The Thesis Committee for Michael Charles Passarello
Certifies that this is the approved version of the following thesis:

New Methods for Quantifying and Modeling Estimates of Anthropogenic and Natural Recharge: A Case Study for the Barton Springs Segment of the Edwards Aquifer, Austin, Texas

APPROVED BY
SUPERVISING COMMITTEE:

Supervisor: John M. Sharp Jr.

Co-Supervisor Suzanne A. Pierce

Meinhard Bayani R. Cardenas

New Methods for Quantifying and Modeling Estimates of Anthropogenic and Natural Recharge: A Case Study for the Barton Springs Segment of the Edwards Aquifer, Austin, Texas

by

Michael Charles Passarello, B.S.

Thesis

Presented to the Faculty of the Graduate School of

The University of Texas at Austin

in Partial Fulfillment

of the Requirements

for the Degree of

Master of Science in Geological Sciences

The University of Texas at Austin

May 2011

Acknowledgements

Thanks to:

Jack Sharp and Suzanne Pierece for being such great supervisors, mentors, and friends. Working with you has been a true privilege and pleasure.

Mark Helper, Bayani Cardenas, and other UT faculty members for all of their help and support.

Brian Smith and Brian Hunt from the Barton Springs / Edwards Aquifer Conservation District.

Nico Hauwert, Roger Glick, and other staff from the City of Austin Watershed Protection Department.

Wendy Robertson, Katie Markovich, Ian Rogers, and other members of my research group who have provided unparalleled support, guidance, and friendship.

Michael Ciarleglio

The Jackson School of Geoscience and the Geological Society of America for financial support.

My family and friends, who without, I would have never made it as far.

Abstract

New Methods for Quantifying and Modeling Estimates of Anthropogenic and Natural Recharge: A Case Study for the Barton Springs Segment of the Edwards Aquifer, Austin, Texas

Michael Charles Passarello, M.S. Geo. Sci.

The University of Texas at Austin, 2011

Supervisors: John M. Sharp Jr. and Suzanne A. Pierce

Increased population and recent droughts in 1996 and 2009 for the Barton Springs segment of the Edwards Aquifer have focused attention on groundwater resources and sustainability of spring flow. These springs serve as a local iconic cultural center as well as the natural habitat for the endangered Barton Springs salamander. In response to the potential compromise of these vulnerable groundwater resources, a two-dimensional, numerical groundwater-flow model was developed for the Barton Springs / Edwards Aquifer Conservation District and other governmental entities to aid in aquifer management. The objective of this study is to develop new methods of quantifying and distributing recharge for this model. The motivation for conducting this study includes the following: recent availability of more extensive data sets, new conceptual models of the aquifer system, and the desire to incorporate estimates of urban recharge. Estimates

of recharge quantities and distributions for natural and artificial sources were implemented within this model to simulate discharge at Barton Springs and water-level elevations from January, 1999 to December, 2009. Results indicate that the new methods employed generated good agreement amongst simulated and observed discharge and water-level elevations (Root mean square error of 0.5 m^3 sec^{-1} and 10.5 m, respectively). Additionally, these recharge calculations are decoupled from Barton Springs discharge which eliminates the circular logic inherent with the previous methodology. Anthropogenic, or artificial, recharge accounts for 4% of the total recharge between January, 1999 and December, 2009. Using observed data to quantify contributions from leaky utility lines and irrigation return flows, recharge estimates were completed with spatial and temporal resolution. Analyses revealed that on a month by month basis, anthropogenic contributions can vary from <1 to 59% of the total recharge. During peak anthropogenic recharge intervals, irrigation return flow is the most significant contributor. However, leakage from utility lines provides more total recharge during the study period. Recharge contributions from artificial sources are comparable to the mid-size watershed contributions over the ten-year analysis period. Urban recharge can be a critical source for buffering seasonal fluctuations, particularly during low flow periods. Outcomes are relevant for habitat conservation, drought response planning, and urban groundwater management.

Table of Contents

List of Tables

List of Figures

CHAPTER 1

INTRODUCTION

This study focuses on a region of the karstic Edwards Aquifer known as the Barton Springs segment which is within and adjacent to Austin, Texas (Figure 1). The Barton Springs segment of the Edwards Aquifer (BSEA) is separated from the rest of the Edwards Aquifer by no-flow boundaries. The BSEA provides water to approximately 60,000 residents (Hunt et al., 2007) and discharges primarily at Barton and Cold Springs. Barton Springs consists of a recreational pool created by a dam directly downstream of the springs located in Zilker Park, downtown Austin. These springs serve as a local iconic cultural center as well as the natural habitat for the endangered Barton Springs salamander. Increased population and recent droughts in 1996 and 2009 have focused attention on groundwater resources and sustainability of spring flow. In response to the potential compromise of these vulnerable groundwater resources, several numerical groundwater flow models have been developed for the Barton Springs / Edwards Aquifer Conservation District (BSEACD) and other governmental entities to aid in aquifer management.

The objective of this study was to develop new methods of quantifying recharge values from observed datasets to reinterpret spatial and temporal distribution create a revised input for the Barton Springs Groundwater Availability Model (BS GAM) developed by Scanlon and others (2001). Research is motivated by the need to understand the relative sensitivity in groundwater behavior to changes in recharge that are related to spatial shifts due to land use change and karst feature locations as well as the influence of temporal patterns as they relate to rainfall variability. Original

interpretations of recharge for the BSEA depended on limited spring flow observations. This study refines the recharge calculations by incorporating extensive precipitation and land use data sets that are newly available, modifying conceptual models of the aquifer system, and integrating estimates of urban recharge. The model developed by Scanlon and others (2001) was employed for this study because it represents a baseline interpretation of groundwater behavior, the model is readily accessible, and the model can be used to compare the decision relevance of scientific uncertainty because it is included within a Groundwater Decision Support System developed by Pierce (2006). The modified interpretation of recharge was completed using a workflow that included expanded data sets, spatial analysis using a geographic information system (ArcGIS 9.3), a scientifically vetted groundwater simulation for BSEA (MODFLOW-96), and analytical interpretations of recent research findings in relation to recharge functions. Study results include:

- new estimates for natural and artificial recharge values that are based upon more extensive data sets and are decoupled from observed discharge,
- new methods of determining the distributions of these recharge values,
- an updated version of the BS GAM for the ten-year study period (1999 – 2009), and
- new insights into the significance of urban-induced recharge for Austin, Texas.

Study Area

PHYSIOGRAPHY AND CLIMATE

The Edwards Aquifer is located along the Balcones Fault Zone of Central Texas which lies on the eastern margin of the Edwards Plateau. The BSEA study area is located

within and adjacent to Austin, Texas and includes parts of Travis and Hays Counties. The BSEA is approximately 400 km^2 in area with surface elevations ranging from approximately 130 to 520 meters AMSL (427 to 1,706 feet AMSL) (Figure 2). This region of Texas is within the subtropical humid climate zone (Larkin and Bomar, 1983) with annual precipitation ranging from 279 to 1,651 mm (11 to 65 in) (1860 through 2000) and averaging 851 mm (33.5 in) (Scanlon et al., 2001). Mean annual potential evapotranspiration, temperature and relative humidity for the study area are 1460 mm (57.5 inches), 26.1 °C (79.0º F), and 43.6 % respectively (TexasET, 2010).

GEOLOGY

The Edwards Aquifer is a narrow band (less than 64 km) of thick and regionally extensive Lower Cretaceous carbonate rocks along the Balcones Fault Zone. The aquifer spans from a groundwater divide near the Rio Grande River in the southwest to the northeast near Salado, Texas, stretching some 400 km (Sharp, 1990). The Edwards Aquifer is divided into the following four components, separated by groundwater divides: the northern segment of the Edwards Aquifer, the Barton Springs segment, and the San Antonio segment (Figure 3). During a Lower Cretaceous sea-level rise, the North American craton was flooded resulting in the deposition of the sediments which would eventually host the Edwards, Trinity Plateau and Trinity Aquifers (Scanlon et al., 2001). Deposits of conglomerate, sandstone, shale, and limestone in the lower and middle Trinity Group represent two transgressive-regressive cyclic genetic sequences (Moore, 1996). Continued transgression and cyclic sedimentation deposited the Glen Rose Formation and the overlying Kainer and Person Formations which constitute the Edwards Aquifer. The Glen Rose Formation consists of two thick carbonate-dominated sequences

in the upper Trinity Group and is overlain by four sequences that comprise the Edwards Aquifer and facies equivalent limestones (Figure 4). Sea-level continued to increase cyclically through part of the Late Cretaceous differing from previous sedimentary patterns by depositing alternating bands of shales and limestones / chalks (Scanlon et al., 2001). The Del Rio Formation is the first shale unit and forms the aquitard at the top of the Edwards Group and is a selenitic, calcareous, pyritic, and fossiliferous clay (Sharp, 1990). The major clay minerals of the Del Rio Clay are kaolinite and illite making the formation very low in permeability. Portions of the Del Rio Clay are eroded throughout Central Texas including portions of the study area where recharge to BSEA occurs. The Buda Formation and Eagle Ford Formation overlay the Del Rio Formation and are dominantly limestone and shale respectively. Above these units is the Austin Chalk which denotes the maximum water depth of sea-level rise. After the maximum water depth was reached, progradation, aggradation, and sea-level fall followed bringing deposition of the clastic Taylor and Navarro Formations (Scanlon et al., 2001). Miocene-age uplift of the Edwards Plateau along the Balcones Fault Zone constitutes the major episode of structural deformation affecting aquifer development. Uplift was accommodated by normal faulting along en echelon faults and graben systems which produced a total of 427 meters (1,400 ft) of displacement down to the coast across the BSEA (Scanlon et al., 2001). Faults associated with this uplift cross-cut the aquifer and control the distribution of confined and unconfined conditions (Sharp, 1990). Fault strike is approximately northeast and coincides with the buried Ouachita fold belt trend (Caran et al., 1981).

HYDROGEOLOGY

The BSEA is approximately 400 km^2 with 80% of this area consisting of unconfined aquifer conditions but this percentage fluctuates with hydrologic conditions. Aquifer thickness ranges from 137 meters along the east side to 0 meters along the west side of the recharge zone (Slade et al., 1986). Barton Springs is the primary discharge point for the BSEA with an average discharge of 1.56 $m^3 s^{-1}$ (55 cfs). Cold Springs is the second largest discharge point followed by pumping. Discharge from Cold Springs cannot be directly measured since it is beneath Town Lake but discharge is often thought to be approximately 3 - 28% of Barton Springs. The BSEA has several hydrologic boundaries which include a no-flow boundary to the west from the Mount Bonnell fault (Senger and Kreitler, 1984), a groundwater divide to the south along Onion Creek (Guyton and Associates, 1958), the "bad-water" line to the east (Sharp, 1990), and the Colorado River to the north. The groundwater divide in the south isolates the BSEA from the San Antonio segment of the Edwards Aquifer which discharges primarily at San Marcos and Comal springs (Scanlon et al., 2003). This divide's location is not static and fluctuates according to hydrologic conditions (LGB-Guyton Associates, 1994). The bad-water line represents a generally abrupt transition in water chemistry from the fresh-water zone of the Edwards aquifer to the more saline bad-water zone (Sharp, 1990). This saline bad-water zone is characterized by a decrease in the relative transmissivity (Flores, 1990) and is described as hydrodynamically controlled rather than separated by a distinct hydrologic barrier, although local fault control is noted (Hovorka et al., 1998).

Recharge

Approximately 85% of long term recharge to the BSEA is derived from six ephemeral losing streams originating in a region west of the recharge zone known as the

contributing zone (Slade et al., 1986) (Figure 5). Stream channels carry runoff from precipitation events downstream to the recharge zone where water within the stream channels recharge the aquifer through various discrete recharge features such as caves, sinkholes, swallets, and fractures. Of the six losing streams, Onion and Barton Creek contribute the majority of recharge derived from the losing streams (~53%). The remaining 15% of recharge occurs throughout the recharge zone as precipitation diffusely percolates into the subsurface (Slade et al., 1986) but recent studies (Hauwert, 2009) suggest that this percentage is greater (~32%). It is thought that mean surface recharge should approximately equal mean discharge (1.56 $m^3 s^{-1}$ or 55 cfs) but has been observed to approach 11 $m^3 s^{-1}$ (400 cfs) during flood events (Slade et al., 1986). Studies have indicated that recharge is highly variable in space and in time and is focused within discrete features (Smith et al., 2001) with Antioch Cave being the largest-capacity recharge feature with an average recharge of 1.3 $m^3 s^{-1}$ (46 cfs) and a maximum of 2.7 $m^3 s^{-1}$ (95 cfs) (Fieseler, 1998). Other sources of recharge include anthropogenic sources such as leaky utility lines, stormwater management structures, and stormwater sewers as well as irrigation return flows (Garica-Fresca and Sharp, 2005; Garcia-Fresca, 2004). Contributions from these sources were quantified for the entire Austin area including areas outside of the recharge zone of the BSEA and are estimated to be approximately 85 mm $year^{-1}$. Recharge from cross-formational flow occurring through adjacent aquifers is unknown but is thought to be relatively small based on water-budget analysis for surface recharge and discharge (Slade et al., 1985). The potential for cross-formational flow from the saline zone and the San Antonio segment of the Edwards aquifer increases under drought and low water-level conditions (Hunt et al., 2007). For example, Massei and others (2007) attribute up to 20% of the increasing conductance at Barton Springs during low flow conditions to flow from the saline zone and Hauwert and others (2004) estimate

that the flow path along the saline zone can contribute about 10-20% of flow to Barton Springs under these conditions.

Groundwater Flow

The Edwards Aquifer is a karst aquifer that is inherently heterogeneous and anisotropic. Consequently, groundwater flow and storage are highly dependent upon these aquifer characteristics (Slade et al., 1985; Maclay and Small, 1986; Hovorka et al., 1996 and 1998; Hunt et al., 2005). Additionally, the aquifer is characterized as a triple porosity and permeability system consisting of matrix, fracture, and conduit porosity. Permeability values vary with the direction and scale of measurement and range over nine orders of magnitude (Halihan et al., 1999). This suggests that the groundwater system can be characterized as having a slow flow system (diffuse matrix flow) and a fast flow system (fracture/conduit flow) (Hunt et al., 2005). Matrix permeability is significantly smaller than values for fractures and conduits with regional scale flow paths dominated by conduit permeability. It is thought that the matrix is connected to the conduit system via fractures (Hunt et al., 2005) and that the majority of groundwater flow occurs in a network of conduits, caves, and smaller dissolution features (Hauwert et al., 2002). Groundwater flow paths interpreted from various dye tests indicate that groundwater generally flows from west to east across the recharge zone and converges with preferential flow paths sub parallel to major faulting and then flows north towards Barton Springs (Figure 6) (Hauwert et al., 2002; Hunt et al., 2007). Additionally, these conduit dominated flow paths generally coincide with troughs in the potentiometric surface. Rates of groundwater flow along preferential flow paths derived from dye tracing range from 2 – 11 km hr^{-1} (1 – 7 mi hr^{-1}) depending upon hydrologic conditions

(Hauwert et al., 2002). Dye tracing studies have also identified several groundwater basins such as the Cold Springs, Sunset Valley, and Manchaca sub-basins within the BSEA (Hunt et al., 2007).

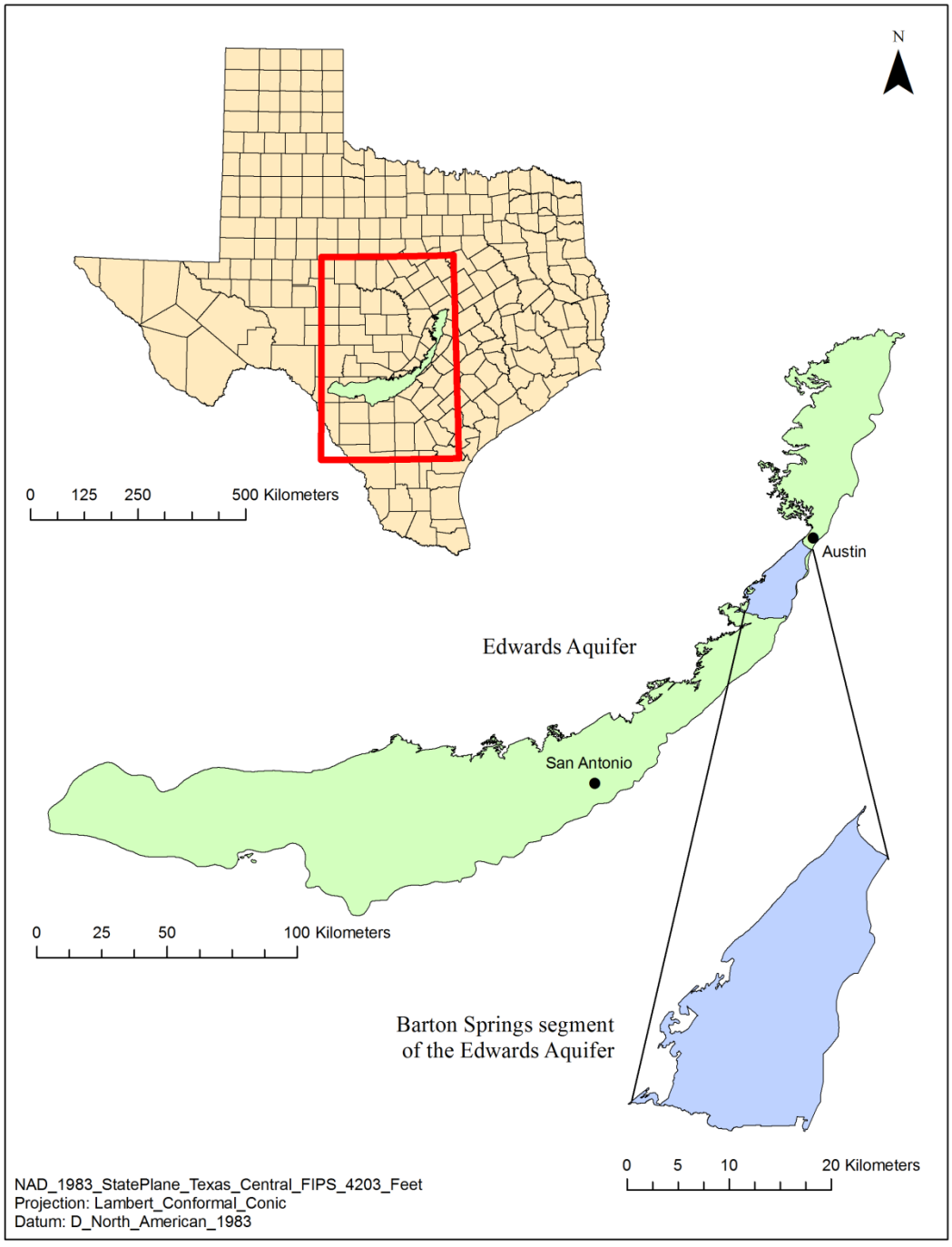

Figure 1: Site map of the study area.

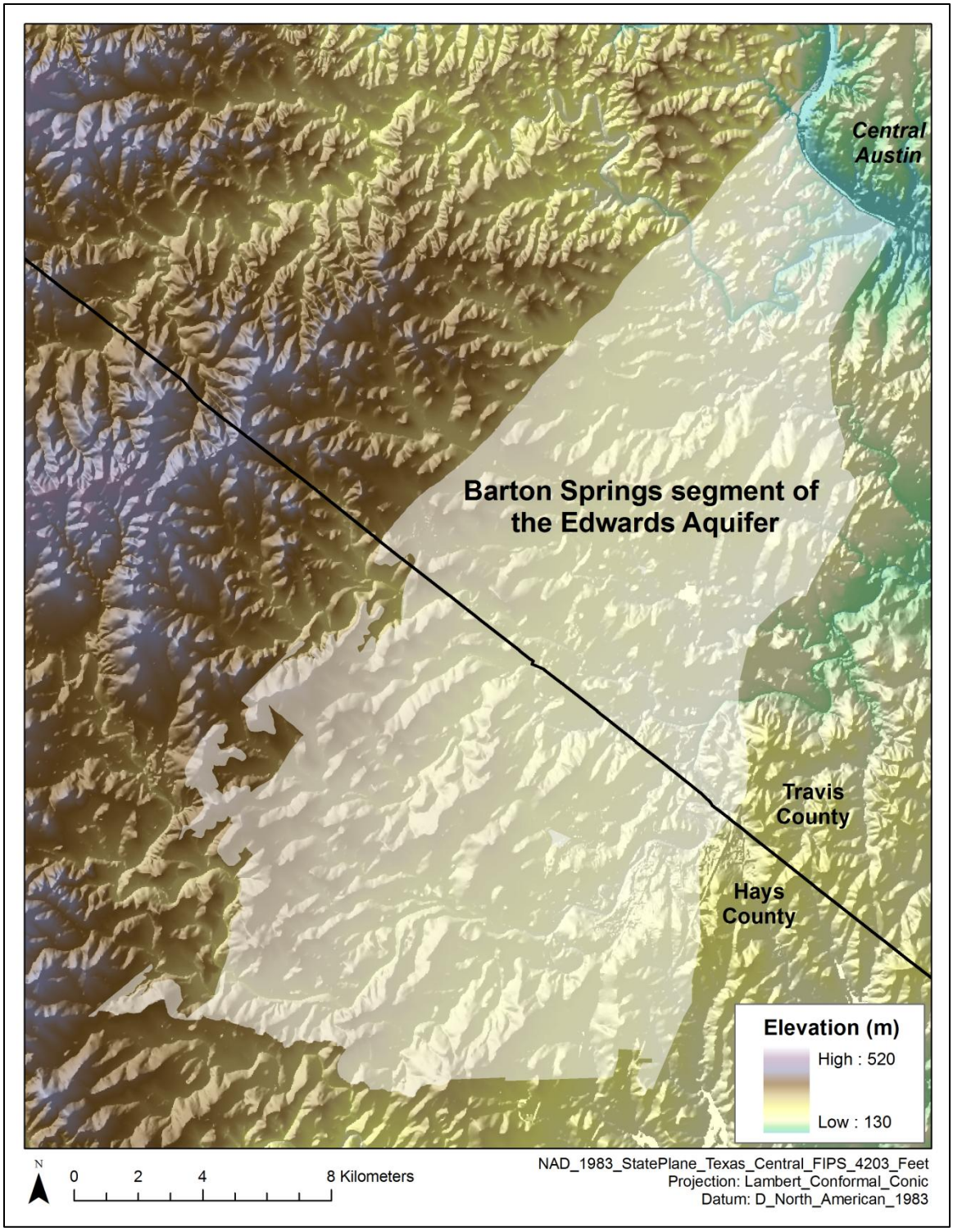

Figure 2: Topographic map of the Barton Springs segment of the Edwards Aquifer.

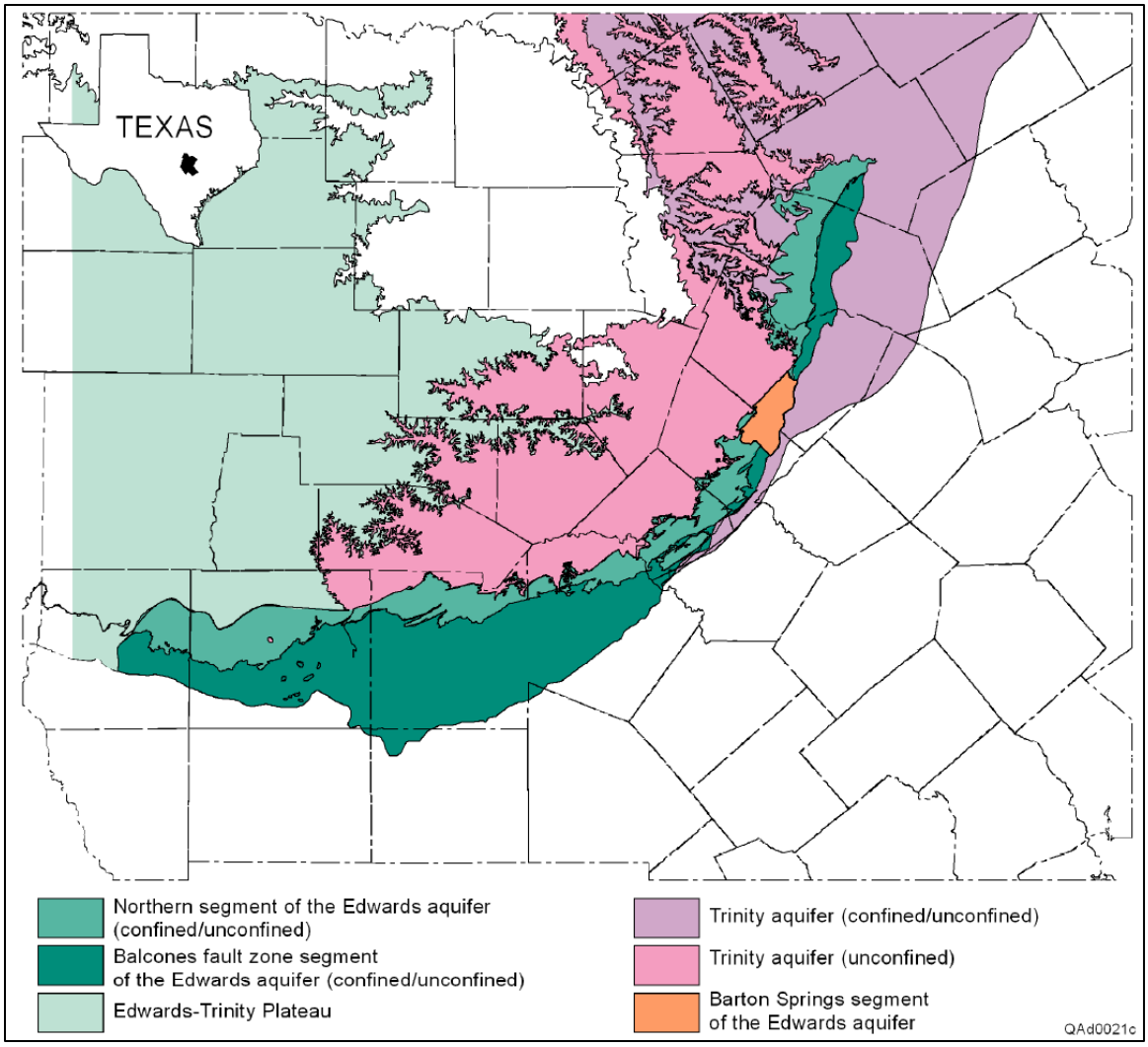

Figure 3: Geologic setting of the Barton Springs segment of the Edwards Aquifer (from Scanlon et al., 2001).

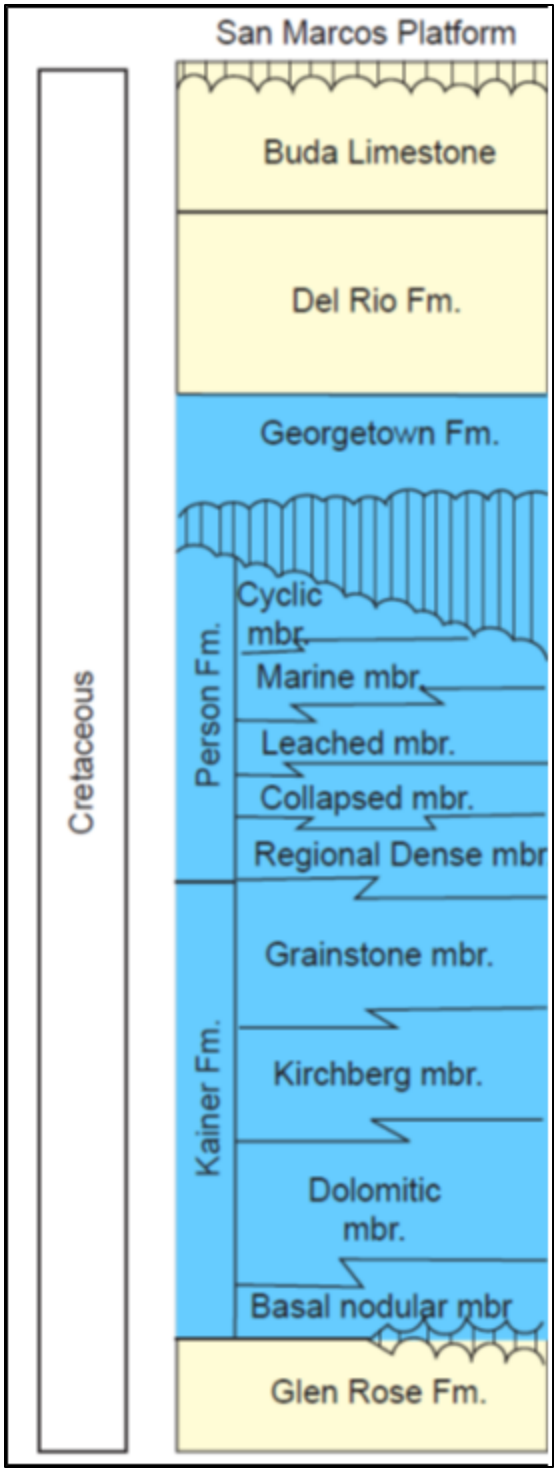

Figure 4: Stratigraphic and hydrostratigraphic section of the study area (from Scanlon et al., 2001).

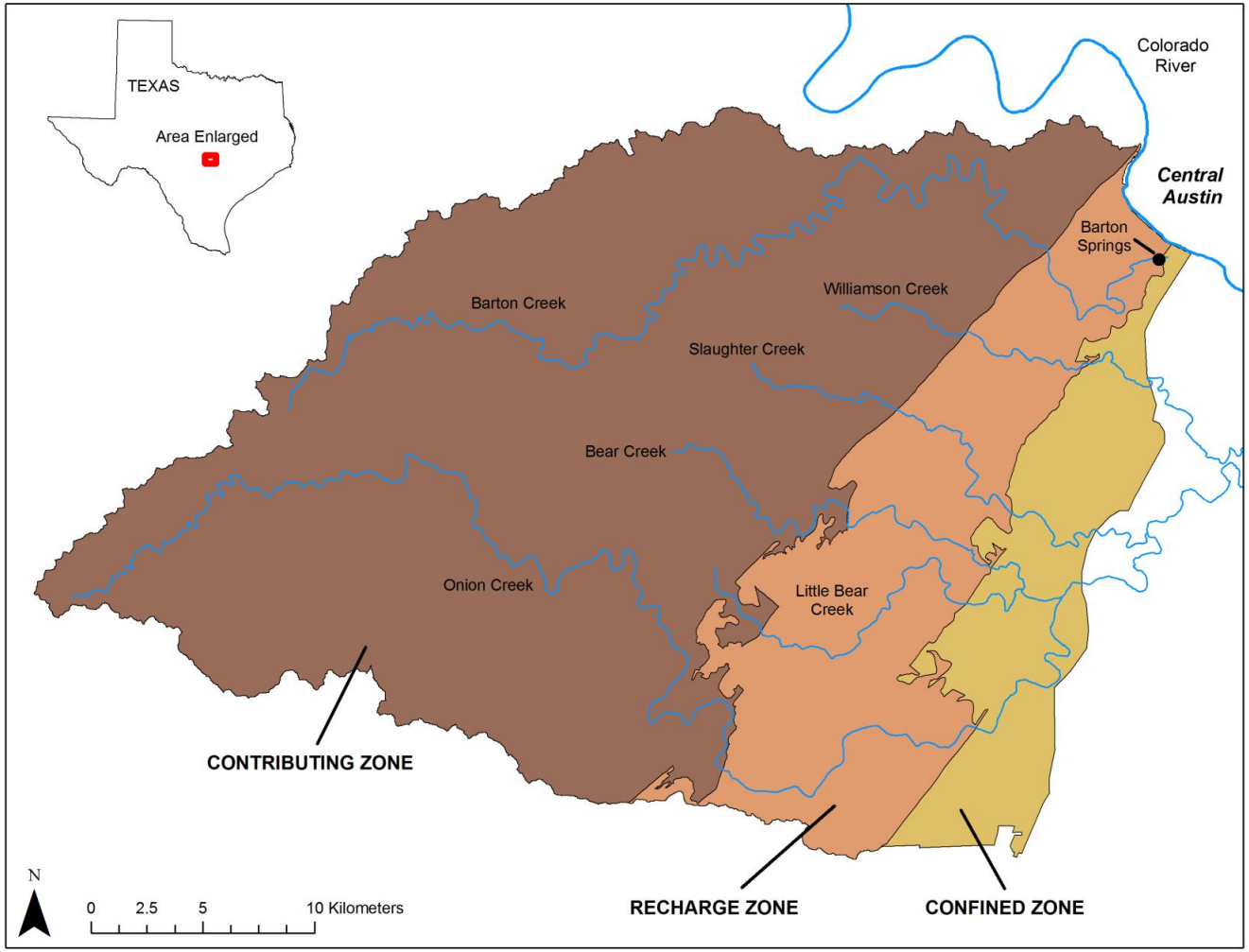

Figure 5: Map of hydrogeologic zones and losing streams for the study area.

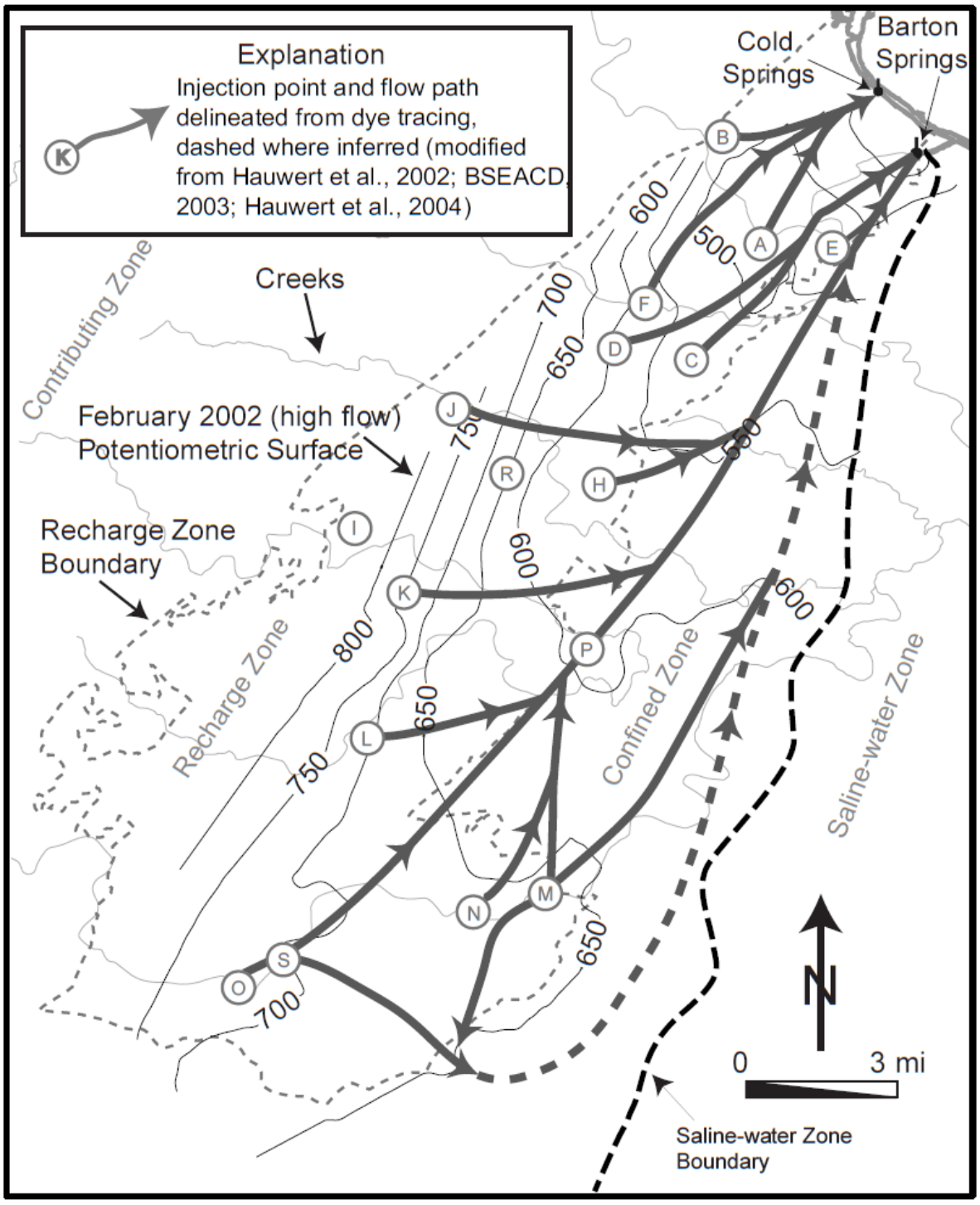

Figure 6: Flowpaths from injections sites to Barton and Cold Springs (from Smith et al., 2005).

CHAPTER 2

URBAN-INDUCED EFFECTS ON GROUNDWATER SYSTEMS

There have been numerous studies that have been conducted to assess the physical and chemical impacts of urbanization on surface water and groundwater for Austin, Texas (Garcia-Fresca and Sharp, 2005; Garcia-Fresca, 2004; Wiles and Sharp, 2008; Wiles, 2007; Krothe, 2002; Christian et al., 2011). Results of previous inquiry have generated a rich interpretation and understanding of processes that control aquifer recharge and motivate this research to assess the significance of urban-induced recharge using the combined knowledge and computational tools. One of the objectives of this study is to determine the relevance of several anthropogenic recharge sources for the BSEA utilizing a water budget approach and a numerical groundwater flow model developed by Scanlon and others (2001).

Introduction

Urbanization and its associated construction of impervious cover and subsurface infrastructures is the major process now affecting the land surface and shallow subsurface around the world. The recognition of humans as an important geologic agent has been well documented for a long time (Sherlock, 1922; Legget, 1969). These effects are compounded in areas of dense populations or urban areas. In 1900, only 10% of the world's population lived in urbanized areas (United Nations, 1991) but current estimates place this percentage at over 50% with some projections estimating an increase to 67% by 2025 (Ramsey, 2003). As more populations migrate towards urban centers, the aerial extent of urbanization will increase through time and often grows at a faster rate than

population growth leading to a phenomenon known as "urban sprawl." In the New York City metropolitan region, the urban area grew 64% between 1964 and 1989 but the population growth was much less (Sharp, 1997). Similar observations have been made for cities like Bangkok, which experienced expansion rates of over 3,200 hectares per year (Lowe, 1992), and for the study area, Austin, TX, where the urban area has increased 640% since 1964 (Garcia-Fresca, 2004). It is estimated that in the United States, urbanized areas are growing at a rate equivalent to two New York Cities per year (Sharp, 1997). These rapid changes to the land surface and local hydrologic cycles are occurring on decadal scales or what can be considered a geologic instant (Sharp et al., 2001). Humankind's alterations to the natural environment from urbanization is found throughout the globe and is taking place at a rate faster than any other geomorphic process for this scale. A thorough understanding of the effects of urbanization is critical in order to maintain future urban populations and towards effectively and sustainably managing future water resources.

Surface Alterations

TOPOGRAPHY

When developing an area during the process of urbanization, major alterations to topography are made. Land surfaces are often leveled for ease of transportation, construction, and infrastructure installation with topographic lows and highs being filled in and lowered through time. By altering the topography, hydrology in urban areas can drastically change. A major consequence of this process includes the burial of streams which are often covered, filled in, converted into a storm sewer or canal, or forgotten. The same fate is observed for many springs in urbanized areas as well (Sharp, 2010).

VEGETATION

Increases in urbanized areas leads to increases in the extent of impervious cover. Thus, vegetation cover can be dramatically decreased and often completely eliminated. These decreases in vegetation cover can effectively decrease the rates of transpiration for urban areas but by planting lawns, gardens, parks, recreational sport fields, and other irrigated land types, transpiration in cities can actually increase. This is especially true for arid climates and/or when invasive species of plants that can include phreatophytes are introduced (Sharp, 2010). Introducing these invasive plant species and the associated irrigation can increase recharge due to irrigation return flows and is especially true for wealthy cities within arid climates.

IMPERVIOUS COVER

Man's most rapidly expanding effect on the natural environment is urbanization and its corresponding construction of roads, buildings, and infrastructures; all of which have dramatic effects on groundwater recharge and permeability distributions (Sharp et al., 2003). The general increase in impervious cover associated with urbanization has long been understood, including the hydrologic effects this has on the urban water cycle (Leopold, 1968). These effects include increasing runoff and decreasing direct infiltration resulting in increased flooding, introduction of non-point source contaminants, and a decrease in diffuse recharge from precipitation (Wiles and Sharp, 2008).

The secondary permeability of impervious cover and the associated infiltration of water through paved surfaces have not been studied extensively and are often ignored. A

recent study for Austin, TX (Wiles and Sharp, 2008) demonstrates that although the low permeability of "impervious" cover decreases diffuse recharge, it does not necessarily lead to an overall decrease in total recharge. The authors utilized double-ring infiltrometers to quantify the permeability of fractures and joints in paved surfaces within the Waller Creek Watershed of Austin, TX. The equivalent hydraulic conductivity for paved surfaces due to these fractures and joints for this study area is 5.9×10^{-5} cm/s. This is equivalent to fine-grained sands, sandstones, silts, and loams (Bear, 1972). Fractures and expansion joints concentrate infiltration which decreases the time and volume of water necessary for saturation and potentially leads to increased recharge potential (Wiles and Sharp, 2008). Currently, the contributing, recharge, and confined zones of the BSEA are 8, 35, and 57% urbanized, respectively (Figure 7). These regions represent the increases in impervious cover (Table 1) for the BS GAM.

Temperature Alterations

One of the main changes to local temperatures due to urbanization is the well documented "heat island effect." According to the U.S. Environmental Protection Agency (US EPA, 2011), urbanized areas endure drastic changes to the landscape that promote heat generation. Buildings, roads, and other infrastructure will replace open land and vegetation essentially changing the land surface from permeable and moist to impermeable and dry. These changes are responsible for urban areas becoming warmer than their rural surroundings due to man-made surfaces such as roofs and pavements heating up from the sun and becoming hotter than the surrounding air. The annual mean air temperature of a city with 1+ million residents can be 1 – 3 °C warmer that its surroundings. Groundwater temperatures are also affected and often increase in the

shallow subsurface (Sharp, 2010). Examples include Tokyo, Japan (Taniguchi et al., 1999; 2001) and Minneaspolis/St. Paul, Minnesota, USA (Taylor and Stefan, 2009).

Pumping Effects

WATER TABLE ELEVATIONS

Urbanization has been documented to cause water table elevations to fall or rise (Sharp, 2010; Simpson, 1994; George, 1992; Whitesides et al., 1983) as imported waters are introduced, transitions from local groundwater systems to surface water systems are made, reservoir-induced changes in river stages, and the utilization of new technologies such as desalinization or aquifer storage and recovery (Sharp, 2010). Water table elevations can rise in urbanized areas when water demands are supplemented by large surface water bodies. Additionally, using imported water rather than local groundwater resources and can lead to flooding of basements, tunnels, and utility systems as well. The opposite can be observed in urban centers where overdraft has led to falling water table elevations and has caused land subsidence, salt water intrusion, and deterioration of groundwater dependent ecosystems (Sharp, 2010).

AQUIFER DEPLETION

Complete resource exhaustion of an aquifer system is typically rare but arid or semi-arid regions can be more susceptible due to little recharge input. Total depletion of an aquifer is generally not a threat. Rather, problems arise when water demands exceed the safe or permissive yields of an aquifer. When these yields are exceeded, consequences can include drops in water levels which raise the cost of pumping, and

water yields become severely diminished. Many cities throughout Texas have experienced the effects of over allocating groundwater resources. Artesian aquifers in Waco and Dallas have had hydraulic head drops of tens of meters forcing these cities to switch to surface water resources. El Paso is currently seeking additional water supplies because the Hueco Bolson Aquifer can no longer meet the projected water demands. These challenges are exacerbated during drought conditions (Sharp et al. 2003, Sharp, 1997).

SUBSIDENCE

Land subsidence due to excessive exploitation of groundwater and petroleum as well as mining is a common human-induced hazard (Holzer and Johnson, 1985; Singh, 1992; Hu et al., 2004; Xue et al., 2005, and Lixin et al., 2011). Over pumping of an aquifer can lead to subsidence and is typical of coastal cities including Houston, Jakarta, Shanghai, Venice, and Calcutta, but is also observed for inland cities like Mexico City and Las Vegas (Sharp et al., 2003; Sharp, 1997). For groundwater dependent areas, land subsidence typically cannot be avoided but can be sustainably managed by a combination of governmental legislation, monitoring, industrial plans and technological advances (Singh 1992; Abidin et al., 2008; Hu et al., 2004; Zhang et al., 2007). Some effects of land subsidence include structural disruption to roads, utilities, and other urban infrastructure, changes to topography resulting in flooding, and many other geological, hydrogeological, environmental, and/or economic impacts (Holzer and Johnson, 1985; Holla and Barclay, 2000; Abidin et al., 2008; Phien-wej et al., 2006; Wang et al., 2009; Wu et al., 2008).

SALT-WATER INTRUSION

The overexploitation of groundwater resources, especially for coastal aquifers, is the most important anthropogenic cause of salt water intrusion. For coastal cities relying upon groundwater resources, salt water intrusion is common due to the proximity of saline groundwater and the ease of which upconing of saline groundwater can occur (Oude Essink, 2003). In regions where saline groundwater is present below fresh groundwater, falling piezometric head levels due to well extraction may cause the interface between fresh and saline groundwater to rise and is known as interface upconing. Cities within arid or semi-arid coastal zones like the Gaza Strip are especially vulnerable to upconing which commonly threatens domestic water supplies (Oude Essink, 2003). Salt-water intrusion can occur inland and has been observed in cities like Kansas City, Missouri and El Paso, Texas (Sharp et al., 2003). In Kansas City, overdraft of the local carbonate aquifers has induced the downward migration of saline water from overlying clastic rocks. Over-exploitation of groundwater in El Paso has caused the intrusion of poor quality brackish river water from the Rio Grande River into the Hueco Bolson alluvial aquifer (Sharp et al., 2003).

Water Quality

A common side effect of urbanization is the introduction of pollution and contaminants into shallow aquifers and/or surface waters. Sources of pollution can include runoff from paved surfaces, leaky storage tanks, surface spills, illegal dumping of hazardous waste, leaky sewage lines, and lack of sanitation facilities (Sharp et al., 2003). Wastewater disposal in developing countries typically consist of pit latrines, cesspits or

septic tanks and represent a significant source of poor quality groundwater recharge (Mather et al., 1996; Lerner, 2002). Urban contamination can also be problematic for underlying deep aquifer systems when over pumping induces downward hydraulic gradients which can potentially introduce pollution into these systems (Sharp et al., 2003).

Recharge

One of the main effects of urbanization can be increases in recharge from anthropogenic sources. Traditionally it has been thought that recharge in urbanized regions decreases due to increases in impervious cover and associated runoff (Leopold, 1968; Coldewey and Meβer, 1997) but numerous studies have shown the opposite (Lerner 1986, 1990; Brasington and Rushton, 1987; Rushton et al., 1988; Price and Reed, 1989; Foster, 1990; Foster et al., 1994, Hutchinson and Woodside, 2002; Garcia-Fresca and Sharp, 2005). The conceptual model for the claim that recharge decreases in urban areas is tied to observed increases in stream flows attributed to increased runoff volumes but several studies have demonstrated that observed increases in stream flow are not tied to decreases in recharge and there is little difference in stream baseflows between urbanized and rural watersheds (Asquith and Roussel, 2007; Drouin-Brisebois, 2002; Lerner, 1997; Scheuler, 1994). Unlike the natural environment, urbanized areas typically have an additional source of water that can potentially become recharge: imported water. Since the majority of cities import water in order to satisfy municipal and industrial demands (Lerner, 2002), significant portions of urban induced recharge can originate from imported water sources; therefore, additional water is introduced into the local

urban hydrologic cycle that would not be present under natural conditions. This additional source of water provides many opportunities for recharge to take place and can account for the increased recharge observed in numerous cities around the world (Figure 8). The fluxes of imported water are often equal to or greater than precipitation; this is especially true of cities within arid climates. For example, rates for both precipitation and imported water for Birmingham, UK average 650 – 750 mm $year^{-1}$ whereas values for Lima, Peru average 10 and 1650 mm $year^{-1}$ for precipitation and imported water respectively (Lerner, 1990).

According to Wiles and Sharp (2008) and Lerner (1990), there are four major types of recharge in the urban environment: *direct*, *indirect*, *localized*, and *artificial* (Figure 9). The focus of this study is to quantify the artificial component and more specifically contributions from leaky utility lines and irrigation return flows. Artificial recharge includes leakage from water mains, sewers, storm drains, stormwater catchments, and other man-made structures as well as contributions from irrigation return flows. Other means of artificial recharge could include soakways, injection wells, drain fields, diversion of surface waters into sinkholes, etc (Sharp, 2010). In cities where no sewers are present to transport wastewater, artificial recharge is typically dominated by the infiltration of wastewater from septic tanks, latrines, and soakways; thus, the majority of imported water eventually recharges the aquifer. The opposite is observed for cities with a wastewater network installed where much of the imported water is re-exported and is no longer available as a potential recharge source (Lerner, 2002). For cities with this

infrastructure in place, importance shifts from wastewater to the water distribution network in terms of artificial recharge contributions.

As explained in Garcia-Fresca and Sharp (2005), water mains generally leak at greater rates than their wastewater counterparts because they are under pressure. Water mains are pressurized in order to keep contaminants out and to transport water to the far reaches of the network. Wastewater networks are typically driven by gravity flow and therefore are not pressurized. Pressure is the main cause of leakage from water distribution networks with leakage rates ranging from 10 – 60% of water distributed. Efficient cities like Austin, TX report leakage rates on the lower end of this spectrum whereas the average rate for developed and less developed countries are typically between 20 – 30% and 30 – 60% respectively. Few publications exist that estimate leakage rates from wastewater pipes but estimates average ~5% (Garcia-Fresca, 2004; Yang et al., 1999; Lerner, 1997; Grischeck et al., 1996; Foster et al., 1994).

Irrigation return flows from the overwatering of lawns, parks, golf courses, etc. are difficult to estimate but their effects are relatively well understood and accepted (Sharp, 2010). Irrigation return flows can be estimated through mass balance calculations of supply and water use while considering soil and evapotranspiration characteristics (Garcia-Fresca and Sharp, 2005; Berg et al., 1996), but this requires extensive data sets and is often oversimplified. According to Oad and DiSpigno (1997), in order to quantify these return flows, all components of the system must be quantified. The first step begins

with quantifying the volume or percentage of applied water that is not consumed by the turf grass followed by determining the amount or percentage of deep percolation water that eventually recharges the groundwater system. Differences between applied water and consumptive use are assumed to be deep percolation water. The downward percolation of this water has been measured in various lysimeter studies (Oad and DiSpigno, 1997; Oad et al., 1997; Danielson et al., 1980; Howell et al., 1991) but all of it cannot be assumed to recharge since some of this water is consumed by deep root plants such as trees, bushes, and other vegetation. Irrigation return flow can contribute significant amounts of artificial recharge and is especially prevalent in arid and semiarid regions. One example would be Riyadh, Saudi Arabia, where excess recharge attributed to irrigation return flow caused groundwater flooding in road underpasses (Rushton and Alothman, 1994).

The quantity of artificial recharge in urban areas can constitute a significant portion of the total water budget. Quantifying these recharge contributors is becoming increasingly important and a thorough understanding of their effects and spatial distributions is needed in order to manage future water resources and maintain future urban populations.

Permeability Field Alterations

The network of water mains, sewer lines, electrical and telephone lines, storm sewers, subways, underground structures, and other subsurface infrastructure associated with urbanization can drastically alter permeability fields (Sharp et al., 2003). For example, in order to install utility lines (water, electric, gas, sewage, etc.), municipalities

and utility companies will often dig trenches in which to place the pipes or housing structures. The bottom of the trench is generally filled with well-sorted, clean sand or gravel to protect the pipes from the rock walls and settlement whereas the top is filled with a varying combination of backfill material. Sharp and others (2003) have demonstrated that the permeability within these trenches is commonly orders of magnitude greater than the surrounding natural materials. Additionally, if the pipe walls are compromised, permeabilities can be much greater within the pipes themselves than the surrounding fill. It is also recognized that urban soils tend to become less permeable with compaction (Pitt et al., 2002) and the difference in permeability inside and outside of utility trenches can be even greater (Sharp et al., 2003).

The urban environment is analogous to a karstic system partly due to the double- or triple-permeability found in the shallow subsurface. According to Sharp (2010), this highly altered permeability field can lead to the following: 1) altered groundwater flow systems, 2) maintenance of stream baseflows and spring flows during times of limited rainfall or alternatively, 3) reduced or increased spring flows, if flow is diverted from spring orifices, 4) diversion of groundwater to different streams or catchments, 5) artificial recharge caused by leakage of water, sewage, and storm waters along the utility lines, 6) difficulty in predicting, modeling, and remediating subsurface contamination, 7) creation of multiple contaminant plumes that can migrate in different directions than might be predicted from standard analyses, and 8) utility trenches and mains/sewers serving as “French drains” to limit rising water tables.

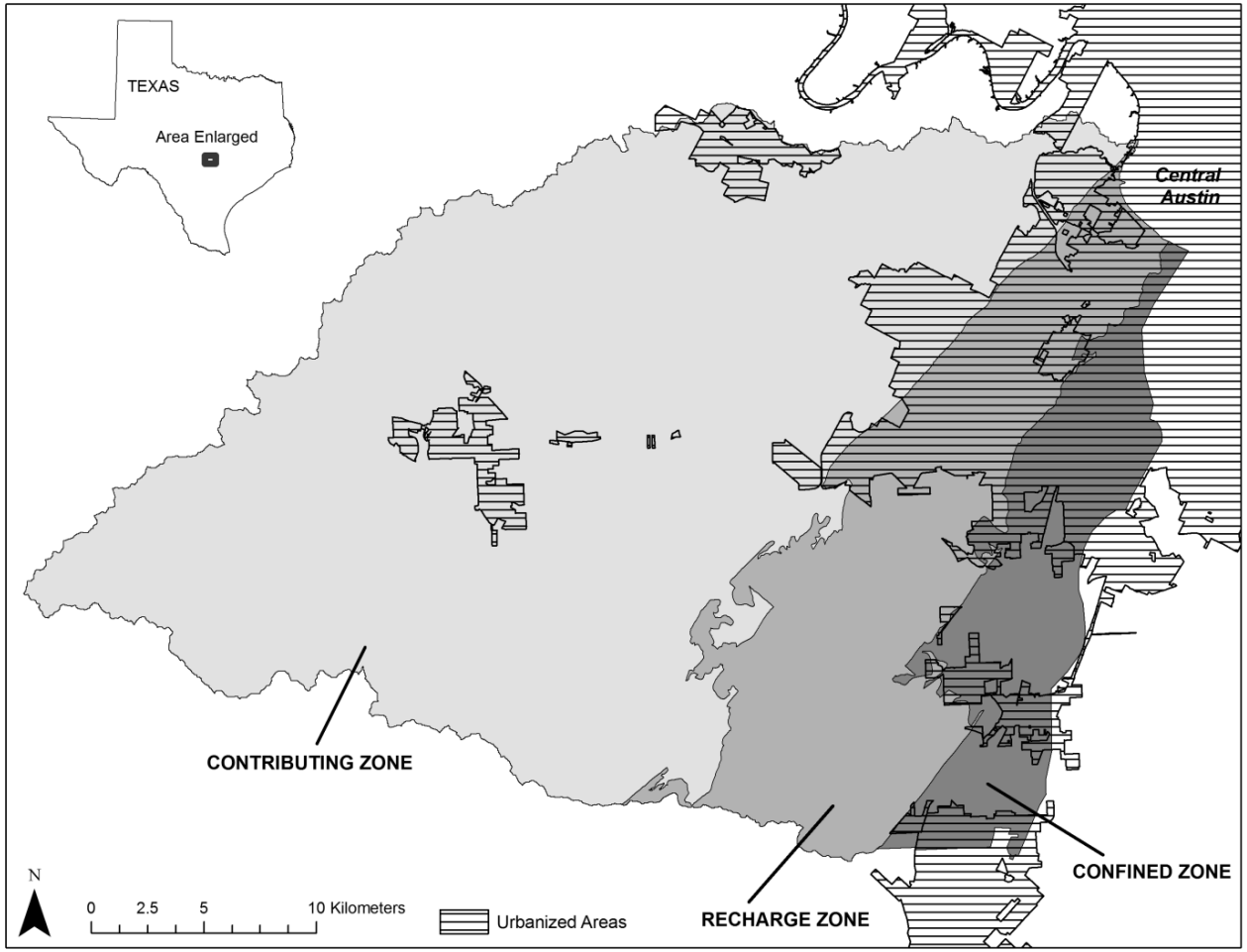

Figure 7: Map of urbanized areas (2010) within the Barton Spring segment of the Edwards Aquifer, TX.

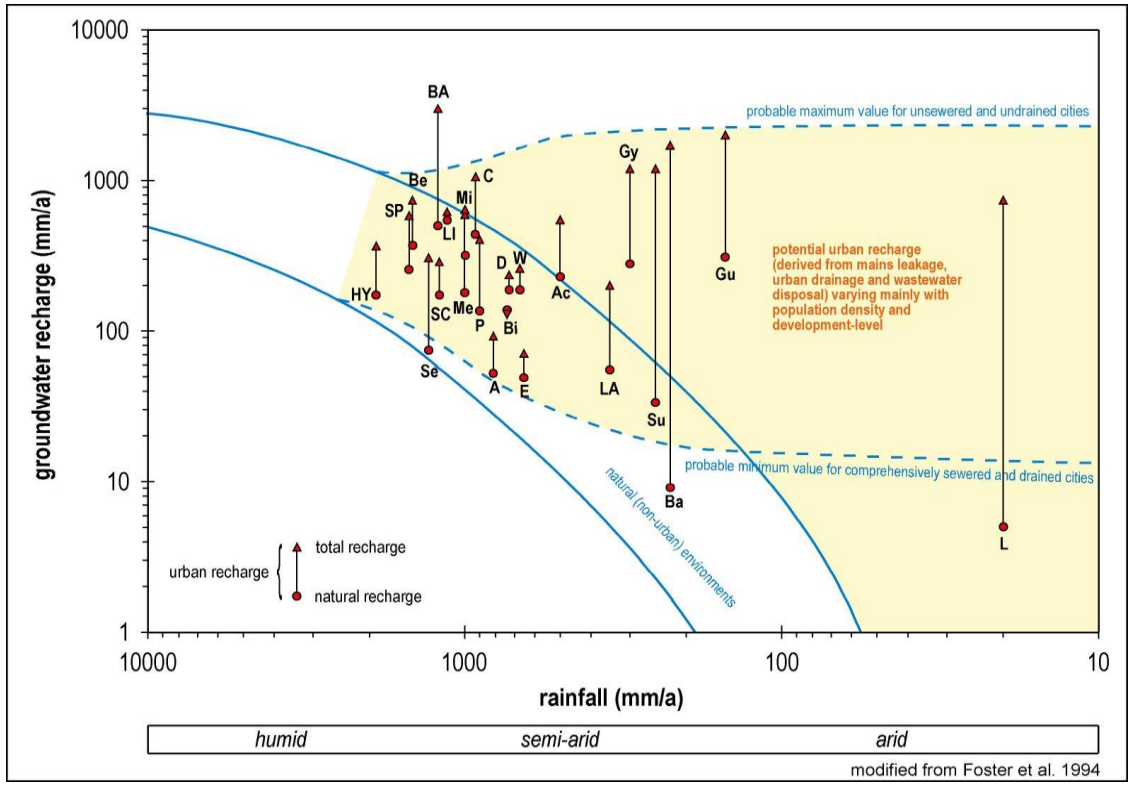

Figure 8: Estimates of groundwater recharge in cities prior to (circle) and after urbanization (triangle) (from Sharp, 2010; Garcia-Fresca and Sharp, 2005 and Foster, 1996). HY – Hat Yai, Thailand; SP – São Paulo, Brazil; Be – Bermuda, UK; Se – Seoul, Korea; BA – Buenos Aires, Argentina; SC – Santa Cruz, Bolivia; LI – Long Island, USA; M – Mérida, Mexico; C – Caracas, Venezuela; Bi – Birmingham, UK; Mi – Milan, Italy; P – Perth, Australia; D – Dresden, Germany; W – Wolverhampton, UK; E – Évora, Portugal; Ac – Aguascalientes, Mexico; LA – Los Angeles, USA; Gy – Gyandja, Azerbaijan; Su – Sumgayit, Azerbaijan; Ba – Baku, Azerbaijan; Gu – Gulistan, Uzbekistan; L – Lima, Peru

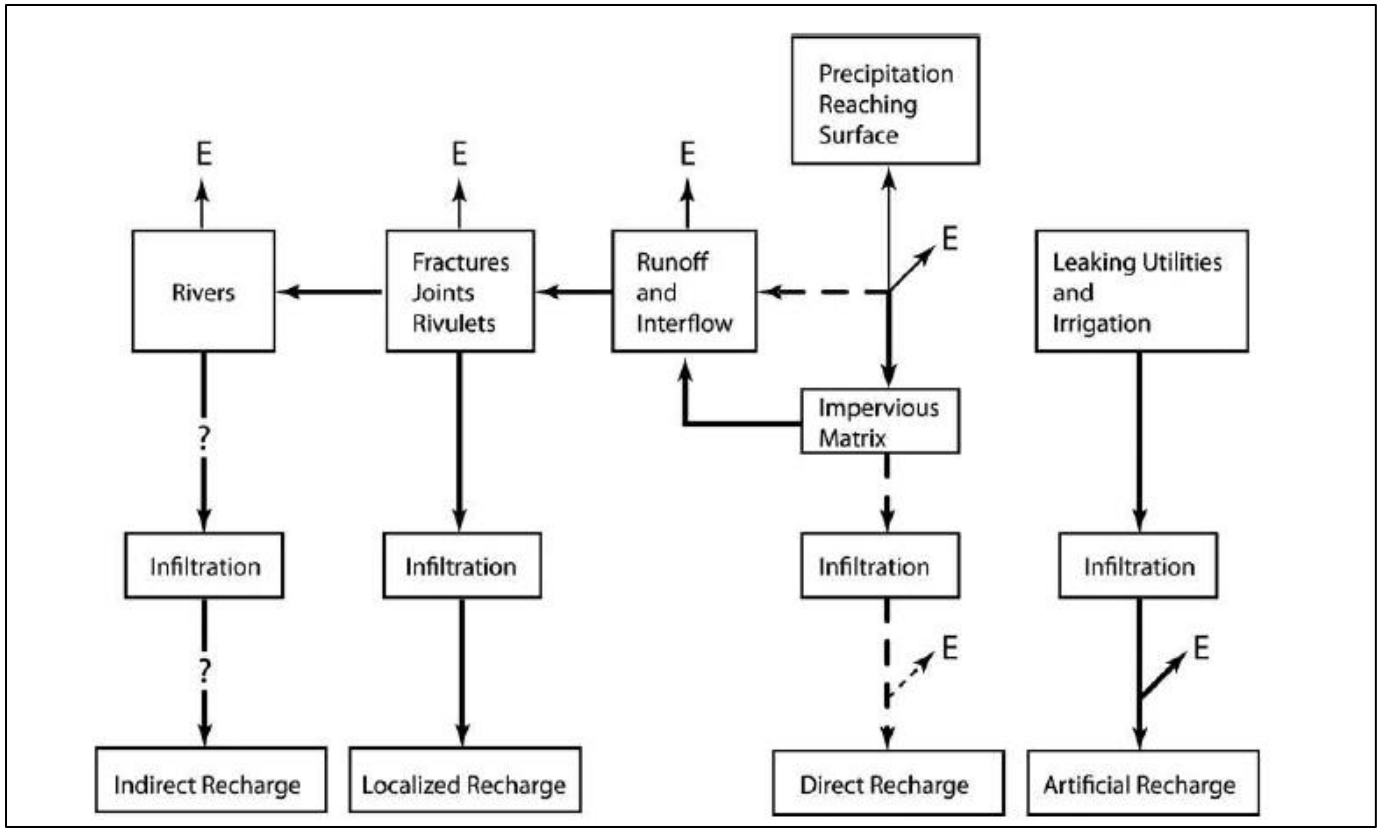

Figure 9: The urban rainfall-recharge relationship (from Wiles and Sharp, 2008; after Lerner, 1997). Bold arrows denote general increases in flux with urbanization; dashed arrows denote general decreases. In areas of losing streams (bold arrows with question marks), indirect recharge can also increase. Evapotranspiration is indicated by E. Recharge can either increase or decrease with urbanization. Data suggest that it more often increases. Impervious cover can increase localized and indirect recharge.

Table 1: Summary table of the area of impervious cover over the BS GAM. Values were calculated from City of Austin land use surveys (City of Austin, 2011)

Year	Impervious Cover (km^2)	Percentage of BS GAM Area
1990	27	8.2%
1995	32	9.9%
2000	42	13.0%
2003	47	14.3%
2006	48	14.8%
2008	49	15.1%

CHAPTER 3

PREVIOUS GROUNDWATER FLOW MODELS

Several digital groundwater flow models have been created for the San Antonio and Barton Springs segments of the Edwards Aquifer (Klemt et al., 1979; Slade et al., 1985; Thorkildsen and McElhaney, 1992; Barrett and Charbeneau, 1996; Scanlon et al., 2001; Smith and Hunt, 2004; Lindgren et al., 2004; Lindgren, 2006; Painter et al., 2007) partly in order to assess the sustainability and susceptibility to contamination of source water provided by public water system wells (Lindgren et al., 2009). In this thesis, I quantify natural and artificial recharge and their spatial distributions for the BSEA. Below is a summary of the previous models for the BSEA that emphasizes how each study quantified and distributed recharge.

Recharge values for this study were calculated and assigned to the spatial grid constructed by Scanlon and others (2001), this simulation model was the first state approved Groundwater Availability Model (GAM) for the BSEA and represents a baseline model for comparison. The BS GAM is a part of the Texas Water Development Board's (TWDB) Groundwater Availability Modeling program (TWDB, 2011) and has undergone two updates since its implementation (Smith and Hunt, 2004; Painter et al., 2007). Although the original version of this model (Scanlon et al., 2001) was utilized for this study, recharge values that were determined can be implemented with the two updated versions as part of future work. However, it is important to note that the model created by Painter and others (2007) distributes recharge values differently from this study. If recharge values from this study were to be utilized for that model, recharge distributions and methods would need to be recalculated and applied to the model

parameters for the 2007 model. An earlier example of refining the recharge file with spatial and urban considerations was completed using the alpha version of the Groundwater Decision Support System (Pierce, 2006; Pierce et al., 2006; Sharp et al., 2008; Cain et al., 2008) and this approach reflects the systems perspective for testing uncertainty in scientific interpretations reflected in those results.

Three of the four numerical groundwater flow models described below are finite-difference groundwater flow models with the mathematical objective of solving groundwater flow in three dimensions. When assuming that fluid density is constant, the three-dimensional movement of groundwater flow through a heterogeneous and anisotropic aquifer can be described by the following partial-differential equation (see Rushton and Redshaw, 1979 for example derivation):

$$\frac{\Delta}{\Delta x}\left(K_{xx}\frac{\Delta h}{\Delta x}\right) + \frac{\Delta}{\Delta y}\left(K_{yy}\frac{\Delta h}{\Delta y}\right) + \frac{\Delta}{\Delta z}\left(K_{zz}\frac{\Delta h}{\Delta z}\right) - W = S_S\frac{\Delta h}{\Delta t} \qquad \textbf{(1)}$$

where,

K_{xx}, K_{yy}, *and* K_{zz}: values of hydraulic conductivity along the x, y, and z coordinate axes, which are assumed to be parallel to the major axes of hydraulic conductivity [L t^{-1}]

h: potentiometric head [L]

W: volumetric flux per unit volume and represents sources and/ or sinks of water [t^{-1}]

S_S: specific storage of the porous material [L^{-1}]

t: time [t]

A groundwater flow system can be mathematically represented by combining Equation (1) with specification of flow and/or head conditions at the boundaries of an aquifer system as well as specification of initial-head conditions (McDonald and Harbaugh, 1988). When solving this relationship, a time-varying head distribution can be derived that measures both the energy of flow and the volume of water in storage. This can be used to calculate directions and rates of movement (McDonald and Harbaugh, 1988).

In general, analytical solutions of Equation (1) are rarely possible except for very simple systems. Numerical methods are often employed to obtain approximate solutions with the finite-difference method being one of them. This method replaces the continuous system described in Equation (1) by a finite set of discrete points in space and time (McDonald and Harbaugh, 1988). The partial derivatives are replaced by terms calculated from the differences in head values at these points. This process leads to systems of simultaneous linear algebraic difference equations whose solutions yield values of head at specific points and times. Therefore, the time-varying head distribution that would be given by an analytical solution of the partial-differential equation of flow is approximated (McDonald and Harbaugh, 1988).

The focus of this thesis is to quantify and distribute (spatially and temporally) values of recharge that will be implemented to solve these linear algebraic difference equations. These recharge values are expressed as W in terms of Equation (1).

Original Finite-Difference Groundwater Flow Model for the BSEA

One of the first digital groundwater flow models for the BSEA was developed by Slade and others (1985). Urban development within this region prompted concerns regarding the quantity and quality of water in the aquifer. The USGS was tasked with developing a numerical groundwater model in order to more effectively manage this resource. The two-dimensional finite-difference groundwater flow model described by Trescott and others (1976) was utilized within Slade and others (1985) to estimate the transmissivity, hydraulic conductivity, and specific yield of the aquifer. The procedure for applying the finite-difference approach to groundwater flow is as follows:

1. A finite-difference grid is superimposed upon a map showing the extent of the aquifer, thus for computational purposes the continuous aquifer is simulated by a set of discrete blocks (cells).
2. Pertinent hydraulic and hydrologic characteristics of the aquifer are coded for appropriate cells within the grid.
3. The governing partial-differential equation is written in finite-difference form for each of the discrete cells.
4. The resulting set of linear finite-difference equations are solved numerically for hydraulic head at the center of each cell (or node) by a digital computer.

Recharge to the aquifer was determined through methods described by Garza (1962) where recharge consists of infiltration of stream flow and direct infiltration of runoff in the inter-stream areas. A water-balance approach was utilized for each watershed of the six major losing streams where recharge within the watershed is the

difference between gauged stream flow upstream and downstream from the recharge zone plus estimated runoff in the intervening area. Based on monthly volumes of recharge for each watershed for July 1979 to December 1982, approximately 85% of total recharge in the watersheds occurs along the main channels of the six creeks with the remaining 15% attributed to diffuse infiltration throughout the recharge zone. Flow-loss studies were also conducted as a means of defining the distribution of recharge within reaches of each creek and to determine the maximum recharge capacity of the main channels for each creek (Slade et al., 1985).

Conclusions of this study were:

1. The hydraulic characteristics determined from an individual well are not necessarily representative of the aquifer on a local basis.
2. The transmissivities derived from the steady-state simulation vary from 100 ft^2/d (9.3 m^2/day or 1.1 x 10^{-4} m^2/sec) in the western part of the aquifer to more than 1,000,000 ft^2/d (92, 903 m^2/day or 1.07 m^2/sec) near Barton Springs.
3. The simulated hydraulic heads are more sensitive to changes in transmissivity in the western and southern portions of the aquifer than in the area near Barton Springs.
4. The average specific yield derived from the model is 0.014 and varied from 0.008 to 0.06.
5. Using projected pumping rates, a simulation for the year 2000 indicates that the aquifer will be dewatered in the southwest part of the aquifer and have large declines in the south east.

According to Scanlon and others (2001), "The model developed by Slade and others (1985) is not appropriate for regional water planning because the model was developed with a code that is no longer in use (Trescott et al., 1976), the grid cell size is large (minimum 2,250,000 ft^2 or 209,031 m^2), the aquifer thickness is not explicitly represented in the model, and the transient simulation period was short (5 months)." Additionally, the aquifer was not dewatered by the year 2000 as predicted. Thus, agreeing with the notion put forth by many (Konikow, 1986; Stewart and Langevin, 1999) that groundwater models typically are poor at forecasting groundwater flow.

Original Lumped Parameter Model for the BSEA

The next significant model for the BSEA was conducted by Barrett and Charbeneau (1996). Once again, one of the objectives of this study was to predict the impacts of urban development on the quantity and quality of water in the BSEA. The authors developed a new type of lumped parameter model in which the aquifer was divided into five cells corresponding to the five major watersheds contributing recharge to the aquifer (Figure 10). In this model, aquifer properties within cells were allowed to vary vertically. Each cell was treated as a tank with a single well utilized to characterize the conditions in that cell.

Model recharge was determined from flow-loss studies and did not differ greatly from the methods utilized in Slade and others (1985) except for Barton Creek. Recharge from all of the creeks except for Barton Creek exhibit a similar behavior: recharge is assumed to increase linearly with discharge until a recharge threshold is met. After discharge exceeds the recharge threshold, recharge remains constant at the recharge

threshold until discharge drops below it again. The rate of recharge for Barton Creek was determined by comparing discharge rates at two stream gauge stations. One of the stations was located above the recharge zone and another was located about half way across the recharge zone. At the downstream gaging station, the bed of the creek is always above the aquifer level. Therefore, recharge above this station was assumed to be unaffected by aquifer level and recharge below this station was assumed to be negligible. Recharge between the two stations was determined by subtracting the downstream discharge from that upstream. This relationship between discharge and recharge is similar to the other streams for flows less than 3.7 $m^3 s^{-1}$ but at higher flow rates recharge increases dramatically. The relationship between discharge and recharge for these high flow rates is described by a quadratic equation.

Diffuse recharge was estimated utilizing the Groundwater Loadings Effects of Agricultural Management Systems model developed by the US Department of Agriculture (Knisel, 1993). Inputs for this model included historical rainfall data from 1979 – 1993 as well as descriptions of soil and vegetation types for the recharge zone. Average infiltration was estimated to be about 50 mm $year^{-1}$ or 6% of average annual precipitation. The conclusions of this study were:

1. The lumped parameter model is capable of predicting regional water levels and discharge comparable to those of traditional groundwater models with fewer data requirements and calibration parameters.
2. The model was able to reproduce measured average nitrogen concentrations in the Edwards Aquifer and at Barton Springs.
3. Results indicate that increased development will reduce spring flow and increase nitrogen concentrations in the aquifer.

According to Scanlon and others (2001), "The resolution of the model (cells equivalent to river basins) is too coarse to evaluate the impact of more local pumpage on spring discharge, therefore, the lumped parameter model is inadequate for regional water planning."

Barton Springs Groundwater Availability Model

As a part of TWDB's Groundwater Availability Modeling (GAM) program (TWDB, 2011), a MODFLOW-96 groundwater flow model was developed for the BSEA by Scanlon and others (2001). The purpose of the Barton Springs Groundwater Availability Model (BS GAM) was to provide a groundwater management tool to the Barton Springs/Edwards Aquifer Conservation District (BSEACD) and the Regional Water Planning Group with. This model was aimed at evaluating groundwater availability and predicting the response of water levels and spring flows to increases in pumpage and droughts during the period 2001 – 2050. Implications of this study are not only important for Austin residents but also important for the federally-listed endangered species, the Barton Springs salamander (*Eurycea sosorum*) that relies upon Barton Springs as its natural habitat.

MODFLOW-96 is a modular finite-difference groundwater flow code developed by the U.S. Geological Survey (Harbaugh and McDonald, 1996). The model is an equivalent porous media model constructed as one layer of 120 rows and columns with a total of 14,400 cells. Each cell is 1,000 feet (304.8 m) long and 500 feet (152.4 m) wide and is aligned parallel to the strike of the Edward's Aquifer (Figure 11). Not all of the

cells within the model are "active" and were determined based upon the hydrogeological boundaries of the aquifer: 1) the northern boundary is the Colorado River, 2) the southern boundary is a groundwater divide located along Onion Creek as determined by Stein (1995), 3) the eastern boundary is the bad-water line as described by Sharp (1990), and 4) the western boundary is the no-flow boundary established by the Mount Bonnell fault (Senger and Kreitler, 1984). Cells within these boundaries are considered "active" resulting in 7, 043 cells. The four model parameters include elevations of the top and bottom of the layer, horizontal hydraulic conductivity, specific yield, and specific storage. Several major faults, based upon Small and others (1996), were incorporated into the model and act as horizontal no flow boundaries. Recharge for this model was modified from the methods described in Slade and others (1985) and Barrett and Charbeneau (1996). Recharge from losing streams was determined from gauging stations and recharge thresholds whereas diffuse recharge from precipitation was set equal to 15% of the total stream recharge. Recharge from the losing streams was uniformly distributed where the streams intersect the recharge zone and diffuse recharge values were equally distributed to all active cells. Pumping was assigned to cells based on values and locations reported by the BSEACD. Unreported domestic pumpage was estimated by the BSEACD and assigned to all active cells.

Two model scenarios, steady-state and transient, were utilized to calibrate the model. Measured water levels in July and August of 1999 were employed to evaluate the steady-state model calibration. Recharge values and distributions for this model scenario were based upon the average recharge from 1979 – 1998. It is important to note that the total amount of recharge for this time period was reduced to equal the average spring discharge for Barton and Cold Springs of 55 $ft^3\ sec^{-1}$ (1.6 $m^3\ sec^{-1}$) and pumpage for 1989

of 5 ft^3 sec^{-1} (0.14 m^3 sec^{-1}). The authors state, "Recharge was assumed to be known and was not changed during calibration." The distribution of hydraulic conductivities was estimated from the steady-state scenario by employing trial and error as well as automated inverse approaches which resulted in 10 zones of hydraulic conductivity that range from 1 to 1,000 ft day^{-1} (0.348 to 304.8 m day^{-1} or 4.3 x 10^{-6} to 3.5 x 10^{-3} m s^{-1}) (Figure 12). Simulated heads and the calibrated distribution of horizontal hydraulic conductivities from the steady-state model scenario were used as inputs for the 10-year transient scenario (1989 – 1999). This time period was broken up into monthly stress periods with 12 time steps in each stress period or 120 stress periods. Each monthly stress period represents a time interval within MODFLOW-96 where all inflow, outflow, properties, and boundary conditions are constant. Values for specific yield (0.005) and specific storage (5 x 10^{-5} ft^{-1} or 1.5 x 10^{-5} m) from Slade and others (1985) were utilized as initial estimates.

Sensitivity analyses of each scenario demonstrate that the model is most sensitive to changes in recharge and hydraulic conductivity distributions. The steady-state scenario was able to simulate water levels with a RMS error of 24 feet (7.3 m) The transient simulation generally reproduced measured spring discharge with a RMS error of 12 ft^3 sec^{-1} (0.34 m^3 sec^{-1}). Predictions of the model include small (<35 ft or 10.7 m) water level declines under average conditions and projected pumping. However, there would be much greater declines (<270 ft or 82.3 m) in response to projected pumping during drought-of-record conditions. Declines in discharge from Barton and Cold Springs are predicted to be small and proportional due to increased pumpage during average conditions, but could go dry during drought-of-record conditions as early as 2030.

As described by Lindgren and others (2009), there are various limitations to this model that need to be addressed in order to model this aquifer system more confidently. These limitations include the quality of input data (i.e. properties and data are based on sparse or clustered information for hydraulic conductivity, storativity, and water level data), the appropriate scale of application (i.e., models should only be utilized for regional scales, thus are inappropriate for site-specific issues), assumptions associated for conceptual and numerical models (i.e., discretization of the model gird, temporal discretization for transient simulation – monthly stress periods, and uncertainties regarding the hydrogeological boundaries of the model). One of the main data uncertainties of this model are the spatial and temporal distribution of recharge and withdrawals from wells.

All recharge inputs are in some way tied to discharge observations from Barton Springs and well withdrawals. For example, recharge values for precipitation are not based on actual precipitation data; rather they are calculated as a percentage of total stream recharge based on water budget analyses conducted by Slade and others (1985) who estimated that 85% of all recharge comes from losing streams and the remaining 15% from diffuse recharge. Additionally, total recharge calculations were lowered to match discharge at Barton Springs and well withdrawals for the steady-state scenario. All of this creates a circular logic situation where properties such as calibrated hydraulic conductivities, specific yields, and specific storages are based on the previous stated assumption by Scanlon and others (2001): "Recharge was assumed to be known and was not changed during calibration." This is not the case and is particularly problematic

when sensitivity analyses for both scenarios indicate that the model is most sensitive to changes in recharge.

Recalibrated Barton Springs Groundwater Availability Model

The BS GAM was recalibrated by the BSEACD for conditions observed during the drought-of-record in the 1950's (Smith and Hunt, 2004). The main objective of the original BS GAM was to predict future groundwater availability in response to projected pumping and various climatic conditions, but mostly for during drought conditions. The previous BS GAM was calibrated to a time period wetter than that of the 1950's drought and therefore overestimates spring flow and under predicts water level elevations compared with measurements taken during the 1950's drought of record. The BSEACD was especially concerned that during severe drought conditions combined with high rates of future pumping, Barton Springs and some water-supply wells would undergo water-quality degradation because of migration of water from the bad-water zone. Incremental changes were made through trial and error to specific yield, specific storage, and hydraulic conductivity values to recalibrate the transient portion of the previous BS GAM. The conclusions of this report were (Smith and Hunt, 2004):

1. The recalibrated BS GAM provides a better match between simulated and measured spring-flow and water-level values under 1950's drought conditions than does the previous BS GAM
2. Recalibrated BS GAM simulations indicate that for each 1 ft^3 sec^{-1} (0.03 m^3 sec^{-1}) of groundwater pumped from the aquifer under 1950's drought

conditions, discharge from Barton Springs will diminish by ~1 ft^3 sec^{-1} (0.03 m^3 sec^{-1}).

3. The recalibrated BS GAM simulates a mean monthly spring flow of about 1 ft^3 sec^{-1} (0.03 m^3 sec^{-1}), with 2004 pumping rate of 10 ft^3 sec^{-1} (0.28 m^3 sec^{-1}) under 1950's drought conditions. According to a minimum daily discharge of 9.6 ft^3 sec^{-1} (0.27 m^3 sec^{-1}) measured in 1956, spring flow may temporarily cease for periods less than 1 month. At 15 ft^3 sec^{-1} (0.42 m^3 sec^{-1}) of pumping, spring flow will cease for at least 4 months.
4. Simulations of 1950's drought conditions with 2004 and future rates of pumping indicate that significantly lower water levels will occur in most parts of the aquifer, resulting in an increased potential for flow from sources with poor water quality, such as the saline-water zone.

Original Dual Conductivity Model for the BSEA

The BS GAM was updated again by Painter and others (2007) to represent conduit flow within the karst aquifer system utilizing MODFLOW-DCM Version 2.0. The final technical report on this update can be found in Winterle and others (2009). The underlying conceptual and geologic frameworks of the original BS GAM are unchanged within this update. Three major additions to the model were:

1. Implementation of the MODFLOW-DCM (dual conductivity model) through addition of a separate interacting model domain that represents a network of high-permeability conduits nested within the main aquifer layer (Figure 13).

2. Extension of the active model area to the south and west.
3. Initial development of an approach for deriving recharge input to the model based on monthly average precipitation data.

These updates necessitated recalibration of the steady-state and transient model scenarios. The steady-state scenario was for the same time period and assumptions previously discussed in Scanlon and others (2001). The transient scenario was recalibrated to match "qualitatively" spring discharge measurements for Barton Springs and water table elevation responses in three wells for the 10-year period from January 1989 to December 1998. This was achieved through recalibrating the hydraulic conductivity values for 9 diffusive zones and 13 conduits by trial-and-error until head levels within the steady-state scenario matched measured levels of 74 observation points during July and August of 1999 (Winterle et al., 2009). Calibration of the transient model consisted of altering the values for specific storage and specific yield as well as adjusting the precipitation-to-recharge function until a best fit to observed discharge at Barton Springs and water table elevations for the three observation wells were met (Winterle et al., 2009).

The algorithm from Painter and others (2007) for calculating recharge from precipitation assumed that an initial threshold of monthly precipitation must be exceeded before any recharge can occur. After this threshold is met, recharge will occur in either linear or exponential proportion to the amount of precipitation until a precipitation limit is met and any additional precipitation will leave the area as runoff and the recharge rate will remain constant. Precipitation data were provided by the City of Austin as average monthly values for the contributing and recharge zones and did not consider the values on a watershed basis. Volumetric distribution of recharge was based on the same

assumptions in Scanlon and others (2001) where 85% of recharge occurs within six losing streams and the remaining 15% is from diffuse recharge. Spatial distribution of recharge within this model varies from that found in Scanlon and others (2001) by incorporating zones of focused recharge meant to represent highly permeable faults or fracture zones (Figure 14). Instead of uniformly distributing recharge from losing streams throughout each stream reach, clusters of cells along each individual stream recharge a proportion of the total recharge for that stream.

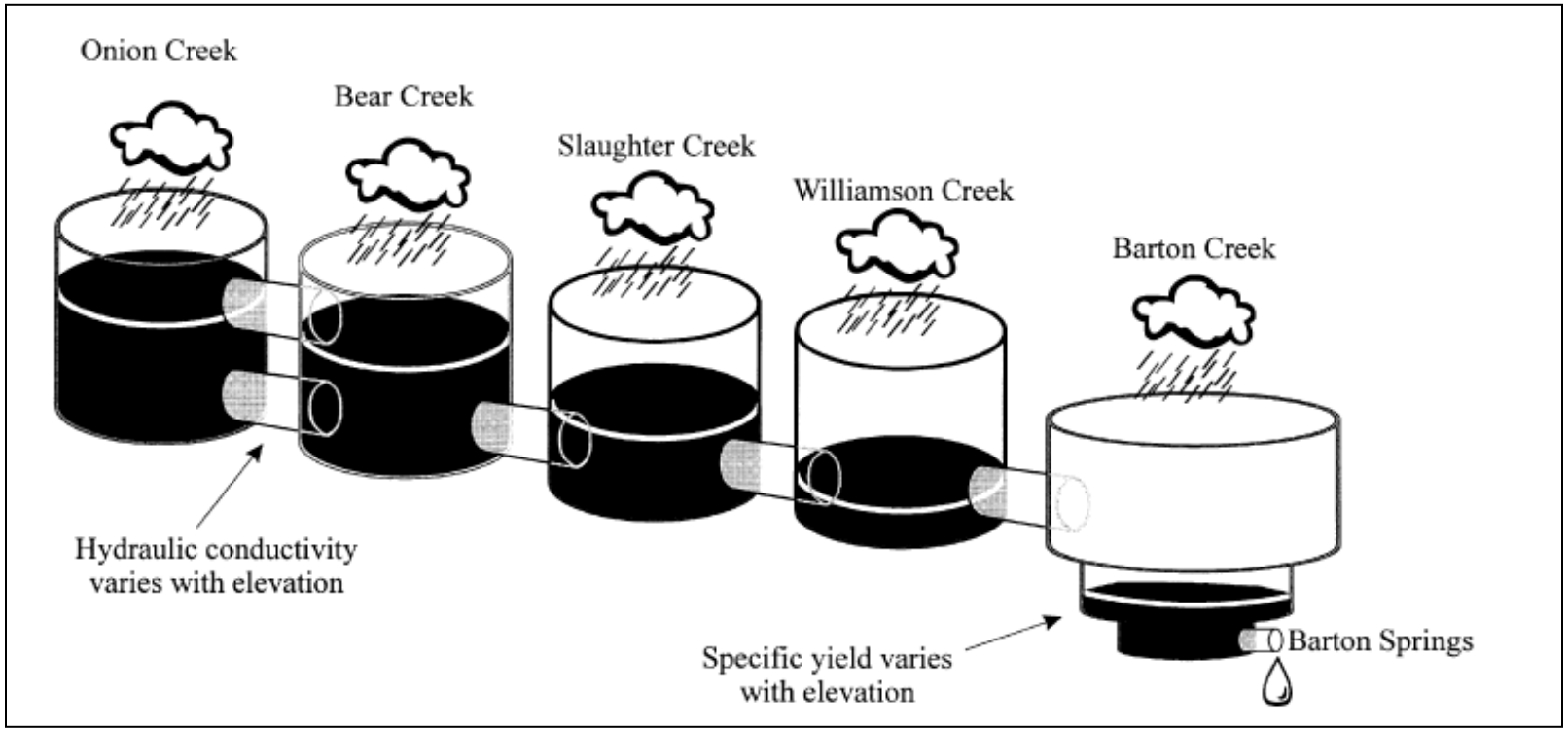

Figure 10: Schematic diagram of the aquifer model developed by Barrett and Charbeneau (1997).

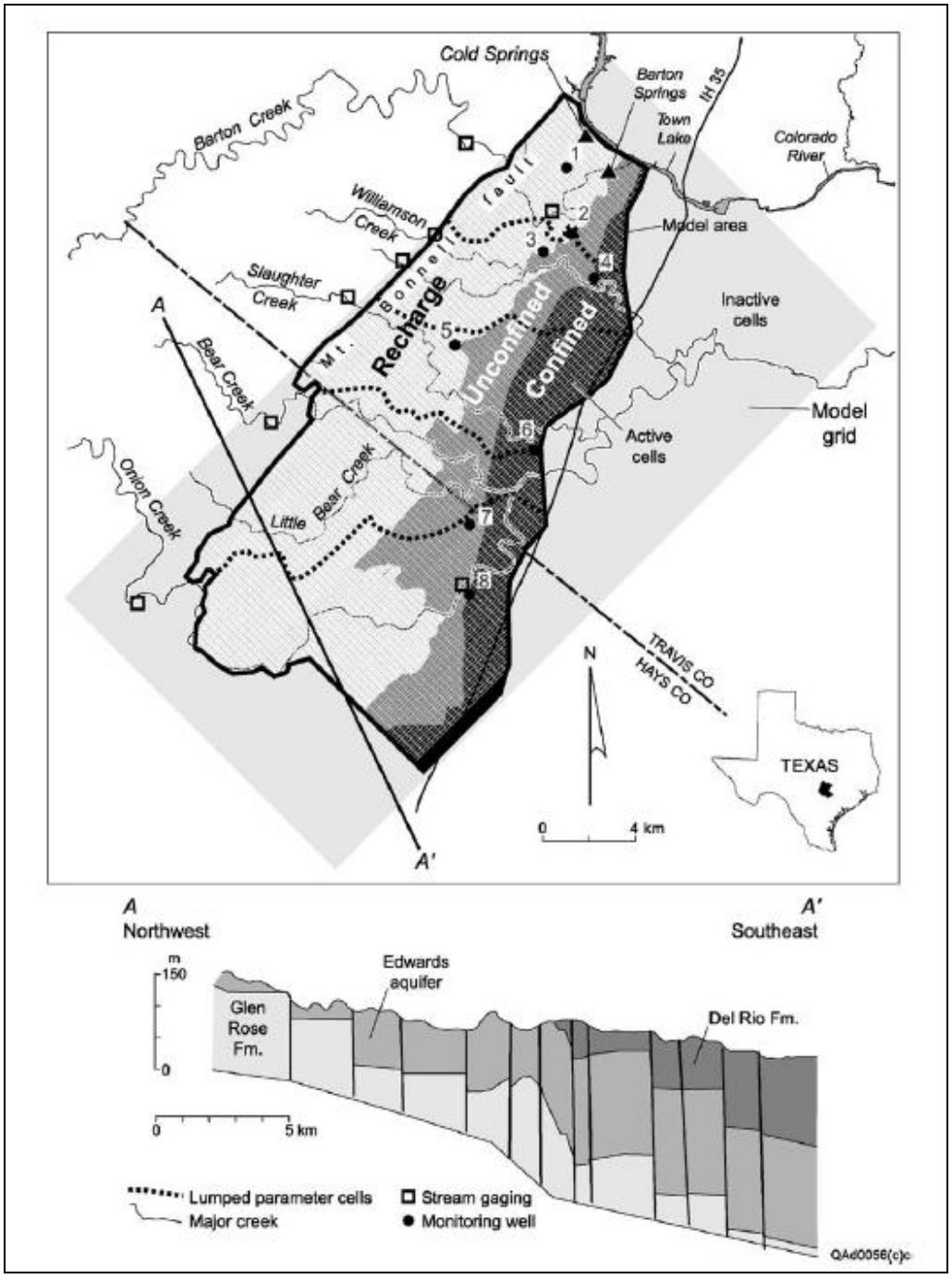

Figure 11: Location of the study area, including cells for the lumped parameter model, stream gauging stations, and long-term monitoring wells (from Scanlon et al., 2003). Recharge, unconfined, and confined zones are also shown. The unconfined zone is overlain by the Del Rio Formation, which precludes recharge from the surface in this zone.

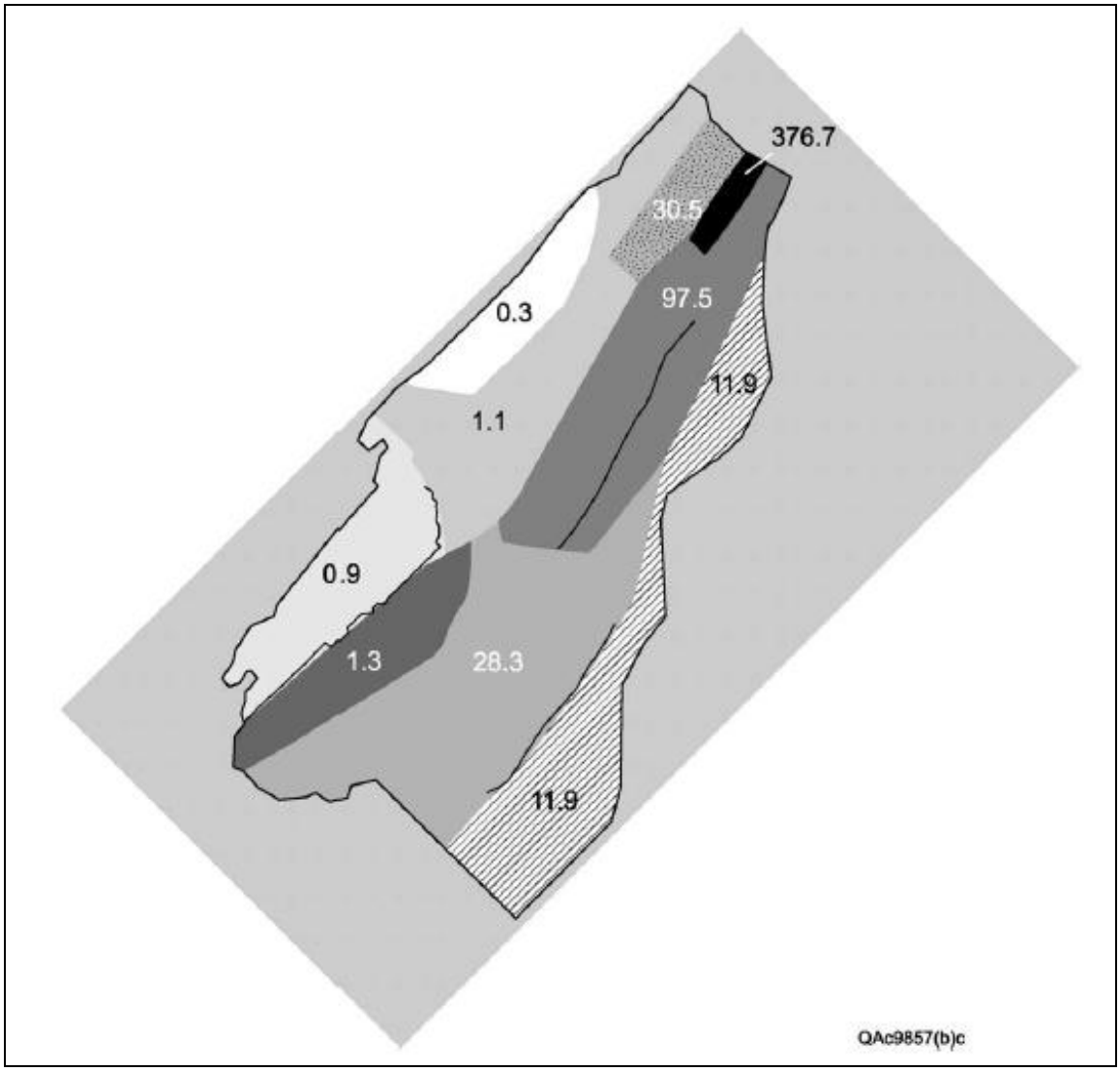

Figure 12: Hydraulic conductivity (m/d) resulting from calibration of the steady state model (from Scanlon and others, 2003). The faults shown on this map were simulated as horizontal flow barriers.

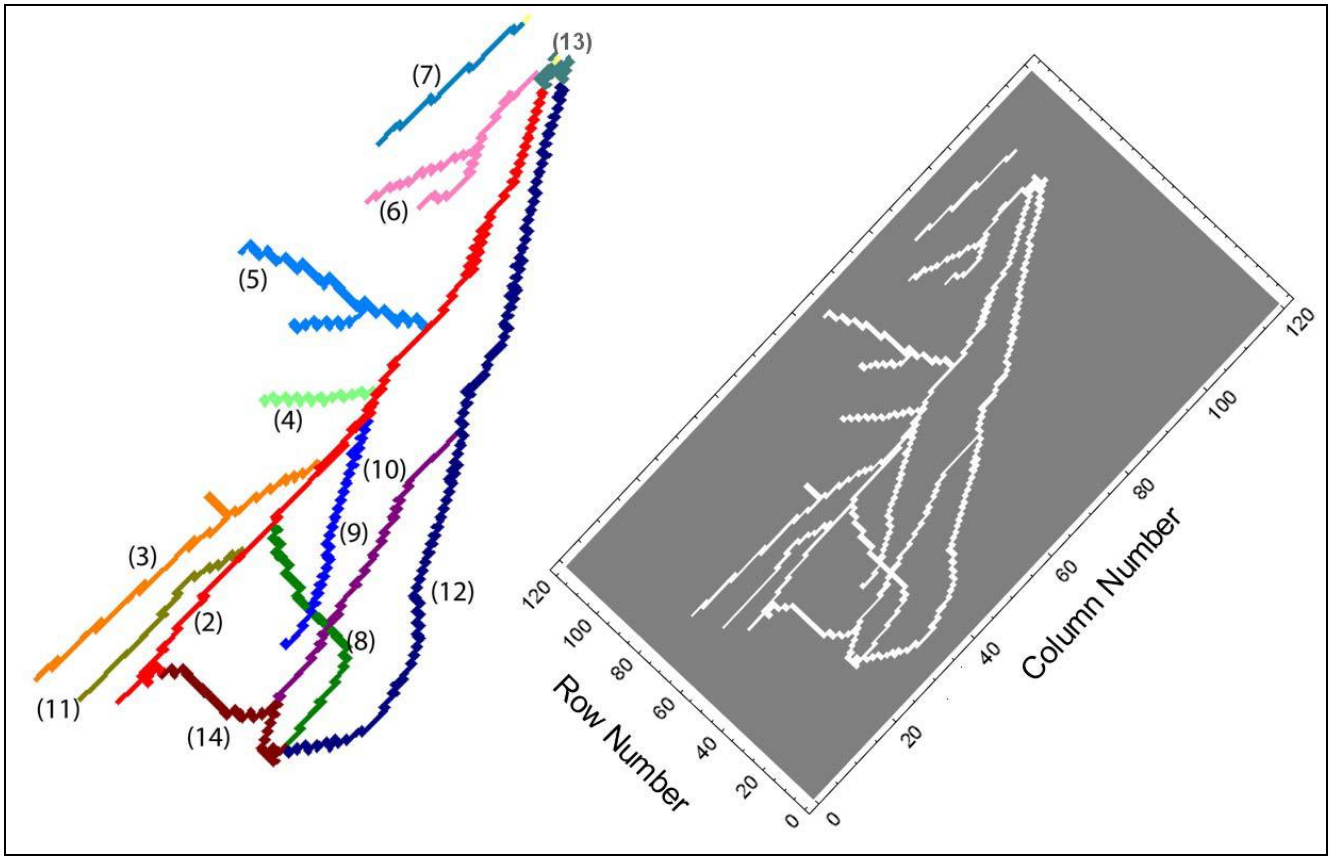

Figure 13: Conduit designations (left) and locations within the model domain (right) (from Winterle et al., 2009). Rows and columns designate model cells with dimensions 500 feet wide by 100 feet long. Cells in grey shaded area are treated as inactive.

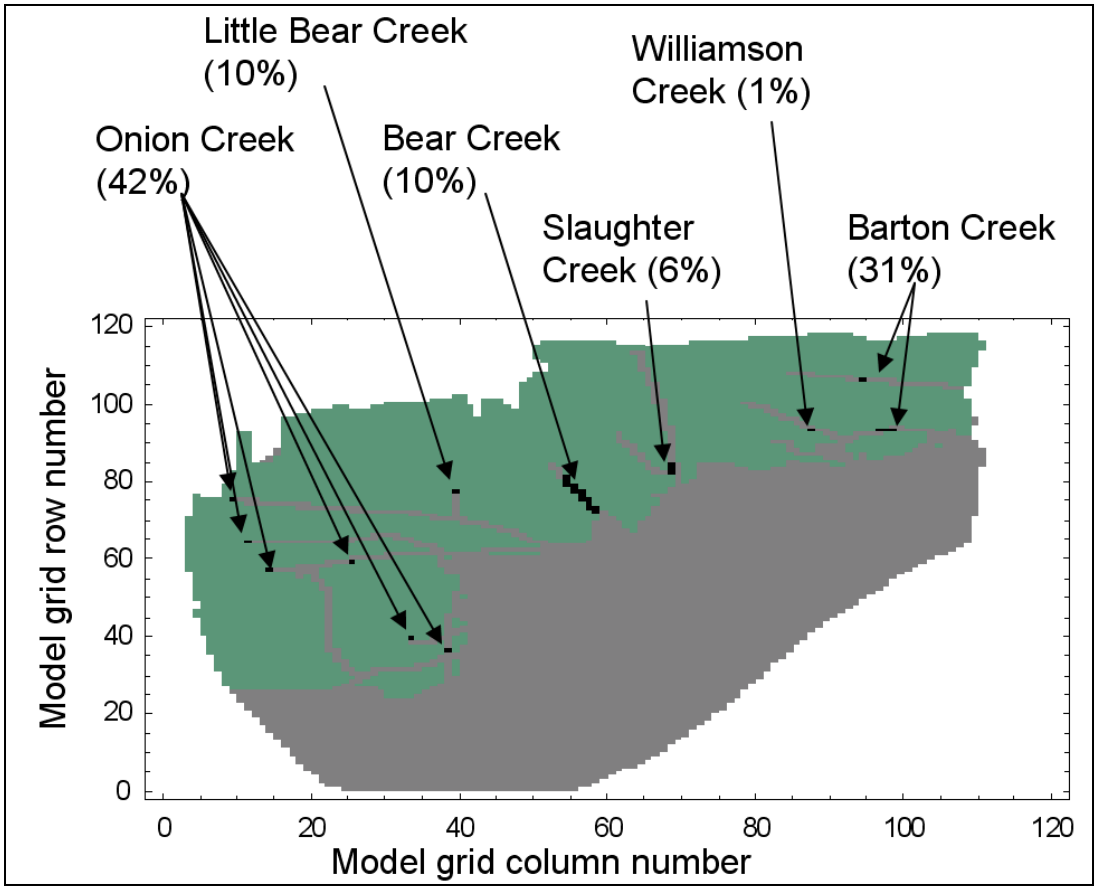

Figure 14: Focused recharge locations (from Winterle et al., 2009). Percentages indicate approximate fraction of focused recharge (85% of total recharge) apportioned to each recharge feature. For features with more than one recharge cell location, the amount of recharge to the feature is evenly divided among the cells. Diffuse recharge is assumed to be 15% of total recharge and is evenly distributed across the green-shaded cells.

CHAPTER 4:

METHODOLOGY

Recharge Calculations

OBJECTIVE

The objective of the methods described in this section is to quantify volumes of various recharge sources from January, 1999, to December, 2009 to modify input for the BS GAM (Scanlon et al., 2001). The BS GAM consists of 7, 038 cells (Figure 15) that correspond to zones within a MODFLOW-96 numerical groundwater flow model. Recharge volumes are quantified on a monthly temporal scale and distributed spatially throughout the BS GAM on a cell by cell basis utilizing ArcGIS 9.3.

DIFFUSE RECHARGE

Diffuse recharge is the precipitation that directly infiltrates into the subsurface and recharges the underlying groundwater system. Majority of this recharge occurs on pervious surfaces where urbanization has not lowered the overall surficial hydraulic conductivity. However, the secondary permeability of paved surfaces allows for contributions to diffuse recharge from impervious areas (Wiles and Sharp, 2008; Wiles, 2007) and should be considered when quantifying the diffuse recharge for an urbanized area (Lerner, 2002). In addition, some such surfaces are now being designed with a significant primary porosity and permeability. See Klenzendorf and other (in press) for a review. Diffuse recharge was previously quantified for the BS GAM by assuming it was equal to 15% of the total recharge from five losing streams intersecting the recharge zone and was distributed equally to all active cells within the model (Scanlon et al., 2001).

Calculating Diffuse Recharge

Diffuse recharge was quantified utilizing multiple land use and precipitation shapefiles within ArcGIS. It is understood that land use has a strong influence on the amount of diffuse recharge that can occur so that the influence of impervious and pervious cover need to be considered for the recharge component of the BS GAM. For this study, diffuse recharge is quantified by:

$$DR = P \times A_{LU} \times IF \qquad \textbf{(2)}$$

where,

DR: diffuse recharge for a given BS GAM cell for a given month and year [L^3]

P: precipitation height for a given BS GAM cell for a given month and year [L]

A_{LU}: area of either impervious or pervious cover for that cell for a given year [L^2]

IF: infiltration factor based on land use type [unit-less]

P and A_{LU} values were determined from methods discussed below. *IF* values were previously determined by Wiles (2007) and Hauwert (2009) who estimated diffuse recharge for the Austin area for impervious and pervious land use types. For impervious cover, Wiles (2007) estimated that 21% of annual rainfall that falls on paved surfaces results in diffuse recharge in the Waller Creek watershed of Austin, TX. In regards to pervious cover, Hauwert (2009) calculated that 32% of annual rainfall that fell on the

Flintridge and Headquarters Flat catchments over the Edwards Aquifer recharge zone on pervious land became diffuse recharge. These are closed basins within the highlands portion of the recharge zone. This infiltration factor may not directly apply to the majority of the BS GAM, but is the only directly-measured estimate available.

Land Use Files

ArcGIS Processing

Land use shapefiles for 1990, 1995, 2000, 2003, 2006, and 2008 were obtained from the City of Austin (COA) online GIS database (City of Austin, 2010). Each shapefile, which covers the Austin area, consists of polygons that outline areas of different land use. Each polygon has an associated land use code. COA shapefiles are available in the desired spatial reference (NAD 1983 State Plane Texas Central FIPS 4203 Feet). Consequently, they were not re-projected like some other data sets discussed below. The first step was to isolate the portions of the land use surveys that are within the BS GAM. This was achieved with the ArcGIS *Clip* tool, using the BS GAM shapefile as the clipping region to produce smaller land use survey shapefiles having areas that precisely correspond to the BS GAM. The remaining steps below describe how land use types were transferred from the surveys to each MODFLOW cell, and how areas for each land use type within each cell were calculated.

Transfer of land use types to MODFLOW cells was done with the *Identity* tool, which, for each survey, created a new land use survey shapefile that contained land use polygons that now conformed to BS GAM cell boundaries; this in essence, dissected land use polygons so that they could no longer span BS GAM cell boundaries. In the process,

each new land use polygon was given an identification code (known as a HydroID) that corresponded to the BS GAM cell in which it resided.

Some BS GAM cells contained multiple polygons with the same land use code after the *Identity* tool was utilized. In order to combine these like polygons and quantify their total areas for each BS GAM cell, the *Dissolve* tool was employed. This function essentially aggregates polygons of similar land use codes and HydroID's into one polygon attribute table record, for which a single area can be calculated. By "dissolving" polygons with the same HydroID and land use code, the total area of each land use code for each BS GAM cell could eventually be computed.

After the "dissolve" was performed, total areas for each land use code in each BS GAM cell was determined by first creating a *Total_Area*, field in the land use survey attribute tables and then using the *Calculate Geometry* function. After creating a new field to store the value (i.e. *Impervious_Area*), the area of impervious cover in each BS GAM cell was then determined with the *Field Calculator* using Equation 2:

$$IA = TA \times ICP \qquad \textbf{(3)}$$

where,

TA: total area for a land use code in a BS GAM cell [L^2]

ICP: impervious cover percentage (based on land use code) [unit-less] (Table 2)

IA: total impervious area for a land use code in a BS GAM cell [L^2]

Similarly, total pervious area was calculated using the *Field Calculator* and stored in a *Pervious_Area* field:

$$PA = TA - IA \qquad \textbf{(4)}$$

Where, PA is the total pervious area for a land use code in a BS GAM cell $[L^2]$.

At this point, each BS GAM cell, identified by a *HydroID*, contained several land use polygons, each with a calculated total area (TA), impervious area (IA) and pervious area (PA). In order to arrive at a total IA and PA for each cell, the *Dissolve* tool was used again, "dissolving" on the HydroID attribute while summing up the *Impervious_Area* and *Pervious_Area* fields. The total pervious area for each BS GAM cell for each year is used in later calculations and is labeled as TPA_{GC}.

ArcGIS Processing of Incomplete Surveys

The original shapefiles for the 1995, 2000, and 2008 land use surveys do not completely cover the BS GAM. In other words, there are areas within these surveys with missing data. Consequently, there are cells within the BS GAM that are completely or partially missing land use data for these years (Figure 16). To only select BS GAM cells that were not missing any land use data after the ArcGIS processing, a *Select by Attributes* function was used with the statement: *Total_Area > 490,000 ft*^{2}. This selects only BS GAM cells with total land use areas greater than 490,000 ft^2 (45, 522 m^2), which are cells that had been completely surveyed. After these cells had been selected, they were exported as new shapefiles.

Excel Processing

Once the ArcGIS processing for each land use survey was completed, each final shapefile was tied to the original BS GAM shapefile based on the HydroID attribute by employing the *Join* function. By performing this action, a master attribute table was created that included the impervious and pervious area of each BS GAM cell for each survey year. This was then exported as a dbase file and opened in Excel. This step ensured that all of the HydroID rows of each survey were lined up and prevented having to manually line them up in Excel. This was a necessary step since some of the land use surveys did not completely cover the BS GAM and consequently did not include all of the BS GAM cells.

In order to accommodate for years that were missing land use data, impervious and pervious areas computed from surveyed years were applied to those which were not. For example, for years 2000, 2001 and 2002, impervious and pervious areas determined from the land use survey of 2000 were assigned. As mentioned, some survey years did not completely cover the BS GAM and therefore were missing some BS GAM cells. For these cells, impervious and pervious areas from the most recent previous year were utilized. For example, for the land use survey of 2000, all missing BS GAM cells were assigned impervious and pervious areas determined from the land use survey of 1995. Values from 1990 would be used if 1995 was missing the same cells as 2000. Once this EXCEL processing was complete, each BS GAM cell had impervious and pervious areas assigned for each year from 1990 – 2010.

Precipitation Files

NEXRAD data sets were employed to more accurately distribute precipitation over the BS GAM both spatially and temporally. These data sets were obtained from the National Oceanographic and Atmospheric Administration (NOAAb, 2010; Shelton, personal communication). These data are point files for each month from 1995 to 2010 of NEXRAD gridded precipitation (4×4 km resolution) of the contiguous United States. These data sets were created using the HRAP projection system; therefore, they needed to be re-projected into the State Plane projection system discussed above. This was done by utilizing the *Project* tool and was performed on each shapefile for each month from January, 1999 to December, 2009. The objective for using NEXRAD shapefiles was to create raster surfaces of precipitation amounts over the BS GAM through interpolation techniques (Figure 17). These raster surfaces are based upon the point data within the NEXRAD shapefiles that represent precipitation amounts. In order to enhance the accuracy of the interpolation technique, point data over the BS GAM as well as all points within a ten kilometer buffer around the BS GAM were utilized. This was done to create a raster surface that is not limited by the BS GAM boundaries and considers the influence of precipitation outside of the BS GAM. In order to only use this portion of the NEXRAD shapefiles, they were selected by employing the *Clip* tool. The area of interest that the shapefiles were clipped upon was created by the *Buffer* tool.

The result of this processing was NEXRAD shapefiles that only include points within the BS GAM and within a 10 kilometer buffer of the BS GAM. Once these shapefiles had been created, *Kriging* was used to generate raster surfaces, which provided the average rainfall for each BS GAM cell for each month from January, 1999, to December, 2009. These values were obtained by utilizing the *Zonal Statistics as Table*

tool. The tables created from the zonal statistics analysis were exported as dbase files and then organized within Excel.

INDIRECT RECHARGE

Indirect recharge is the total water that recharges an aquifer from leaky utility lines, septic tanks, storm sewers, and storm water ponds. This study only considers the leakage from water distribution and wastewater lines. It has been demonstrated by Garcia-Fresca and Sharp (2005) that leakage from utility lines provides potential recharge to the BSEA, but quantification and distribution of indirect recharge through time remains. Garcia-Fresca (2004) determined leakage fluxes from the entire utility network for Austin during the year 2000 to demonstrate how this recharge source could be quantified. Calculating recharge from these leaky utility lines as well as determining its distribution in this research are based on the conceptual model of Garcia-Fresca (2004), but differ by quantifying BS GAM recharge and its distribution based on ArcGIS processes.

Calculating Leakage from Utility Lines

A simple and effective way to quantify leakage from water distribution networks is to assume a certain percentage of the water supplied is leakage (Lerner et al., 1990; Garcia-Fresca, 2004). The same concept can be applied to wastewater networks, but these leakage rates are typically assumed to be lower because these systems are not generally pressurized. From this conceptual model, leakage volumes from each system can be quantified by:

$$WL = W \times L_W \quad \textbf{(5)}$$

$$WWL = \frac{WW}{(1-L_{WW})} \times L_{WW} \quad \textbf{(6)}$$

Where,

WL: volume of leakage from the entire water distribution network for a given month and year [L^3]

W: volume of total water served for a given month and year [L^3]

L_W: average percentage of water lost from distribution network [unit-less]

WWL: volume of leakage from the entire wastewater network for a given month and year [L^3]

WW: volume of total water treated for a given month and year [L^3]

L_{WW}: average percentage of water lost from wastewater network [unit-less]

Values for *W* and *WW* were provided by Austin Water Utility (AWU), which has been responsible for calculating water loss from their distribution network, since October 2004, in compliance with Texas Water Development Board's (TWDB) water audit program. An average L_W value of 8.35% was utilized for this research and was determined from these reports and Garcia-Fresca (2004) (Table 3). AWU is not required to produce similar reports for the wastewater network. Consequently, a L_{WW} of 5% is used. This L_{WW} value was determined from personal communication between the author and authorities at AWU and is consistent with other reported leakage rates from other

wastewater networks, but is probably conservative (Garcia-Fresca and Sharp, 2005; Garcia-Fresca, 2004; Trow and Farley, 2004).

ArcGIS Processing

In order to quantify the proportion of the total indirect recharge within BS GAM boundaries as well as how it should be distributed for the model, various ArcGIS processes were employed. Indirect recharge from the utility networks is likely from point sources, but locating these points spatially and temporally is difficult. Although AWU does keep reports on where, when, and how much water is leaked for major bursts, it is not practical to process this data. Moreover, these data sets only include major bursts or leaks and do not include smaller leaks that are either not immediately detected or never found. This study assumes that the indirect recharge volumes from both the distribution and wastewater networks are distributed equally amongst their respective pipe networks. Indirect recharge volumes could then be calculated for different regions and times based on the total length of pipe throughout the Austin area for a given time interval. By knowing the total length of each pipe network within each BS GAM cell through time, total indirect recharge volumes on a cell by cell basis could be determined.

Water distribution and wastewater line shapefiles were obtained from the COA. These two files contained the fields *Date_Added* and *Installed,* indicating the date that each pipe segment was digitized and the date each pipe segment was physically installed, respectively. The *Installed* field was missing dates for almost all of the pipe segments, thus dates from the *Date_Added* field were assumed to be the date in which they were physically installed. The first step was to determine the total pipe length for each

network for each year. This was done by selecting all the pipes that existed by a given year within the attribute table and then using the *Statistics* tool for the field containing pipe length. This tool reports common statistical information including minimum, maximum, sum, mean, and standard deviation. Once the total pipe length for each network for each year was determined, a leakage rate based on pipe length and type could be calculated:

$$PLR_W = \frac{WL}{TPL_W} \qquad \textbf{(7)}$$

$$PLR_{WW} = \frac{WWL}{TPL_{WW}} \qquad \textbf{(8)}$$

Where,

PLR_W: pipe leakage rate for the water distribution network for a given month and year [L^2]

TPL_W: total pipe length for the entire distribution network for a given year [L]

PLR_{WW}: pipe leakage rate for the wastewater network for a given month and year [L^2]

TPL_{WW}: total pipe length for the entire wastewater network for a given year [L]

After calculating PLR_W and PLR_{WW} values, the length of each pipe network for each BS GAM cell for each year from 1999 to 2009 needed to be determined. This was

achieved by clipping the original pipe shapefiles to the BS GAM area by the process described previously. From these clipped files, all pipe segments in existence each year were selected and exported as individual shapefiles. For example, the 1999 water distribution shapefile includes all pipes for the distribution network that were installed by 1999 (those with *Data_Added* years 1997, 1998, and 1999). The *Identity* and *Dissolve* tools were then utilized, as previously described, in order to associate each pipe segment with a HydroID and then aggregate all common segments. Once this processing was complete, pipe lengths for each BS GAM cell for each had been determined (Figure 18). These new shapefiles were joined to the original BS GAM file by HydroID and exported to Excel as discussed previously. Finally, indirect recharge for each BS GAM cell was calculated by:

$$WL_C = CPL_W \times PLR_W \quad \textbf{(9)}$$

$$WWL_C = CPL_{WW} \times PLR_{WW} \quad \textbf{(10)}$$

$$IR = WL_C + WWL_C \quad \textbf{(11)}$$

Where,

WL_C: water distribution leakage for a BS GAM cell for a given month and year [L^3]

CPL_W: water distribution pipe length for a BS GAM cell for a given year [L]

WWL_C: leakage from the wastewater network for a given month and year [L^3]

CPL_{WW}: wastewater pipe length for a given year [L]

IR: total indirect recharge for a given month and year [L^3]

ARTIFICIAL RECHARGE

Artificial recharge is the water applied to the subsurface from irrigation return flow (IRF) and/or structures built to enhance recharge. IRF is the only source of artificial recharge considered for this study.

Calculating Irrigation Return Flow

IRF is the water directly applied to parks and lawns not lost to evapotranspiration (ET), runoff, or interflow that recharges groundwater. The methods for quantifying IRF were modified from those established in Garcia-Fresca (2004). Two major components of the urban water budget are the volume of potable water distributed and the amount of wastewater treated. The difference between the two is considered to be the total urban water available for recharge or excess urban water:

$$EUW = W - WW \qquad \textbf{(12)}$$

Where, EUW is urban water [L^3]. As mentioned above, monthly values for W and WW were provided by AWU. The two major pathways that explain the difference between the volumes of water served and treated are leakage from utility lines and irrigation. Water is lost from the utility line network when either pipe system leaks. The methods for quantifying these monthly leakage volumes were discussed previously (Equations 5 & 6). Water is also lost from the utility line network when the served water is utilized for irrigation so monthly irrigation volumes can be quantified by:

$$I = EUW - WL - WWL \qquad \textbf{(13)}$$

Where, I is the irrigation applied for a given month and year [L^3]. A portion I is lost to ET, runoff, and interflow while the remaining water becomes IRF. In order to determine the volume of IRF, it was assumed that runoff and interflow are negligible; therefore, ET was assumed to be the only pathway for water besides as IRF. In order to quantify ET rates, a standard ET rate (ET_0) is used since different plants have different water requirements and thus different ET rates. The ET_0 values utilized are PET rates for a cool season grass, 4-inches tall, in a deep soil, and under well watered conditions (Garcia-Fresca, 2004; TexasET, 2010). With these assumptions in mind, standard plant water requirement values can be determined:

$$PWR = ET_0 \times T_c \times Q_f \qquad \textbf{(14)}$$

Where,

PWR: plant water requirement for a given month and year [L]

ET_0: average standard potential evapotranspiration for a given month of the year [L]

T_c: turf coefficient [unit-less]

Q_f: stress coefficient [unit-less]

Average ET_0 rates for the Austin area were obtained from TexasET (2010) (Table 4). The turf coefficient is defined as the water requirement of specific crops and/or turf grasses as a fraction of the PET. This value varies depending on plant type. The turf value used in this research was for a warm season grass with a T_c value of 0.6 (TexasET, 2010). Park and lawn irrigation rarely account for full plant requirements needed to maintain a healthy and attractive turf. These requirements are often not met in order to avoid maximum production of grass clippings and to conserve water and money. Therefore, a stress coefficient is applied to reduce the *PWR*. The Q_f values were assigned based on corresponding Palmer Drought Indices (PDI) (Table 5). The PDI data was obtained from NOAA's online drought monitoring center (NOAAa, 2010). NOAA creates a map each week of the contiguous United States displaying the PDI values for each climate division (Figure 19). These maps were utilized to generate tabular data and were then averaged to determine the mean PDI and corresponding Q_f values for each month from January, 1999, to December, 2009.

It is important to note that the *PWR* is satisfied by both precipitation and irrigation. The relative contribution of these two sources to ET is difficult to discern, and it can be assumed that both contribute. ET is an unbiased "consumer" of water, so that all water applied to a surface is available for consumption and is called the surface water application:

$$SWA = P + I^* \quad \textbf{(15)}$$

Where,

SWA: surface water application for a BS GAM cell for a given month and year [L]

*I**: irrigation height for a BS GAM cell for a given month and year [L]

SWA values were calculated for BS GAM cells. Therefore, *P* values determined for BS GAM cells by methods discussed above were utilized. It was assumed that irrigation is only applied to pervious surfaces within Austin's water service area (WSA) (Figure 20) and is equally distributed. Consequently, *I** is the same for all BS GAM cells within the WSA boundary.

In order to calculate *I** values, various processes within ArcGIS were employed. The proportion of the *SWA* that is irrigation can be determined for each BS GAM cell by:

$$SWAi = \frac{I^*}{SWA} \quad \textbf{(16)}$$

Where, *SWAi* is the proportion of the *SWA* that is irrigation for a given BS GAM cell for a given month and year [unit-less]. It can be assumed that irrigation and precipitation contribute to ET in the same proportions as they were applied to a surface and the proportion of the *PWR* that is satisfied by irrigation can be determined by:

$$PWRi = PWR \times SWAi \qquad \textbf{(17)}$$

Where, *PWRi* is the plant water requirement satisfied by irrigation for a given BS GAM cell for a given month and year [L]. By knowing the amount of irrigation applied and the amount of irrigation lost for any BS GAM cell, *IRF** can be calculated:

$$IRF^* = I^* - PWRi \qquad \textbf{(18)}$$

Where, *IRF** is the irrigation return flow for a given month and year [L]

ArcGIS Processing

Although *IRF** values can be quantified, the distribution of this recharge cannot be easily determinable. It was assumed that irrigation was applied equally to all pervious areas throughout Austin's WSA. Through the methods discussed above and those of this section, the "height" of irrigation applied (*I**) throughout Austin's WSA can be determined. Additionally, by previously quantifying the total pervious area for each BS GAM cell (TPA_{GC}), a total IRF volume can be calculated and distributed throughout the BS GAM.

Converting from an irrigation volume (I) to an irrigation height (I^*) is a necessary step towards calculating and distributing IRF volumes. In the previous section, it was discussed how to calculate the total irrigation volume utilized by clients connected to Austin's water distribution network (I). In order to distribute this volume equally and determine a uniform irrigation height (I^*) throughout Austin's WSA, the total pervious area within the entire WSA was calculated for each year from 1999 and 2009. By dividing the total irrigation by the total pervious area within Austin's WSA, I^* could be calculated by:

$$I^* = \frac{I}{TPA_{WSA}} \qquad \textbf{(19)}$$

Where, TPA_{WSA} is the total pervious area within Austin's WSA for a given year [L^2]. TPA_{WSA} values were calculated utilizing the same land use surveys discussed previously as well as WSA shapefiles provided by AWU. Because the WSA shapefile was only available for the year 2007, it was also assumed for unrepresented years between 1999 and 2009. The first step was to clip the original land use shapefiles by the WSA shapefiles in order to isolate our region of interest. After these files were clipped, they were dissolved based upon land use code with all polygons with the same land use code were aggregated into one polygon. The TPA_{WSA} for each dissolved land use survey was then determined by the same methods employed to calculate the pervious area of each BS GAM cell.

After I^* values were calculated, monthly IRF* values for each BS GAM cell could be determined (Equation 18). TPA_{GC} values had been determined from previous ArcGIS processing but not all of the BS GAM cells are within the WSA boundaries. Therefore, it had to be determined which BS GAM cells are within the WSA boundaries for each year (Figure 20). This was done by utilizing the *Select Layer by Location* tool. Once the desired BS GAM cells were selected, their HydroID values were exported to Excel. Only BS GAM cells within the WSA boundary were used in the Excel calculations. Finally, artificial recharge or IRF volumes for each of these cells could be quantified by:

$$AR = IRF = IRF^* \times TPA_{GC} \qquad \textbf{(20)}$$

Where,

AR: artificial recharge for a BS GAM cell for a given month and year [L^3]

IRF: volume of irrigation return flow for a BS GAM cell for a given month and year [L^3]

TPA_{GC}: total pervious area for a BS GAM cell for a given year [L^2]

STREAM RECHARGE

The majority of recharge to the BSEA is attributed to six major losing streams that flow over the recharge zone (Figure 5) (Slade et al., 1986; Barrett and Charbeneau, 1996; Hauwert et al., in press). Numerous flow loss surveys and dye trace tests have

been performed for each of these studies partly to determine what percentage of Barton Springs discharge is contributed by each of these six streams (Table 6). Total recharge for modeling this system has been traditionally calibrated to springflow (Scanlon et al., 2001; Lindgren et al., 2009) assuming springflow from Barton Springs accounts for the majority of all discharge. Cold Springs discharge has been estimated to range 3 – 28% of that at Barton Springs at different times but is not gauged because it is flooded by Town Lake. For this study, monthly recharge from each losing stream is determined as a function of stream discharge.

Calculating Recharge from Losing Streams

Previously, recharge inputs for the BS GAM were determined from discharge data from USGS gauging stations coupled with recharge thresholds (Scanlon et al., 2003). There have been several studies (Slade et al., 1986; Barrett and Charbeneau, 1996; Hauwert et al., in press; Hauwert, 2009) that estimated these recharge thresholds for each of the six losing streams contributing recharge to the BSEA (Table 7). These threshold values identify the rate of recharge as a function of stream discharge. When discharge in the stream is below the recharge threshold, all of the stream's discharge is lost to the subsurface as recharge. When discharge exceeds the recharge threshold, recharge is equal to the recharge threshold.

$$\begin{aligned} &For\ Q_S < RT \qquad R_S = Q_S \\ &For\ Q_S > RT \qquad R_S = RT \end{aligned} \qquad \textbf{(21)}$$

Where,

Q_S: stream discharge [L^3]

R_S: stream recharge [L^3]

RT: recharge threshold [L^3]

Previously, recharge from Bear, Slaughter, and Williamson Creek was determined by the relationship described in Equation 21. Recharge for Onion Creek was calculated by subtracting average daily discharge downstream from that upstream of the recharge zone (Scanlon et al., 2001; Smith and Hunt, 2004). Barton Creek recharge was determined by methods described in Barrett and Charbeneau (1997). Recharge from Little Bear Creek was accounted for by setting it equal to Bear Creek recharge.

For this study, recharge for Barton, Onion, Slaughter and Williamson Creek was determined by subtracting average daily discharge downstream from that upstream of the recharge zone. Barton Creek had three USGS monitoring station rather than two like the other streams. Therefore, recharge is calculated from these three stations. Recharge for Bear creek was calculated utilizing Equation 21 (below) as no downstream monitoring station existed. Discharge data was obtained online from the USGS as daily averages for all of the streams excluding Little Bear Creek. Since Little Bear Creek does not have a stream gauge, recharge for this stream was calculated as a proportion of Barton Springs discharge (Table 6). R_S values were calculated on a daily temporal scale but were then summed for each month. The monitoring stations are located at or slightly upstream of where the streams intersect the recharge zone (Figure 21). Thus, surface runoff within the recharge zone during storm events is not estimated. These recharge calculations underestimate total recharge and are truly only representative of recharge from the contributing zone. It is important to note that these recharge calculations are only

underestimated during storm events so that they are representative of the total recharge taking place for the majority of the time.

Flow-loss Surveys

For the current version of the BS GAM, recharge is equally distributed in each stream where it intersects the recharge zone. This accounts for 85% of the total recharge to the BSEA with the remaining 15% assigned to diffuse recharge from precipitation (Scanlon et al., 2003). This uniform distribution of recharge is unrepresentative of the discrete recharge points found within this system (Zahm, 1998) as well as karstic aquifers in general. Flow loss surveys from Hauwert et al. (in press) were utilized to incorporate more realistic spatial distributions.

Numerous flow loss surveys for each of the six losing streams have been conducted by the USGS, the COA, and the BSEACD since 1980. The most recent surveys were conducted by Hauwert et al. (in press) and have been combined with past studies to generate a summary of flow-loss surveys (Figures 22 – 27). These combined surveys were utilized to designate segments within each stream where recharge occurred and assign an average contributing percentage to the total recharge for each stream (Table 8). The stream gauging points which delineated the recharge segments consisted of stream-road intersections, recharge features like swallets and caves, permanent gauging stations, and arbitrary distances downstream from an identifiable feature.

ArcGIS Processing

The shapefiles utilized to distribute recharge volumes from the losing streams were obtained from the COA (City of Austin, 2010). The original shapefiles consisted of

a line shapefile of all the creeks and streams in the Austin area as well as a polygon shapefile of the recharge zone for the BSEA. These files did not need to be re-projected, so the first step was to clip the streams file to our region of interest, the recharge zone for the BSEA. This is the only region where the streams can contribute to the overall recharge of the BSEA. Thus, this portion of the streams is where the recharge calculations will be distributed. After the original stream shapefile had been clipped, only the six major losing streams were selected and exported as a new shapefile. With the six losing streams isolated from the rest of the streams, the next step was to determine the total stream length for every BS GAM cell containing a stream. This was done utilizing the *Identify* and *Dissolve* tools.

In order to distribute the total recharge from each stream, stream reaches needed to be associated with recharge segments. The recharge segments were identified and digitized within ArcGIS by creating a new point shapefile (Figure 21). Each stream gauging point utilized to delineate the recharge segments were digitized based on flow-loss surveys within Hauwert et al. (in press) (Figures 22 – 27). After these points were digitized, sections of streams and their corresponding BS GAM cells could be associated with recharge segments. It is important to note that portions of Onion and Bear Creek that intersected the recharge zone of the BSEA were outside of the BS GAM (Figure 21). These were not assigned to a BS GAM cell during the previous ArcGIS processing and were manually assigned to the nearest BS GAM cells and recharge segments. After this processing was complete, each recharge segment had been associated with a collection of BS GAM cells each with known stream lengths. Total monthly recharge for each recharge segment was then quantified by:

$$R_{RS} = R_S \times CF_{RS} \qquad \textbf{(22)}$$

Where,

R_{RS}: total recharge for a recharge segment for a given month and year [L^3]

CF_{RS}: contributing factor for a given recharge segment (Table 8) [unit-less]

R_{RS} volumes were then distributed in each recharge segment based on the total length of stream for each BS GAM cell within the recharge segment:

$$NR = \frac{R_{RS}}{SL_{RS}} \times SL_{GC} \qquad \textbf{(23)}$$

Where,

NR: natural recharge for a BS GAM cell for a given month and year [L^3]

SL_{RS}: total stream length for a given recharge segment [L]

SL_{GC}: total stream length for a given BS GAM cell [L]

TOTAL RECHARGE

Total recharge for a BS GAM cell has been defined as the summation of diffuse recharge (*DR*), indirect recharge (*IR*), artificial recharge (*AR*), and stream recharge (*SR*) for a given month and year:

$$TR = DR + IR + AR + SR \qquad \textbf{(24)}$$

Where, *TR*: total recharge for a BS GAM cell for a given month and year [L^3]. *TR* values were organized in Excel and exported as a text file and eventually imported into the BS GAM as a new recharge file.

Table 2: Summary of City of Austin land use codes and corresponding mean impervious cover percentages.

Land Use Code	Description	Mean Impervious Cover (%)
50, 100	Single Family	16.11
113	Mobile Home	10.87
120	High Density Residential (<1/2 ac)	29.62
130	Medium Density Residential (<2 ac)	12.55
140	Low Density Residential (<10 ac)	6.16
150	Duplex	31.23
160	Large Lot Single Family (>10 ac)	2.98
200	Multi-Family	53.89
210	Three/Fourplex	44.66
220	Apartment/Condominiums	61.29
230	Group Quarters	53.46
240	Nursing Home	56.16
300	Commercial	69.16
400	Office	59.27
500	Industrial	54.25
510	Manufacturing	61.22
520	Warehouses (Excluding Ministorages)	60.59
530	Heavy Equipment Sales, Service & Repair	40.92
560	Mining	4.39
570	Landfill/Salvage	9.46
600	Civic	36.5
610	Semi-institutional Housing	28.55
620	Hospitals	52.88
630	Government Services	41.52
640	Education	31.74
650	Meeting & Assembly	52.41
670	Cemetery	9.04
680	Cultural Facilities	39.37
700	open space / parks	4.49
710	Parks & Recreation	9.31
720	Golf Course	3.24
750	Open Space (Protected)	0.92
800	Transportation Infrastructure	37.5
810	Railroad Facilities	5.11
820	Transportation Terminal	70.43
830	Aviation Facilities	17.8
840	Marina	12.99
850	Parking Lot/Vehicle Storage	71.97
860	Streets & Roads	46.7
870	Utilities	13.13
900	Undeveloped	2.76
910	Agriculture	0.82
999	Unknown	31.24

Table 3: Summary of L_W values from varying sources and time periods.

Year	Source	L_W (%)
2000	Garcia-Fresca (2004)	7.70
2004	AWU	9.30
2006	AWU	7.68
2007	AWU	8.50
2008	AWU	8.58
		Mean: 8.35

Table 4: Average monthly ET_0 values for Austin, TX (TexasET, 2011).

Month	**Mean ET_0 (in/month)**	**Mean ET_0 (m/month)**
Jan	2.27	0.058
Feb	2.72	0.069
Mar	4.34	0.110
Apr	5.27	0.134
May	6.39	0.162
Jun	7.15	0.182
Jul	7.22	0.183
Aug	7.25	0.184
Sep	5.57	0.141
Oct	4.38	0.111
Nov	2.74	0.070
Dec	2.21	0.056
Annual	57.51	1.461

Table 5: Plant stress levels and corresponding stress coefficients and Palmer Drought Indices.

Plant Stress Level	**Stress Coefficient (Q_f)**	**Palmer Drought Indices**
No Stress	1	> 4
Low Stress	0.8	2 – 3.9
Normal Stress	0.6	-1.9 – 1.9
High Stress	0.5	-2 – -3.9
Very High Stress	0.4	< -4

Table 6: Proportions of Barton Springs discharge that is contributed by various sources.

Stream	Slade et al. (1986)	Barrett and Charbeneau (1996)	Hauwert et al. (in press)
Barton Creek Upstream of Highway 360	0.24	0.26	0.00
Barton Creek Downstream of Highway 360	-	-	< 0.12
Bear Creek	0.09	0.06	0.07
Little Bear Creek	0.09	0.06	0.04
Onion Creek	0.29	0.39	0.38
Slaughter Creek	0.10	0.05	0.08
Williamson Creek	0.05	0.03	0.01
Intervening Areas	0.15	0.15	< 0.36

Table 7: Summary of recharge thresholds for each stream (from Hauwert et al., in press).

Stream	**Recharge Threshold (m^3/s)**
Barton Creek – Upstream of Loop 360	1.42
Barton Creek – Downstream of Loop 360	1.13
Bear Creek	0.99
Little Bear Creek	0.85 (Slade et al., 1986)
Onion Creek	3.40
Slaughter Creek	2.40
Williamson Creek	0.57

Table 8: Summary of different recharge segments and their respective contributions to the total recharge of each stream. Values and location of recharge segments are based upon Hauwert et al., (in press) (see Figure 21 for locations).

Stream	Recharge Segment	Contribution to Stream Recharge (%)
Barton Creek	Recharge Swallet – Tucker Sink	29.58
Barton Creek	Tucker Sink – Twin Falls	8.57
Barton Creek	Twin Falls – Jones Sink	11.90
Barton Creek	Jones Sink – Loop 360	14.49
Barton Creek	Loop 360 - Barton Lodge Tributary	15.69
Barton Creek	Barton Lodge Tributary - Gus Fruh	9.29
Barton Creek	Gus Fruh - Skunk Hollow Tributary	7.30
Barton Creek	Skunk Hollow Tributary - Campbells Hole	3.18
Bear Creek	Spillar LWX - 20,000 ft Dnst from USGS 1826 Flow Station	12.74
Bear Creek	20,000 ft - 25,000 ft Dnst from USGS 1826 Flow Station	30.71
Bear Creek	25,000 ft - 30,000 ft Dnst from USGS 1826 Flow Station	12.62
Bear Creek	30,000 ft - 35,000 ft Dnst from USGS 1826 Flow Station	23.38
Bear Creek	35,000 ft - 40,000 ft Dnst from USGS 1826 Flow Station	20.55
Little Bear Creek	FM 967 - 15,600 ft Dnst from FM 967	77.71
Little Bear Creek	15,600 ft Dnst from FM 967 – Stoneledge WQPL Flow Station	20.29
Little Bear Creek	Stoneledge WQPL Flow Station - 28,400 ft Dnst from FM 967	2.00
Onion Creek	USGS Flow Station 08158700 – Walnut Bend Swallet	11.92
Onion Creek	Walnut Bend Swallet – Crippled Crawfish Swallet	25.16
Onion Creek	Crippled Crawfish Swallet – Ruby Ranch Rd	24.00
Onion Creek	Ruby Ranch Rd – Antioch Cave	19.81
Onion Creek	Antioch Cave – Edge of Recharge Zone	19.10
Slaughter Creek	FM 1826 – Escarpment Blvd	35.94
Slaughter Creek	Escarpment Blvd - Mopac	11.28
Slaughter Creek	Mopac – Wyldwood Dr	24.87
Slaughter Creek	Wyldwood Dr – Brodie Ln	6.23
Slaughter Creek	Brodie Ln – Manchaca Rd	21.68
Williamson Creek	Highway 290 – Brush Country Rd	51.78
Williamson Creek	Brush Country Rd - Mopac	22.21
Williamson Creek	Mopac – Brodie Ln	7.80
Williamson Creek	Brodie Ln – Westgate Blvd	18.21

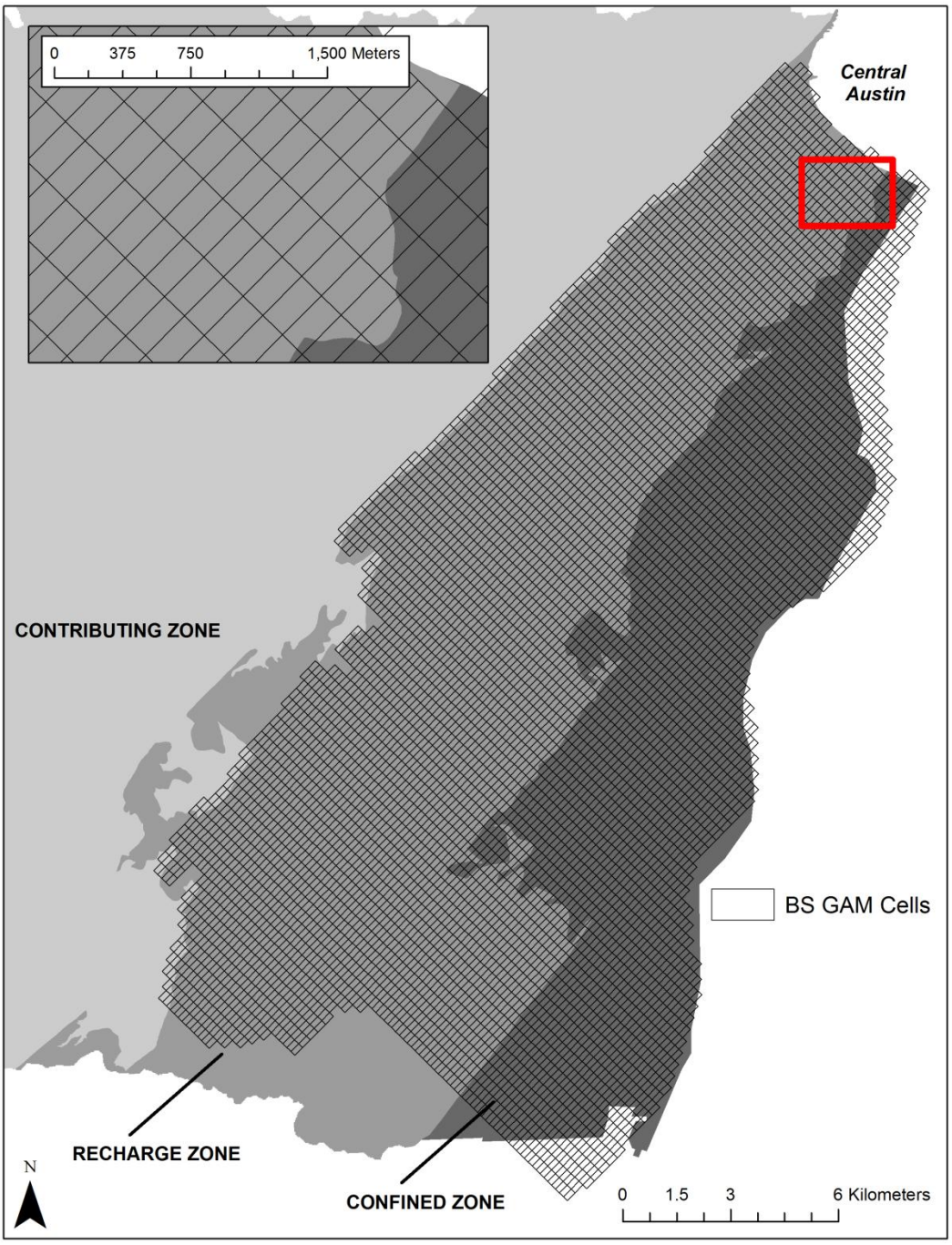

Figure 15: Site map for the Barton Springs Groundwater Availability Model (BS GAM) (Scanlon et al., 2001).

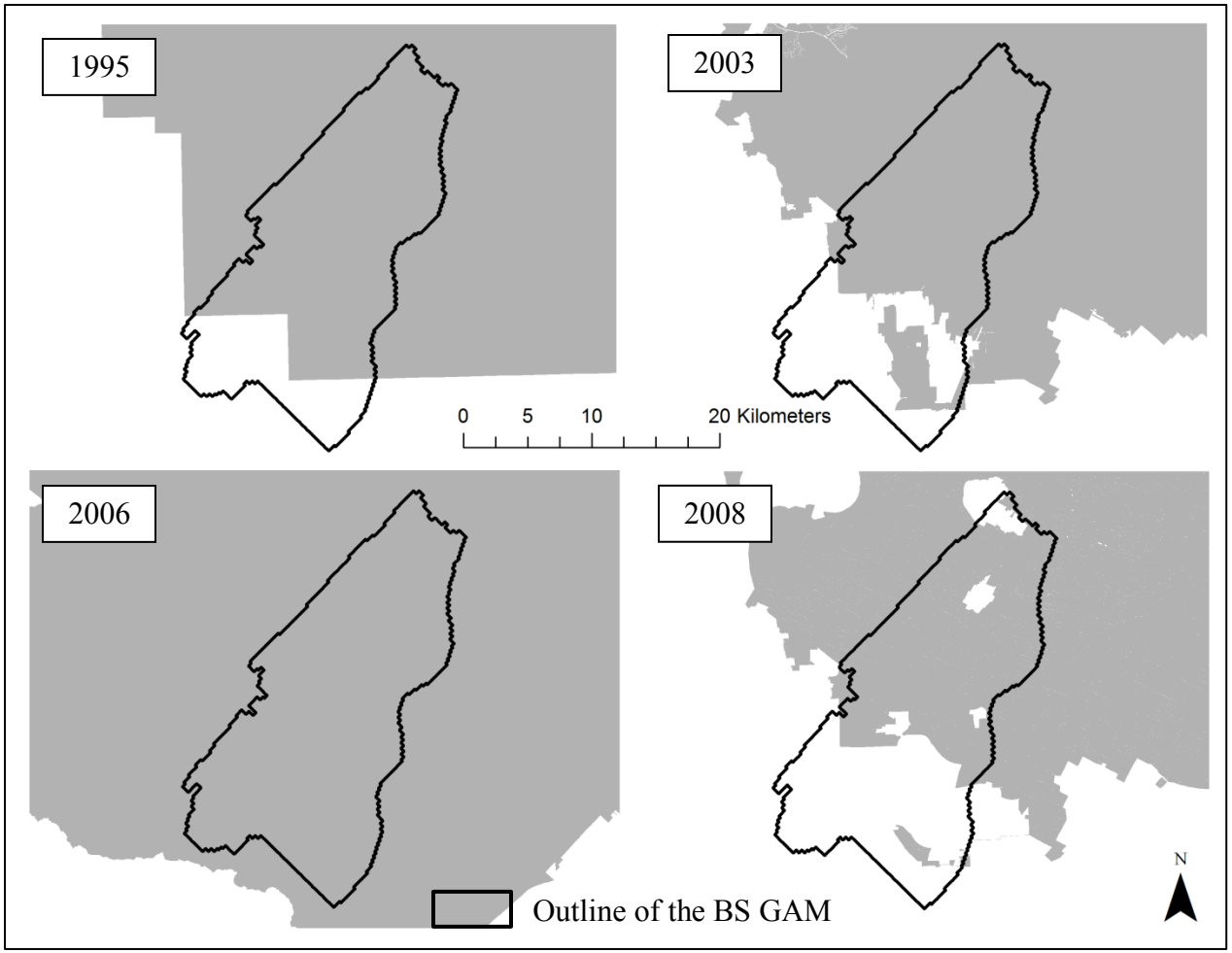

Figure 16: Extents of selected land use surveys conducted by the City of Austin (grey). It is important to note that the BS GAM is not completely surveyed for years 1995 (top left), 2003 (top right), and 2008 (bottom right).

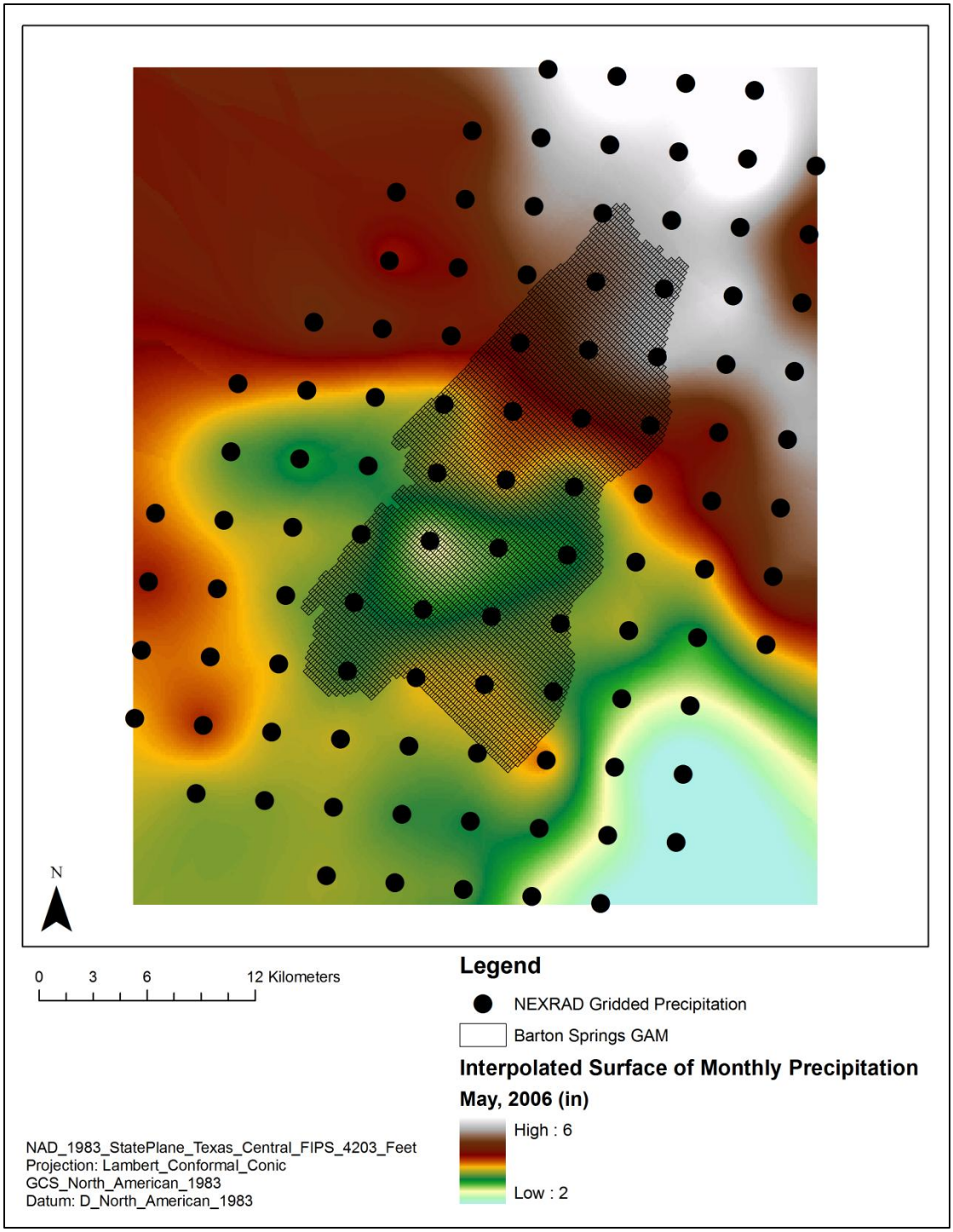

Figure 17: Example raster surface of total precipitation generated from NEXRAD gridded precipitation (May, 2006). *Kriging* is the interpolation technique used.

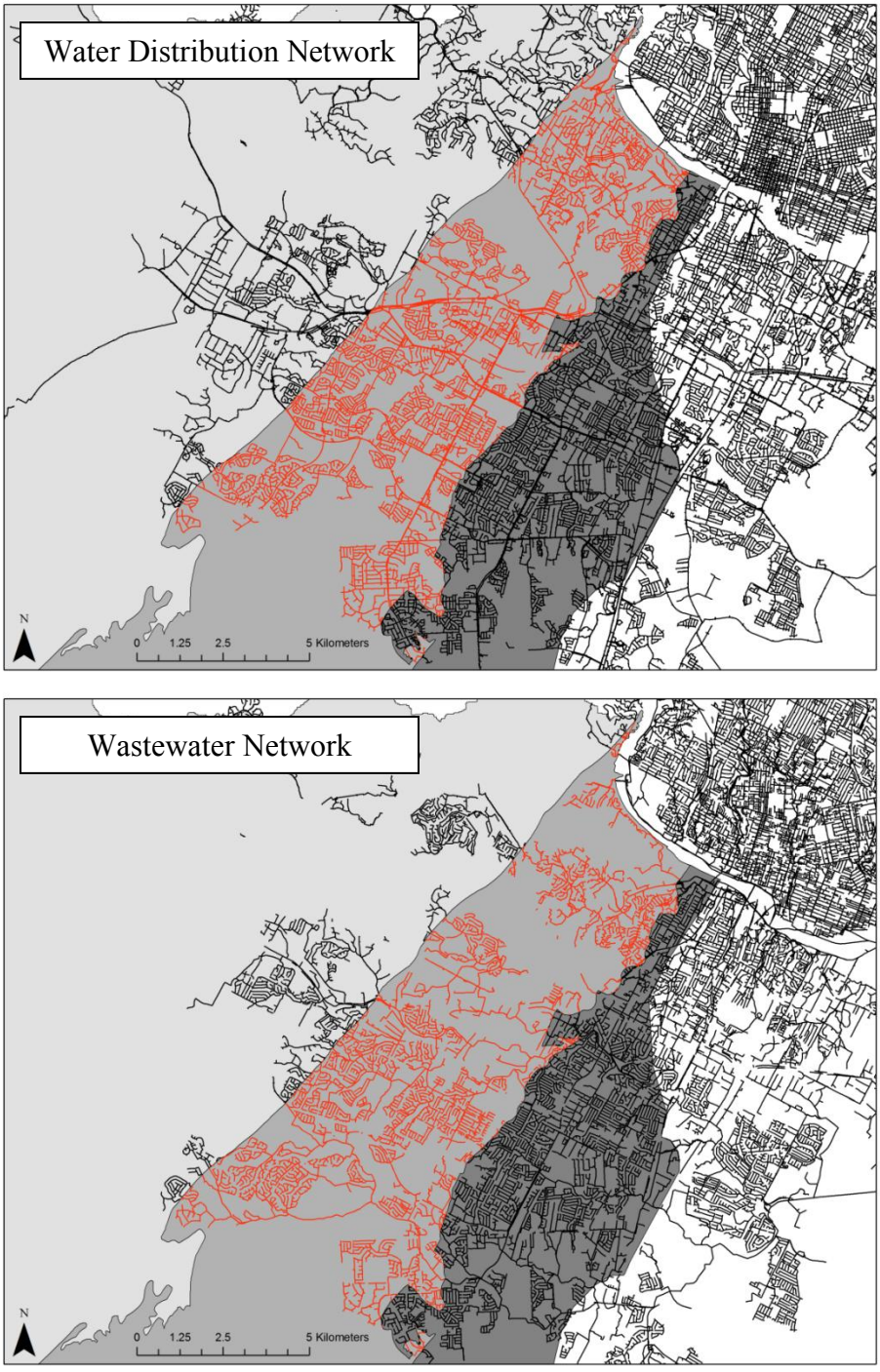

Figure 18: Map of pipe segments from the water distribution (top) and wastewater (bottom) networks within the recharge zone of the BSEA (red) as of January 1st, 2010.

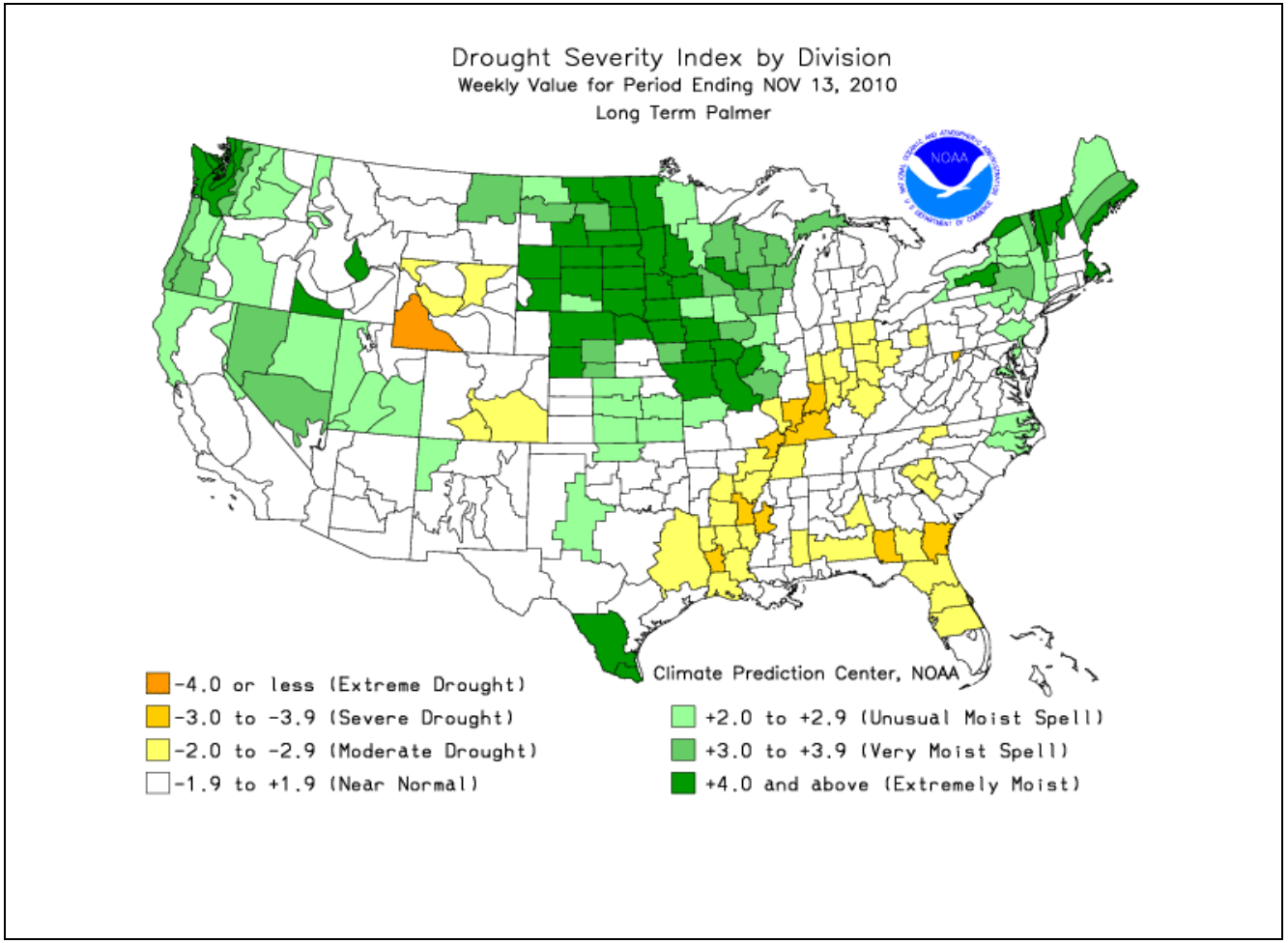

Figure 19: Example map of NOAA's weekly PDI data that was utilized to determine mean monthly values (NOAAb, 2011).

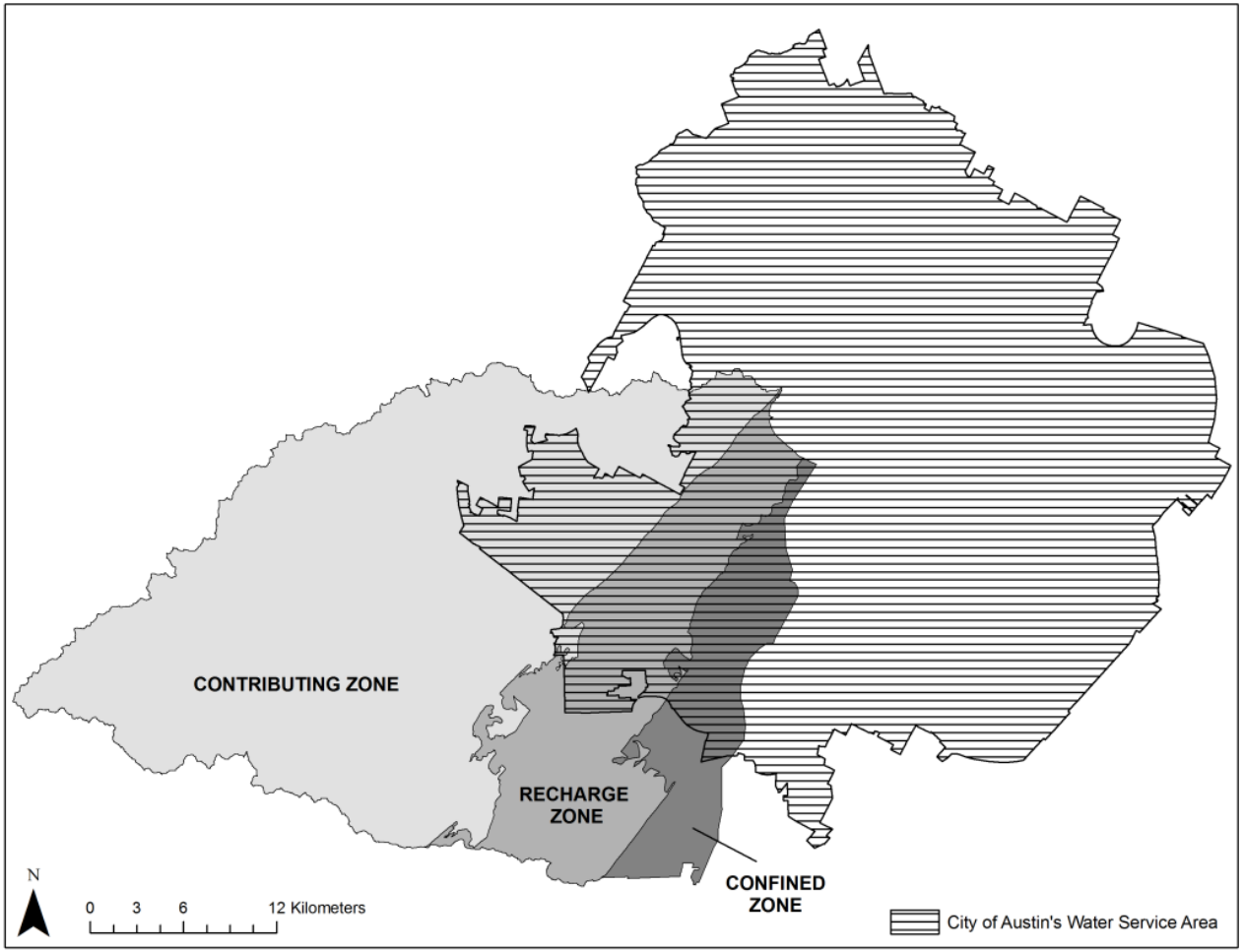
CONTRIBUTING ZONE
RECHARGE ZONE
CONFINED ZONE
N
0 3 6 12 Kilometers
City of Austin's Water Service Area

Figure 20a.

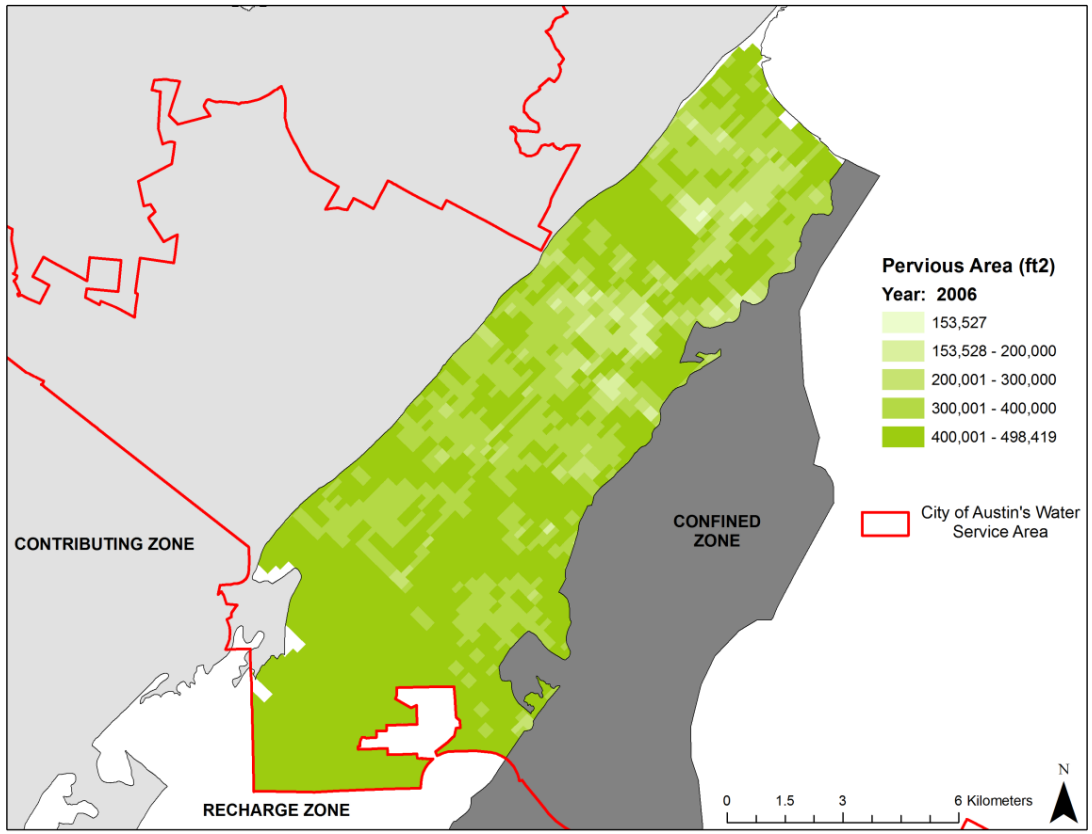

Figure 20b: Map of the extent Austin's Water Service area (Figure 20a) and pervious area calculations for the region within the recharge zone as well as the water service area (Figure 20b). Pervious areas were calculated as a grid of cells each 500,000 ft^2 (46, 452 m^2) in area based on City of Austin land use surveys. Greener cells represent greater pervious areas with a range of 153,527 – 498,419 ft^2 (14,263 – 46, 305 m^2). These analyses were conducted for each year within the study period.

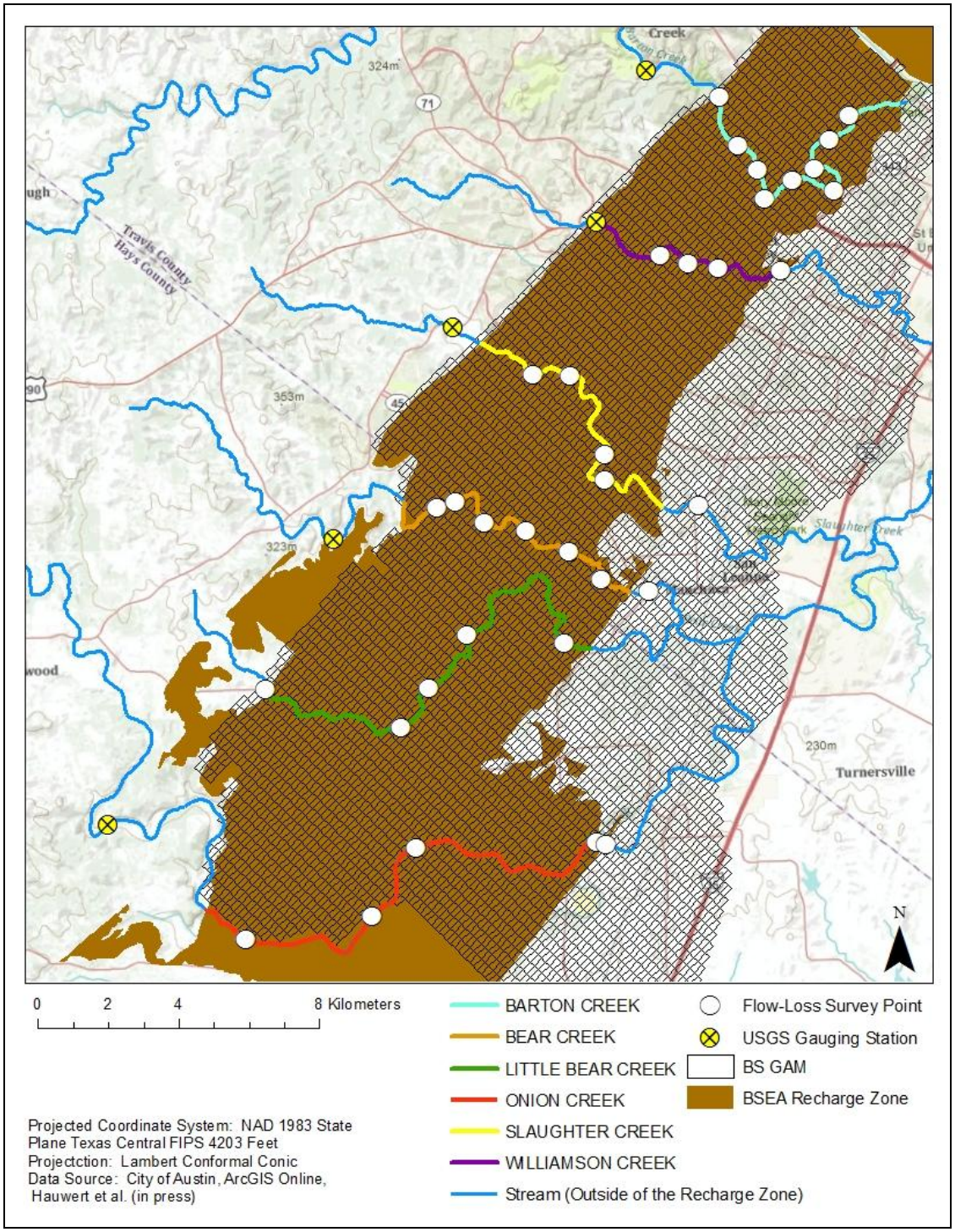

Figure 21: Map of flow-loss survey points. Locations based upon Figures 22 – 27.

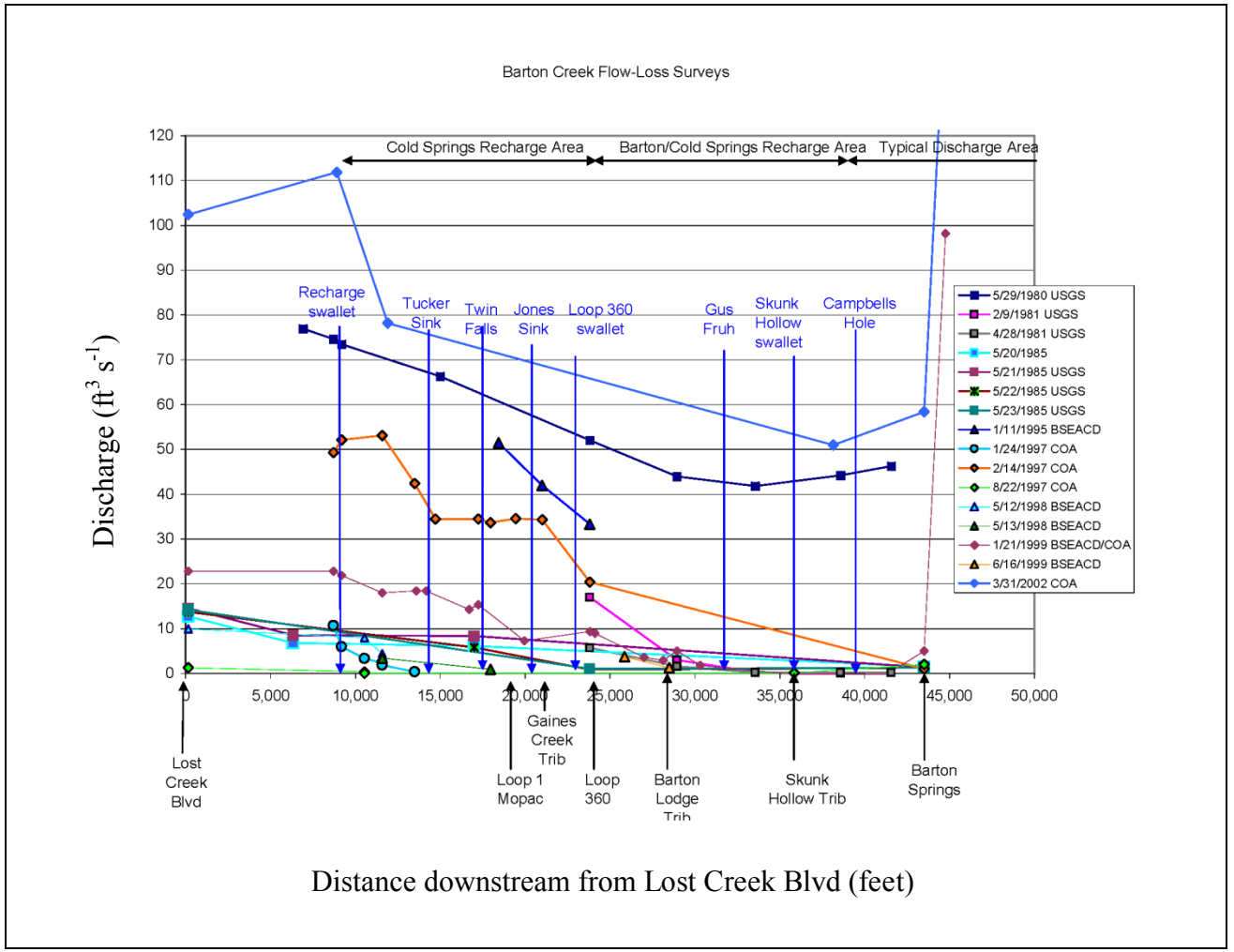

Figure 22: Barton Creek flow-loss surveys (modified from Hauwert et al., in press).

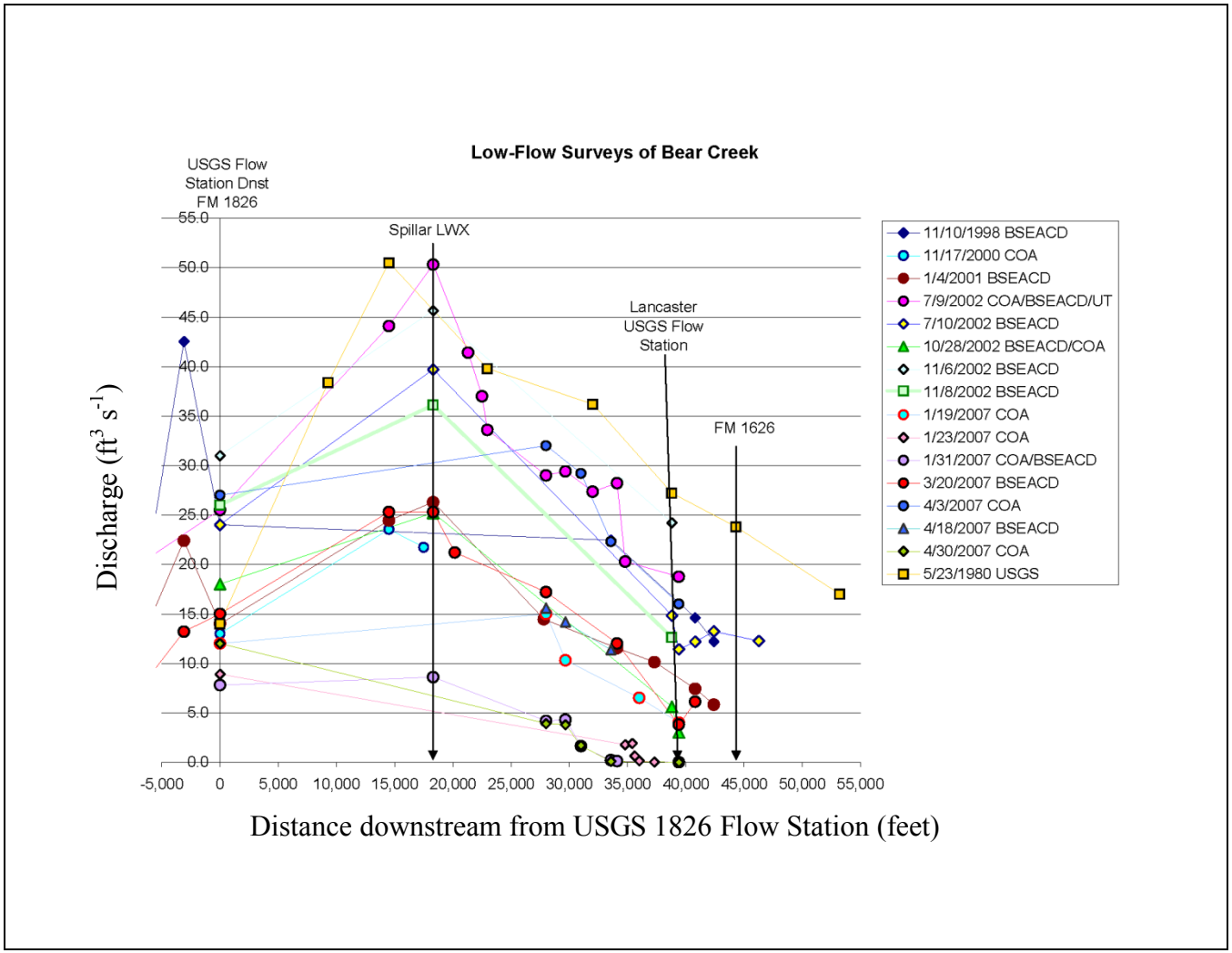

Figure 23: Bear Creek flow-loss surveys (modified from Hauwert et al., in press).

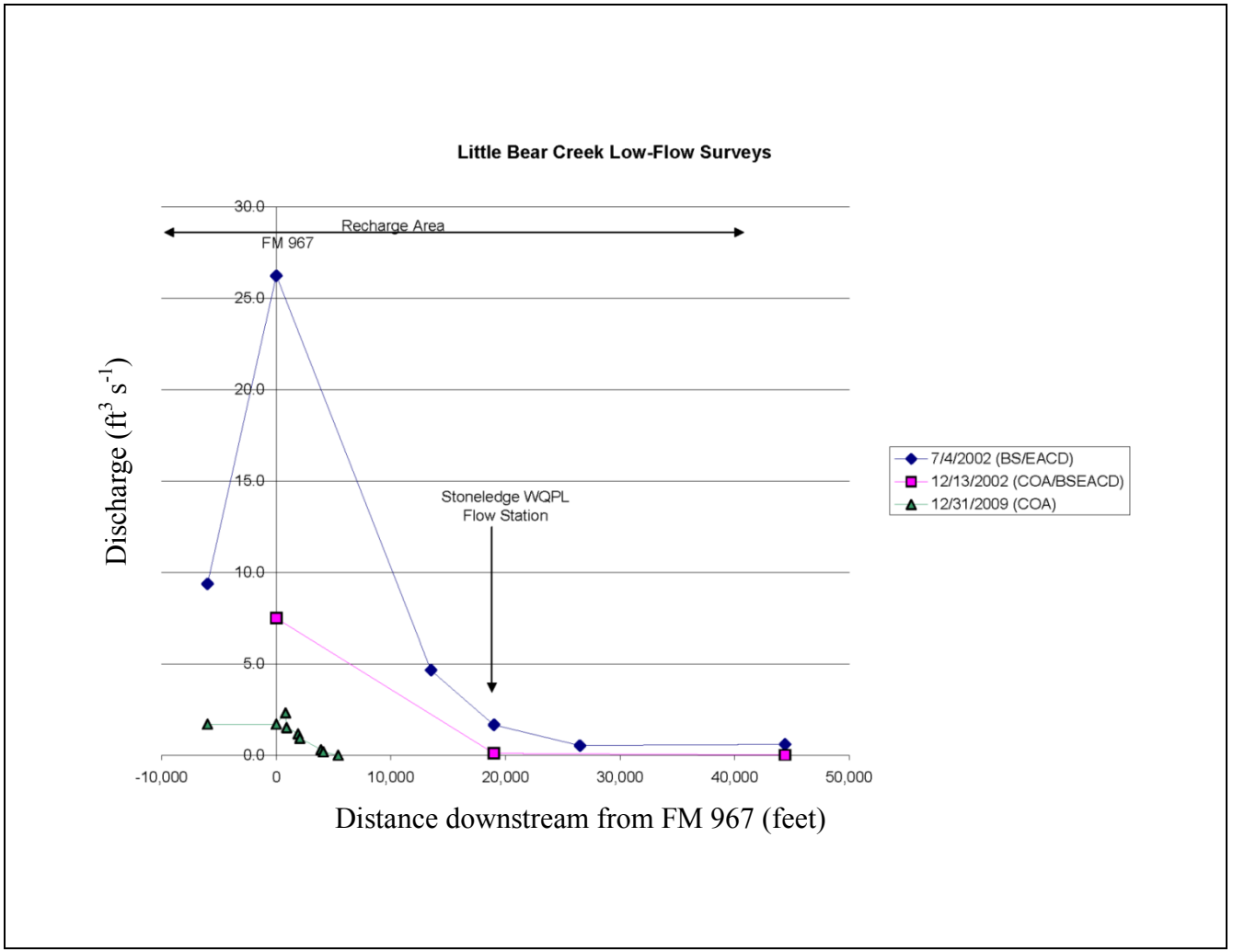

Figure 24: Little Bear Creek flow-loss surveys (modified from Hauwert et al., in press).

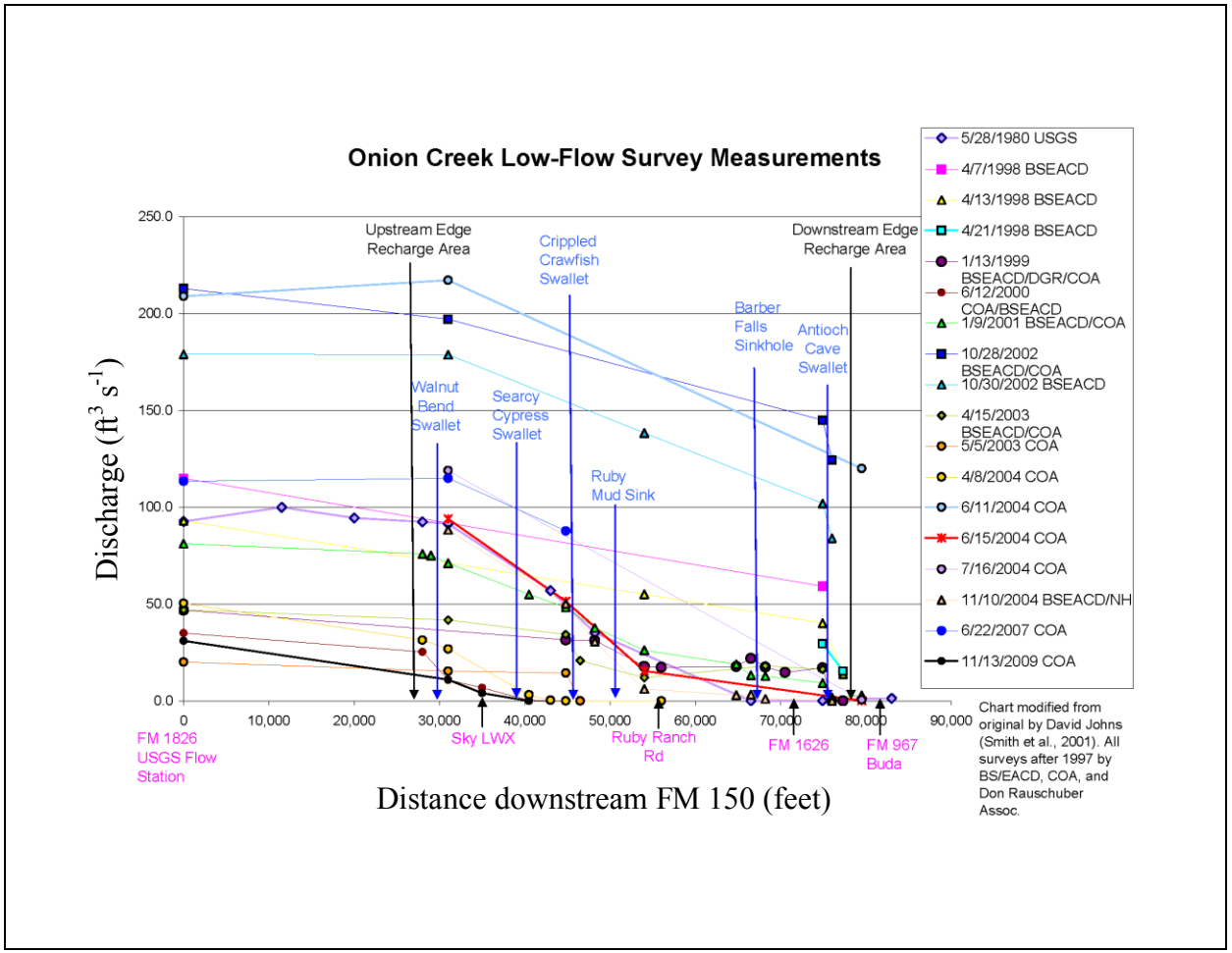

Figure 25: Onion Creek flow-loss surveys (modified from Hauwert et al., in press).

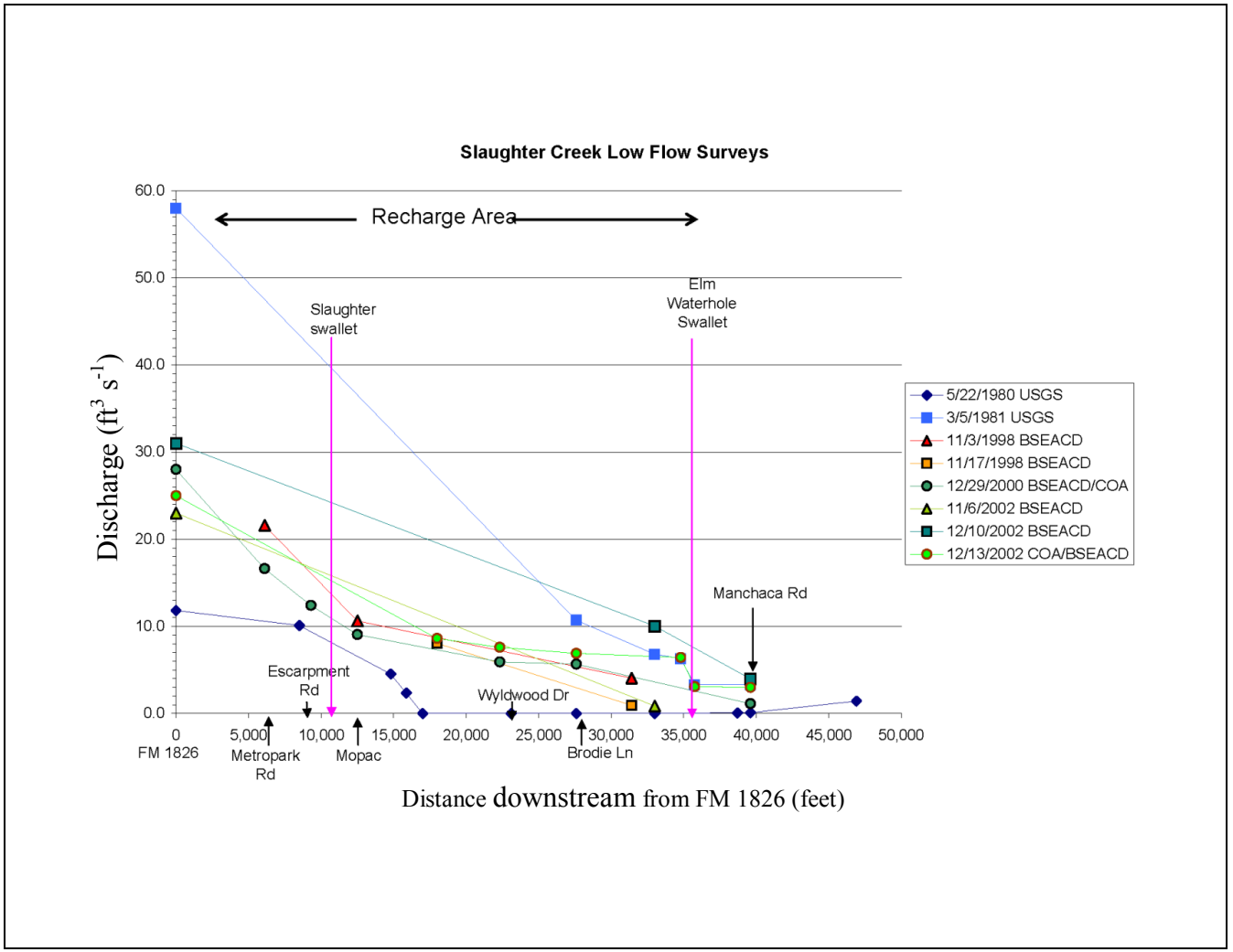

Figure 26: Slaughter Creek flow-loss surveys (modified from Hauwert et al., in press).

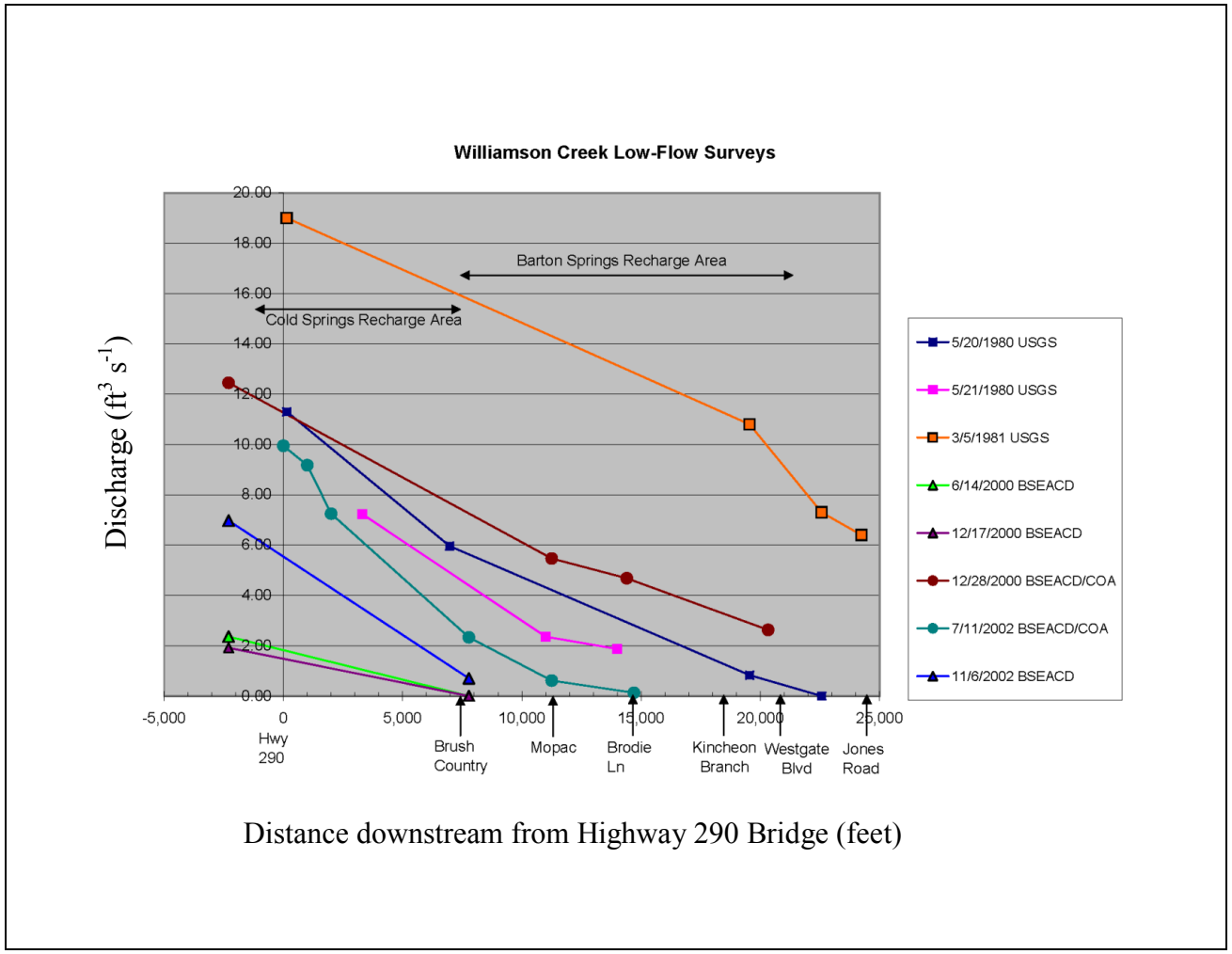

Figure 27: Williamson Creek flow-loss surveys (modified from Hauwert et al., in press).

Updated Pump Data

OBJECTIVE

The model also required quantifying discharge associated with well withdrawals (pumpage) within the BS GAM for years 1999 through 2009. The current GAM only has inputs for years 1989 through 1999so to model the system from 1999 through 2009, the input file for pump data needed updating.

DISCHARGE CALCULATIONS

The BSEACD is the local governmental authority tasked with permitting water supply wells and pump rates for the BSEA. Their most current report with pump data for the BSEA is reported in Hunt and others (2006). Approximately 50,000 to 60,000 people rely upon groundwater from the BSEA for their water supply from about 1,230 water supply wells. These wells are utilized for the following purposes: domestic (71% of the wells), public-supply (9%), monitor (6%), commercial (5%), irrigation (4%), agricultural (3%), closed loop (1%), and industrial (1%).

Total reported monthly pumping volumes from 1988 through 2005 can be found in Hunt et al. (2006), but no individual well data can be found, excluding the year 2004. To determine the total volume of discharge from each well for all months from 1999 through 2009, the proportions of total monthly pumping for each well in 2004 needed to be determined.

$$PP = \frac{W_P}{T_P} \qquad \textbf{(25)}$$

Where,

PP: proportion of total pumping

W_P: total pumping from a given well for a given month

T_P: total pumping from all wells for a given month

PP values were determined for each month during 2004 for each well (Appendix A). These proportions were then applied to T_P values for all other years between 1999 and 2005 to estimate W_P values for this time period. W_P values determined for 2005 were assumed for years 2006 – 2009 since data for these years were unreported. Well withdrawals have not increased significantly since 2005 (Brian Smith, BSEACD, personal communication).

ARCGIS PROCESSING

The location of each well within the BS GAM and the distribution of pumping volumes required the creation of a new shapefile was created. An Excel table was created utilizing data from Hunt et al. (2006) containing the geographic coordinates of each well and was uploaded into ArcGIS. Once the Excel table was uploaded into

ArcGIS, a new shapefile could be created with the well locations (Figure 28). Ultimately, each well needed to be associated with a HydroID in order to associate it with a BS GAM cell. This was done with the same methods previously discussed by utilizing the *Identity* tool. After each well was assigned to a BS GAM cell, a table of total monthly pumping for each well from 1999 – 2009 was created for the input file into MODFLOW-96.

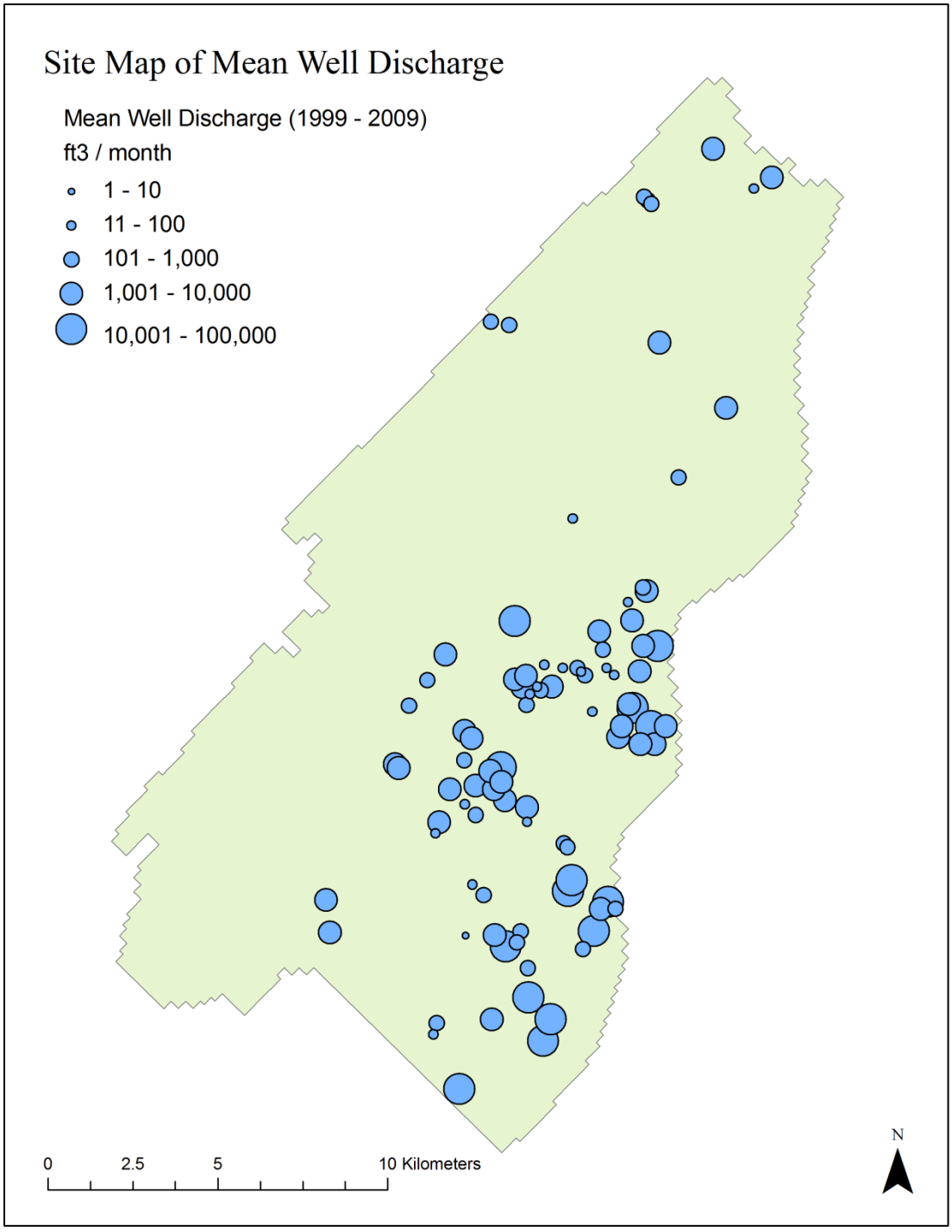

Figure 28: Site map of pumping wells and mean well discharge within the BS GAM. Locations and discharges based upon Hunt and Smith (2006).

CHAPTER 5

MODEL SCENARIOS

A variety of model scenarios were constructed for the BS GAM to test the effects and relevance of the various interpretations of recharge. The BS GAM is a numerical groundwater flow model (MODFLOW-96) (Harbaugh and McDonald, 1996) utilized by the Texas Water Development Board, the BSEACD, and the Regional Water Planning Group to manage groundwater resources for this region. The model scenarios described in this chapter are varying the quantity and distribution of recharge to the BS GAM as well as utilizing updated well pump rates while keeping all other model parameters consistent (aquifer properties, model boundaries, etc.). In order to test the results of each model scenario, outputs are compared to observed data. In particular, simulated Barton Spring discharge as well as water-level elevations are compared to observed measurements. Summaries of recharge inputs for each model can be found in Appendix B.

BASELINE EQUIVALENT SCENARIO

The original and recalibrated BS GAM models (Scanlon et al., 2001; Smith and Hunt, 2004) were designed to simulate monthly stress periods from 1989 to 1998 and 1950 to 1959 respectively. The monthly stress periods for this study are from 1999 to 2009. Consequently, there is no baseline scenario with which to compare the new recharge interpretations. In order to make this comparison, a baseline "equivalent" scenario was created for this new time period by utilizing the previous methods of quantifying and distributing recharge (Scanlon et al., 2001).

Recharge for the baseline equivalent scenario was quantified utilizing various methods but only considers contributions from losing streams and precipitation (Table 9). For Onion Creek, recharge was determined by subtracting daily average flow downstream from that upstream of the recharge zone (Scanlon et al., 2001). Recharge for Barton Creek was determined from stream discharge through a quadratic relationship developed by Barrett and Charbeneau (1996). This quadratic relationship was calibrated to Barton Springs discharge and assumed that all reaches of the stream that contributed to recharge were discharging at Barton Springs. Recent dye trace tests have demonstrated that this assumption is invalid and that a significant portion of Barton Creek actually discharges to Cold Springs (Hauwert et al., 2011 in press; Hauwert, 2009; Hunt et al., 2006; Smith et al., 2005; BSEACD, 2002). Bear, Slaughter, and Williamson Creek are the only other streams accounted for in the previous methods of calculating recharge. For these streams, recharge volumes were calculated from the relationship described in Equation 21. Recharge for each of the five streams was distributed equally throughout each stream. In other words, the monthly total recharge volume for a stream is distributed equally to all BS GAM cells that the stream intersects. Distribution does not consider where within the channels recharge is taking place or which cells have greater stream lengths. Diffuse recharge for these models was set equal to 15% of the total stream recharge and distributed equally to all active cells. These methods of calculating and distributing recharge for the BS GAM as well as all other model details can be found in Scanlon et al., 2001.

NATURAL RECHARGE SCENARIO

New methods for quantifying and distributing recharge from losing streams and precipitation were discussed in the previous chapter. This model scenario seeks to test the effects and relevance of these new interpretations of natural recharge. Within this scenario, changes are made to the recharge inputs for losing streams and precipitation (Table 9). These new interpretations of recharge decouple stream and precipitation calculations from Barton Springs discharge, consider which BS GAM cells have greater stream lengths, and incorporate flow-loss surveys (Hauwert et al., 2011 in press) for greater spatial distribution of stream recharge, and integrate NEXRAD precipitation data with COA land use surveys for diffuse recharge calculations and distributions.

NATURAL + ARTIFICIAL RECHARGE SCENARIO

The BS GAM does not currently consider recharge inputs from anthropogenic sources. This is the first study to quantify recharge from these sources in this detail for Austin, TX. In this model scenario, recharge inputs from the Natural Recharge Scenario are combined with anthropogenic inputs (see Methods). Thus, total recharge for this scenario is defined as the summation of stream loss, diffuse recharge, leakage from utility lines, and irrigation return flow (Table 9).

ALTERED NATURAL + ARTIFICIAL RECHARGE SCENARIO

Barrett and Charbeneau (1997) estimate diffuse recharge rates to the recharge zone of the BSEA with the Groundwater Loading Effects of Agricultural Management Systems model developed by the US Department of Agriculture (Knisel, 1993). Their methods relied upon historical rainfall data from the period 1979 – 1993 and descriptions

of soil and vegetation types from the recharge zone. From this model, average infiltration was estimated to be 50 mm $year^{-1}$, which is about 6% of annual rainfall (Barrett and Charbeneau, 1997).

For the altered natural + artificial recharge scenario recharge inputs from the natural + artificial scenario, excluding the diffuse recharge input, were combined with a diffuse recharge input based upon Barrett and Charbeneau (1997) (Table 9). NEXRAD precipitation data determined precipitation distribution, but instead of utilizing infiltration percentages estimated by Wiles (2007) and Hauwert (2009), the infiltration rate from Barrett and Charbeneau (1997) was employed. An important note is this methodology does not consider land use type like the methods discussed in the previous chapter.

Table 9: Summary table of modeling scenarios and their corresponding recharge and discharge parameters.

Model Scenario	**Simulated Time Period**	**Total Recharge (TR)**	**Well Discharge**
Baseline Equivalent	1999 - 2009	Methods described in Scanlon et al., (2001)	$W_p = T_p \times PP$
Natural	1999 - 2009	$TR = DR + SR$	$W_p = T_p \times PP$
Natural + Artificial	1999 - 2009	$TR = DR + SR + AR$	$W_p = T_p \times PP$
Altered Natural + Artificial	1999 - 2009	$TR = DR^* + SR + AR$ DR^*: altered diffuse recharge calculation where the infiltration percentage from Barrett et al., (1996) (6%) is used instead of the percentages estimated within Wiles (2007) (21% for impervious cover) and Hauwert (2009) (32% for pervious cover).	$W_p = T_p \times PP$

CHAPTER 6

RESULTS

The results presented in this chapter are divided into the following two sections: 1) model runs and 2) water budget analyses. A core premise used to interpret modeled outcomes hinges on the assumption that modeling scenarios with the best fit for key metrics, such as spring flow rates and water table levels at drought indicator wells, represent greater accuracy in terms of scientific interpretation for recharge. The Altered Natural + Artificial Recharge scenario proved to be the most accurate at simulating Barton Springs discharge and water-level elevations for the study period. Consequently, the results of the water budget analyses presented within the Water Budget Analyses section of this chapter are in terms of this modeling scenario.

Model Runs

The four modeling scenarios were tested using the BS GAM based on the MODFLOW-96 code and simulation runs were generated using the GWDSS software platform (Pierce, 2006). These scenarios differed in the methods for quantifying recharge inputs and distributing these values within the BS GAM (Table 9). No other parameters of the original model (Scanlon et al., 2001), besides the pumping file, were altered.

BASELINE EQUIVALENT SCENARIO

A true baseline scenario would be the original transient simulation conducted by Scanlon and others (2001) for the previous decade (1989 – 1999). Since this thesis is

concerned with modeling the following decade (1999 – 2009), a baseline "equivalent" was generated by using the same methods for quantifying and spatially distributing recharge as the original method reported by Scanlon and others (2001) (Table 9). Using these values, MODFLOW-96 was unable to complete the run for the Baseline Equivalent scenario. Error reports indicated that a large number of cells beginning in the southeastern portion of the model were going dry and that the model failed to converge at time step 12 of stress period 93 or near the end of September, 2006 (Figure 29). Consecutive months of minimal precipitation took place between March, 2005, and January, 2007, that lead to minimal recharge. Recharge inputs for this model scenario were possibly insufficient for MODFLOW-96 to converge (i.e., it was mathematically impossible to solve the numerical flow equations and relationships within the model with the given recharge inputs).

Another important factor that potentially led to the failure of the Baseline Equivalent scenario is the spatial distribution of recharge inputs within this scenario. The Baseline scenario has the smallest total recharge input of the four scenarios (Figure 30). The next largest is the Altered Natural + Artificial Recharge scenario that is the most accurate model in terms of simulating Barton Springs discharge and water-level elevations. The difference between the total volumetric input over the study period for these two scenarios is approximately 60,000,000 m^3 or 8%. Although the volumetric difference between these two scenarios is not significant, the distribution of their recharge inputs is greatly different (Figure 31). By distributing recharge in a more uniform manner, the Baseline Equivalent scenario potentially may cause regions within the model to dry up more quickly and unrealistically. However, by accounting for

realistic recharge distributions, as is the case with the other three model scenarios, MODFLOW-96 is able to successfully run.

A prime example of the importance of realistically distributing recharge inputs is observed in the effects of Antioch Cave. Antioch Cave is the largest-capacity recharge feature within the BSEA with an average recharge of 1.3 $m^3 s^{-1}$ (46 cfs) and a maximum of 2.7 $m^3 s^{-1}$ (95 cfs) (Fieseler, 1998). It is located within Onion Creek in the southeastern portion of the model which is also the region where cells started to go dry first (Figure 31). The Baseline Equivalent scenario does not account for this feature and recharge within this portion of the stream is no different from the rest of Onion Creek. This is not the case for the other three model scenarios (Figure 31). For the Altered Natural + Artificial Recharge scenario, the two cells accounting for Antioch Cave average approximately 250,000 and 85,000 $m^3 mo^{-1}$ (9 and 3 million $ft^3 mo^{-1}$ or 3.5 and 1.2 cfs) of recharge over the study period. These mark the upper limit of mean monthly recharge values amongst all of the BS GAM cells (Figure 31). It is important to account for this feature's location and recharge capacity because there are several horizontal no-flow boundaries within the model framework (Figure 12) that hydraulically isolate this section of the model. Consequently, by uniformly distributing Onion Creek's recharge, substantially lower volumes of recharge and groundwater flow reach this portion of the model and are inferred to be one of the reasons why the Baseline Equivalent scenario fails to converge.

NATURAL RECHARGE SCENARIO

The Natural Recharge scenario was able to converge, and simulates Barton Springs discharge moderately well (Figure 32). In general, this scenario captured the general shape of observed Barton Springs discharge but substantially overestimated spring flows with a root mean square error (RMSE) of 1.0 $m^3 s^{-1}$ (35.3 cfs) (Figure 33, Table 10). The simulated spring flow within this scenario is almost always greater (at least 2x) for the entire model period (January, 1999 – December, 2008). Similar results are found for water-level elevations (Figure 34, Table 11) in that this scenario tends to overestimate water-levels as well with a RMSE of 22.6 meters (74.1 feet). Under-prediction of spring flows during the first six months (January, 1999 – June, 1999) of this scenario is attributed to initial conditions from the original BS GAM (Scanlon et al., 2001) not being in equilibrium with boundary conditions (recharge and discharge). This observation can be applied to the results from the other two model scenarios as well. Good correlation between simulated and observed Barton Springs discharge is found during recharge events following months of consecutive minimal recharge (October, 2000 – February, 2001; December, 2006 – April, 2007). Discharge recovery for these time periods are reproduced fairly well but the transition back to lower flows is poorly simulated in terms of discharge rates (i.e. good agreement between fluctuation trends, but not the spring discharge.

Overestimation of Barton Springs discharge and water-level elevations can be explained by the overestimation of recharge from precipitation. The infiltration percentages for precipitation utilized were 21 and 32% for impervious and pervious land cover respectively (see Methods; Wiles, 2007; Hauwert, 2009). Impervious area ranges from approximately 9 – 15% of the total BS GAM for the study period (Table 1) so the

majority of the BS GAM area is considered pervious land cover. This means that the majority of precipitation falls on these areas throughout the BS GAM and 32% is assumed to recharge the aquifer. According to Hauwert (2009), these infiltration rates are representative of closed basins within the highland regions of the recharge zone. Furthermore, this 32% consists of 26% as diffuse recharge and 6% as discrete recharge (into a cave). It is unknown how well these values extrapolate to other parts of the recharge zone, especially where discrete features may not exist. Additionally, the 42-month sampling period that this study was based upon was wetter than average conditions and may have led to artificially higher infiltration percentages (Nico Hauwert, City of Austin, personal communication).

Ultimately, it appears inappropriate to apply the 32% infiltration rate to all pervious areas within the BS GAM, even though such percentages are common in other karstic areas (Hauwert, 2009). The volumes of total recharge for each modeling scenario vary greatly between those which utilize these inflated infiltration rates (Natural Recharge, Natural + Artificial Recharge scenarios) and those which do not (Baseline, Altered Natural + Artificial Recharge scenarios) (Figure 35). Excluding the Baseline scenario, recharge from losing streams and artificial sources are identical for each modeling scenario. Therefore, the variation in cumulative recharge between each scenario is truly a function of varying amounts of diffuse recharge which is a function of these infiltration percentages (Figure 36).

NATURAL + ARTIFICIAL RECHARGE SCENARIO

There are minimal differences between the outputs from the Natural Recharge scenario and the Natural + Artificial Recharge scenario. This scenario was able to simulate spring flows and water-level elevations that are slightly elevated from those observed in the Natural Recharge scenario (Figure 32). The only difference between these two model scenario's inputs is the addition of artificial recharge in the Natural + Artificial Recharge scenario (Table 9). For this scenario, artificial sources only constitute 3% of total recharge for the 10-year study period. Therefore, it is not surprising to not observe significant differences between the two. However, the addition of artificial sources did affect Barton Springs discharge and water-levels within the model indicating that they are substantial enough to influence the modeled groundwater system. The RMSE for Barton Springs discharge and water-level elevations increased to 1.1 $m^3 s^{-1}$ and 24 m (38.8 cfs and 78.7 ft) respectively (Figures 33, 34; Tables 10, 11). The significance of these results is that it demonstrates that artificial sources can potentially influence spring flows and water-level elevations.

ALTERED NATURAL + ARTIFICIAL RECHARGE SCENARIO

Based on the findings from the previous two model scenarios, it is evident that the greatest influence on how well the models scenarios could simulate Barton Springs discharge and water-level elevations was the input volume of diffuse recharge. It is important to note that recharge volumes calculated for losing streams and artificial sources were determined from observed data (stream gauge data and AWU supply and treatment reports). Diffuse recharge calculations utilized infiltration percentages from

previous studies that did employ field measurements (Hauwert, 2009; Wiles, 2007). However, it is likely that these values are site specific and should be scaled up only with great caution. Consequently, the greatest influence of uncertainty in terms of recharge sources is diffuse recharge due to its significance from a volumetric standpoint and the poor understanding of infiltration percentages. The results from the previous model scenarios suggested that diffuse recharge was being overestimated. Additionally, previous studies (Slade et al., 1986; Barrett and Charbeneau, 1996; Hauwert et al., 2011 in press) all estimate that diffuse recharge is approximately 15 – 34% of total recharge. For the Natural Recharge and the Natural + Artificial Recharge scenarios, diffuse recharge is 47 and 46% of the total recharge (Figure 35). This implies that diffuse recharge may be overestimated. Therefore, a lower infiltration percentage was applied (6% instead of 21 and 32%). Instead of lowering the infiltration rate until the best match was found between simulated and observed flows / elevations, an infiltration rate from a previous study was utilized (Barrett and Charbeneau, 1996). The main motivation for utilizing this value is that this infiltration percentage was based upon sampled data (soil and vegetation types, topography, etc) and was independent from Barton Springs discharge (water-budget approach). Thus, the goal of decoupling recharge calculations from Barton Springs discharge could be achieved. Complete decoupling is ultimately not achieved because the accuracy of the model scenarios is based on how well they can simulate Barton Springs discharge but these recharge inputs are not calculated from Barton Springs discharge data as previous methods have done.

There is significantly greater agreement between simulated and measured Barton Springs discharge for the Altered Natural + Artificial Recharge scenario (Figure 32) resulting in a RMSE of 0.5 $m^3 s^{-1}$ (17.7 cfs) (Figure 33, Table 10). The model scenario

also simulated water-level elevations more precisely than the previous scenarios producing a RMSE of 10.5 m (34.4 ft) (Figure 34, Table 11). These RMSE values are comparable to previous model studies where simulated Barton Spring discharge and water-level elevations ranged from 0.17 – 0.39 $m^3 s^{-1}$ and 1 – 26 m (6.0 – 13.8 cfs and 3.3 – 85.3 ft) respectively (Table 10, 11). This scenario generally underestimates both Barton Springs discharge and water-level elevations (Figures 33, 34) suggesting that diffuse recharge was underestimated for this scenario.

This is further substantiated by the change in storage over the study period (Figure 36, Table 12). Change in storage was calculated by subtracting total discharge (springs + pumping) from total recharge. Results indicate that the Baseline and Altered Natural + Artificial Recharge scenarios had decreases in storage by approximately -2.8 x 10^8 and -1.5 x 10^8 m^3 (-9.9 x 10^9 and -5.3 x 10^9 ft^3) over the ten-year study period, respectively. The Natural Recharge and the Natural + Artificial Recharge scenarios observe an increase in storage of approximately 1.7 x 10^8 and 2.0 x 10^8 m^3 (6.0 x 10^9 and 7.1 x 10^9 ft^3) and over the ten-year study period, respectively. In reality, there is probably close to no change in storage since this one of the objectives of the BSEACD and water-level elevations have not demonstrated long-term declines (Brian Smith, BSEACD, personal communication).

MODELING CONCLUSIONS

It was determined from the modeling results that the Altered Natural + Artificial Recharge scenario had the best fit with simulated Barton Springs discharge and water-level elevations. The following water budget analyses are based upon the recharge inputs for this modeling scenario

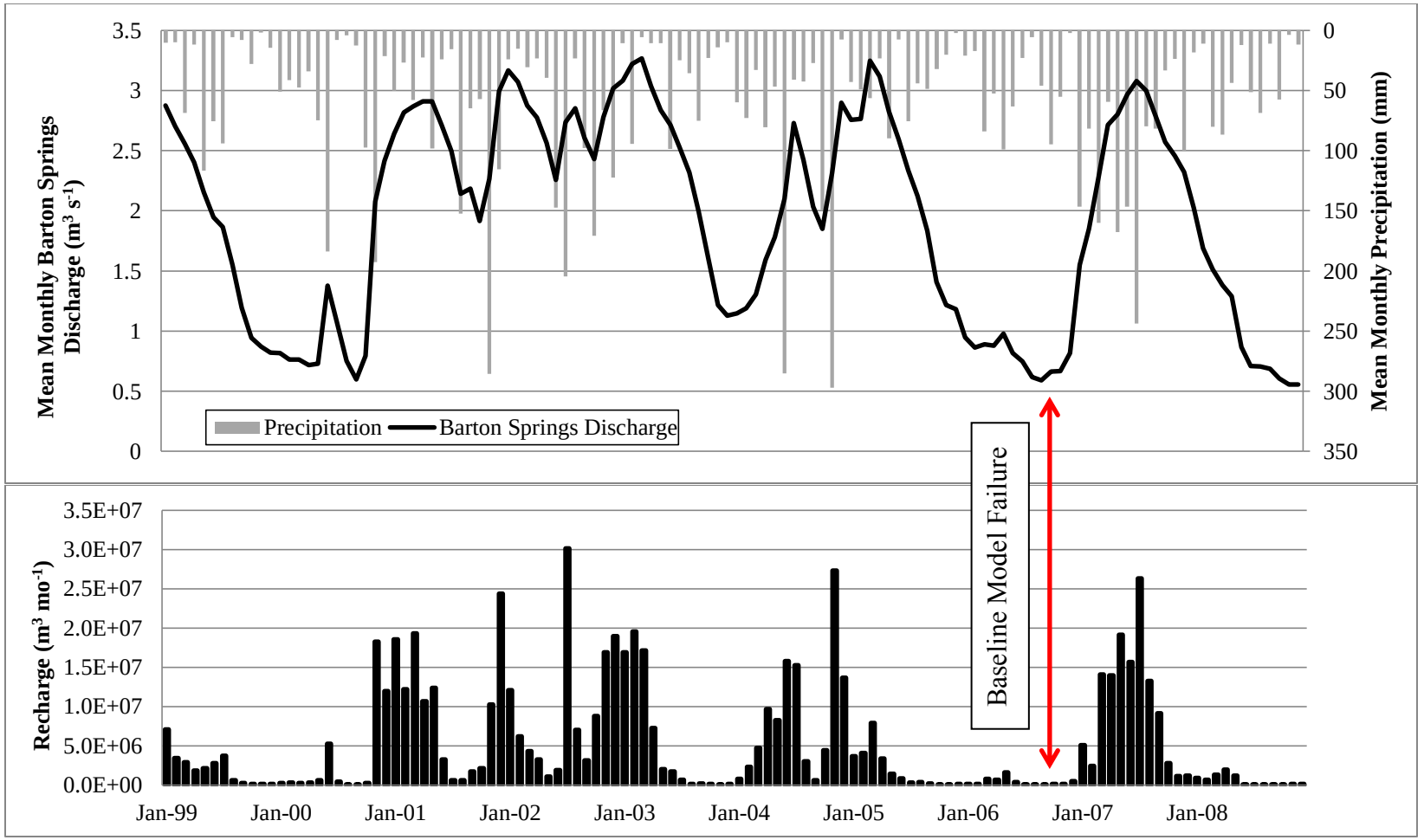

Figure 29: Plots of mean monthly Barton Springs discharge and precipitation (top) and the monthly recharge input for the Baseline model scenario (bottom). The model failed to converge near the end of September, 2006, due to insufficient water attributed to drought conditions.

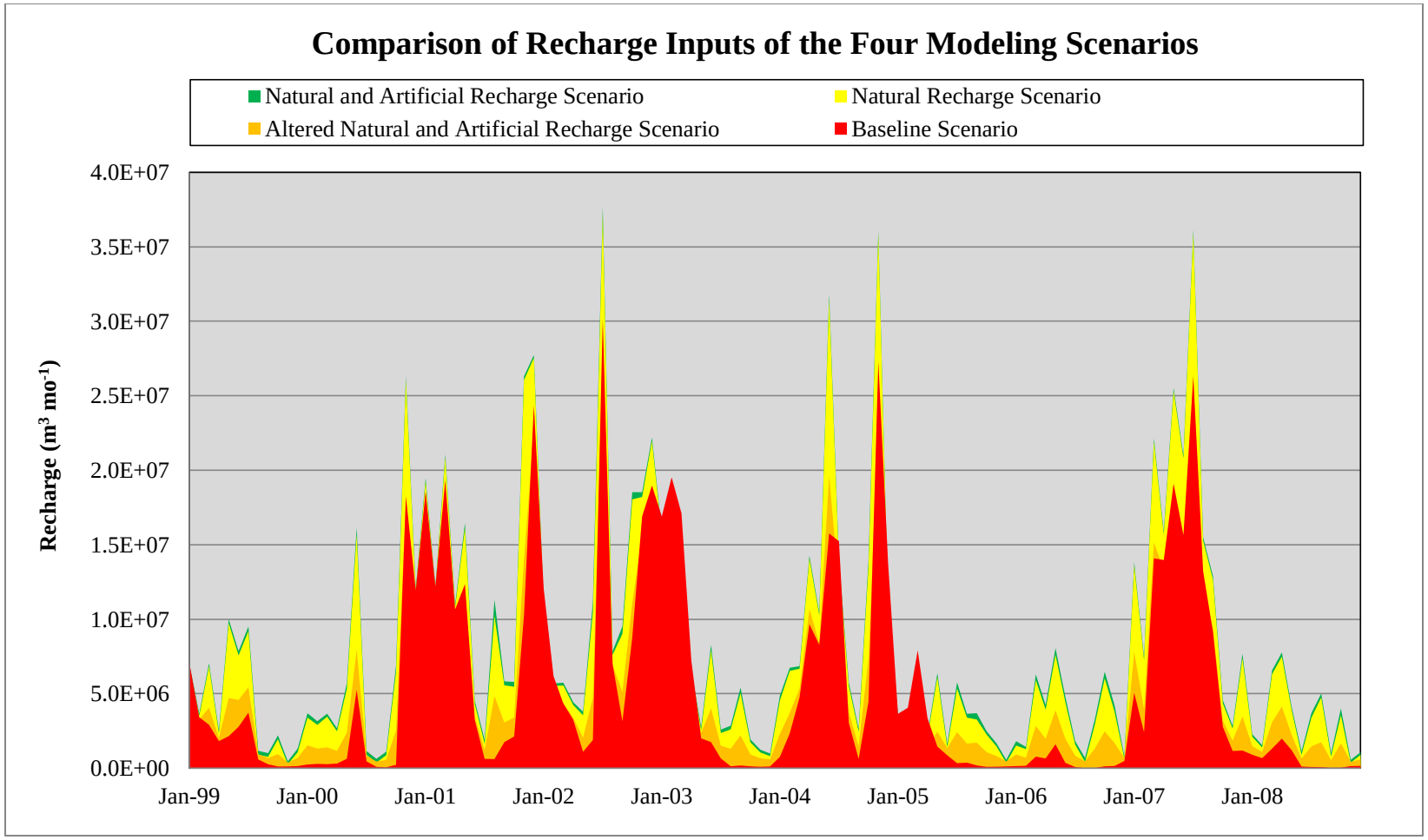

Figure 30: Comparison of monthly recharge inputs for the four model scenarios. The total volumetric difference between the Baseline (red) and the Altered Natural + Artificial Recharge (orange) scenarios is approximately 60,000,000 m^3 (2.1 x 10^9 ft^3) or 8% for January, 1999, – December, 2008.

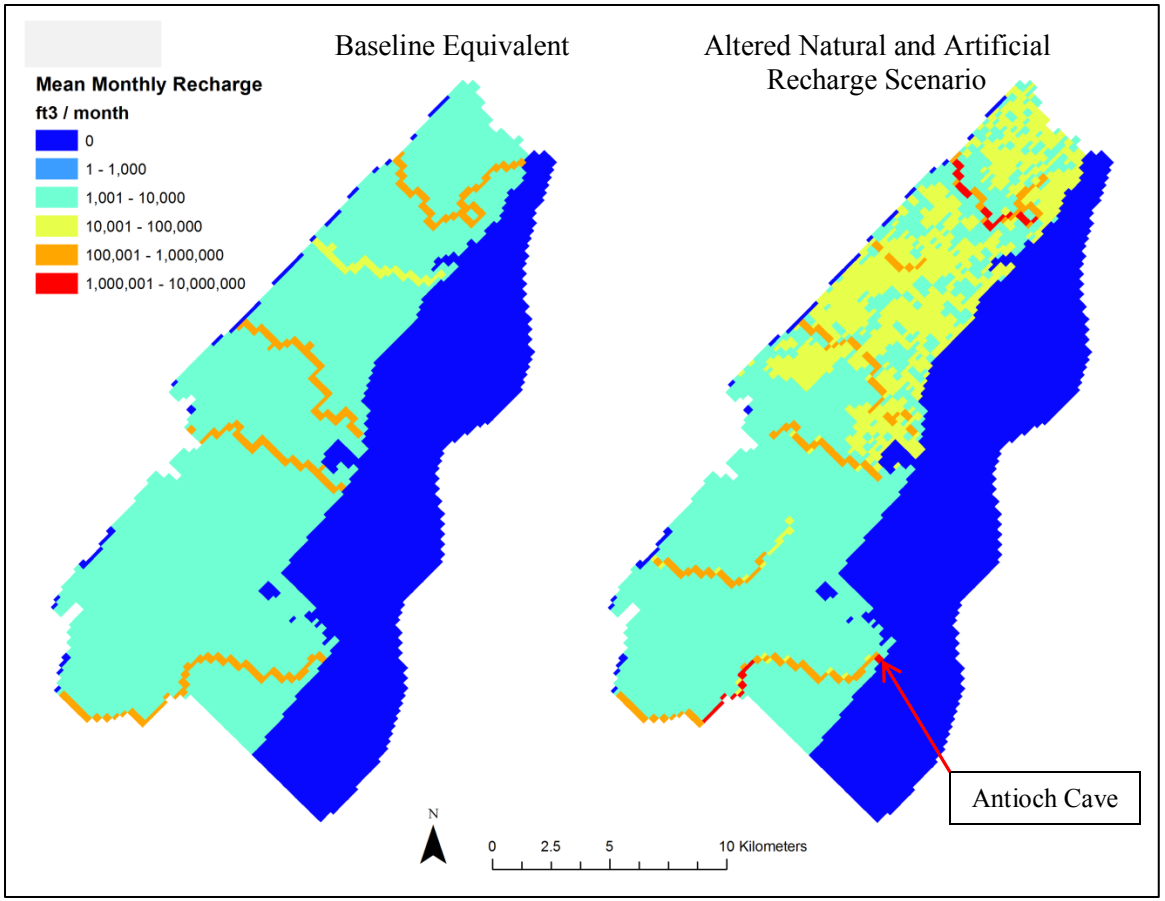

Figure 31: Comparison of mean monthly recharge distributions between the Baseline (left) and Altered Natural + Artificial Recharge (right) scenarios. Units are in cubic feet for labeling convenience (larger range of values) since the color scale is logarithmic. The scatter of yellow colored cells in the top half of the Altered Natural and Artificial Recharge scenario is a direct result of artificial recharge sources and correlates with the portion of the recharge zone that is urbanized (see Figure 7).

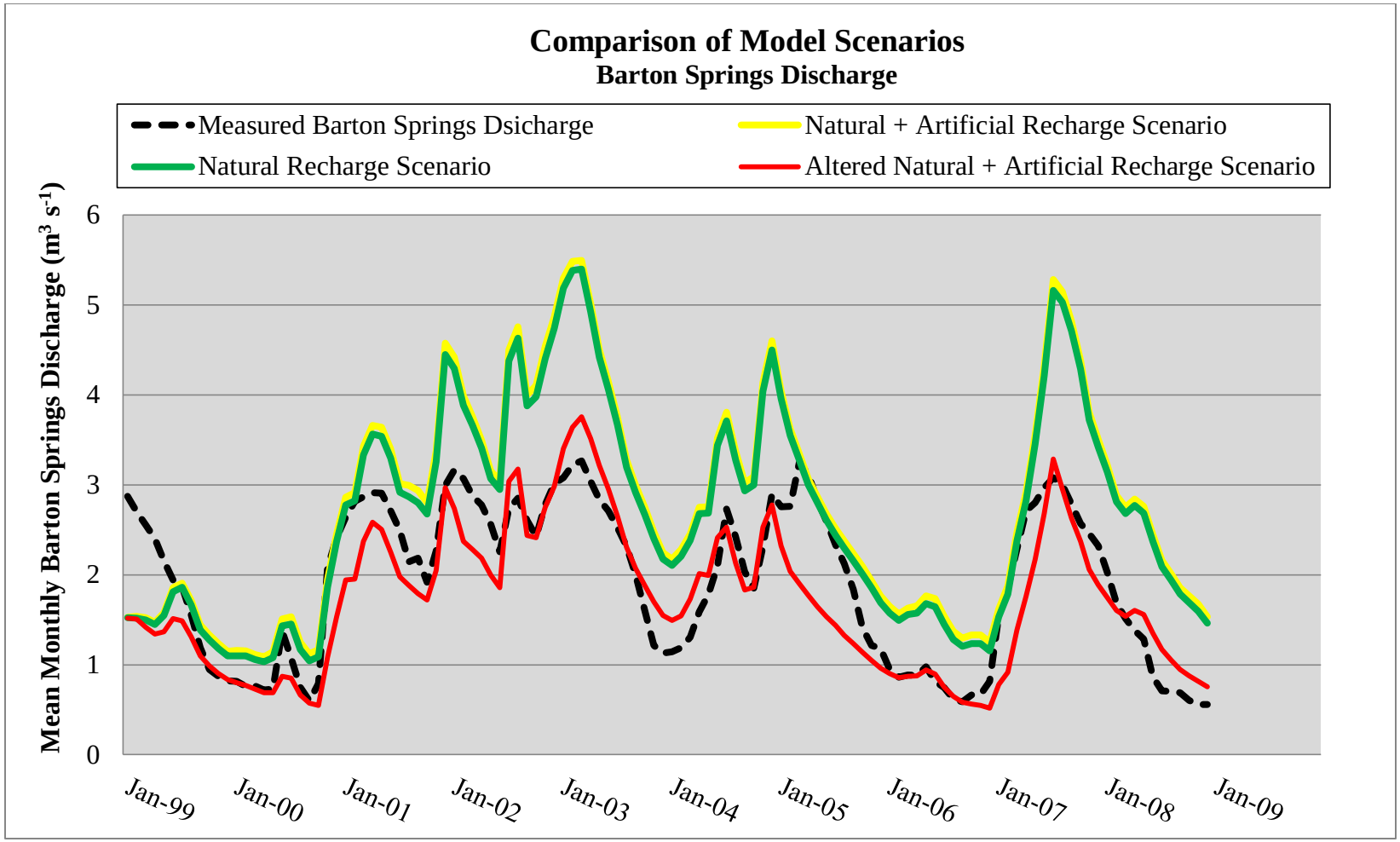

Figure 32: Graph comparing simulated Barton Springs discharge from the model scenarios (green, yellow, and red) to measured Barton Springs discharge (black-dotted line).

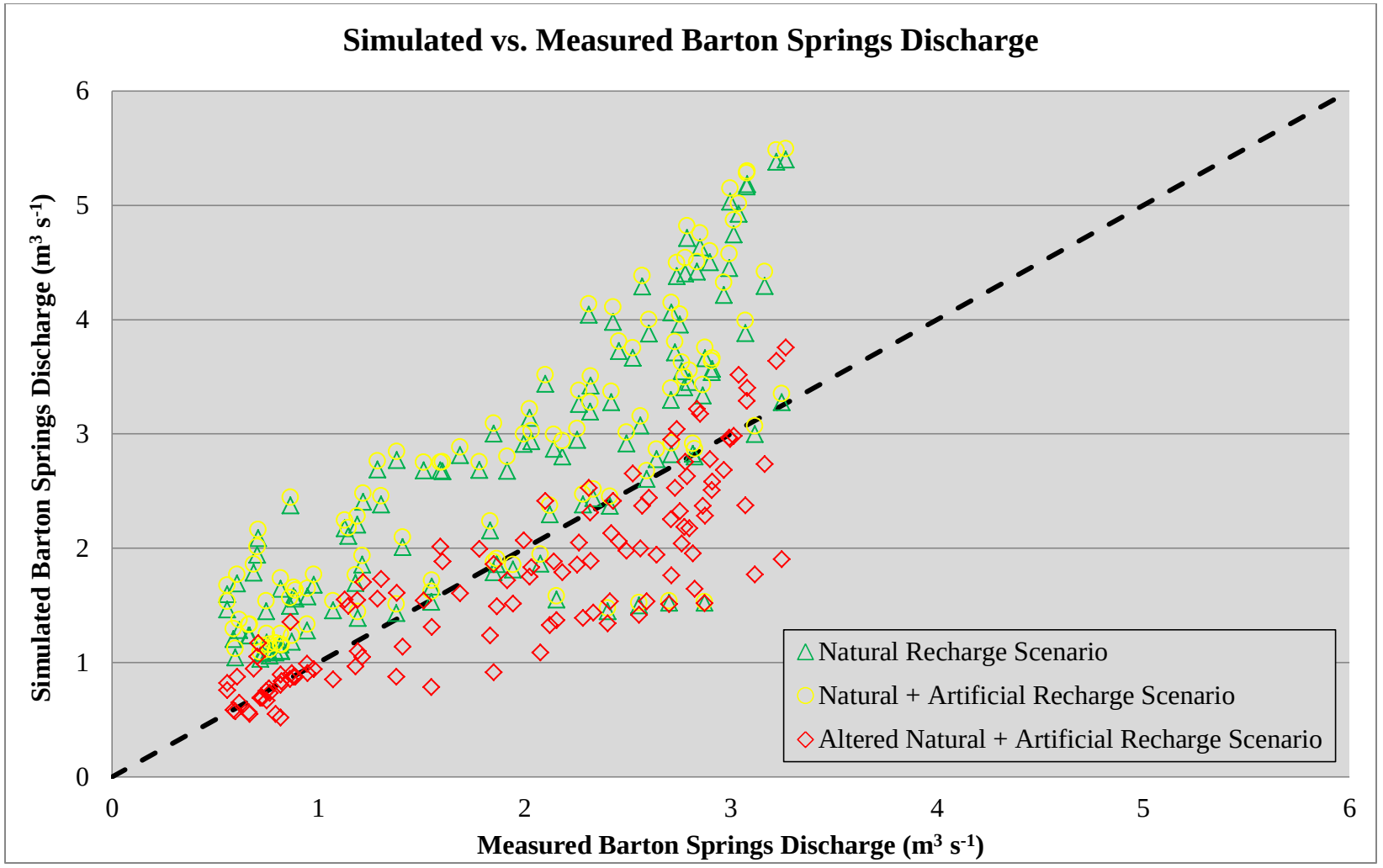

Figure 33: Plot of simulated versus measured Barton Springs discharge.

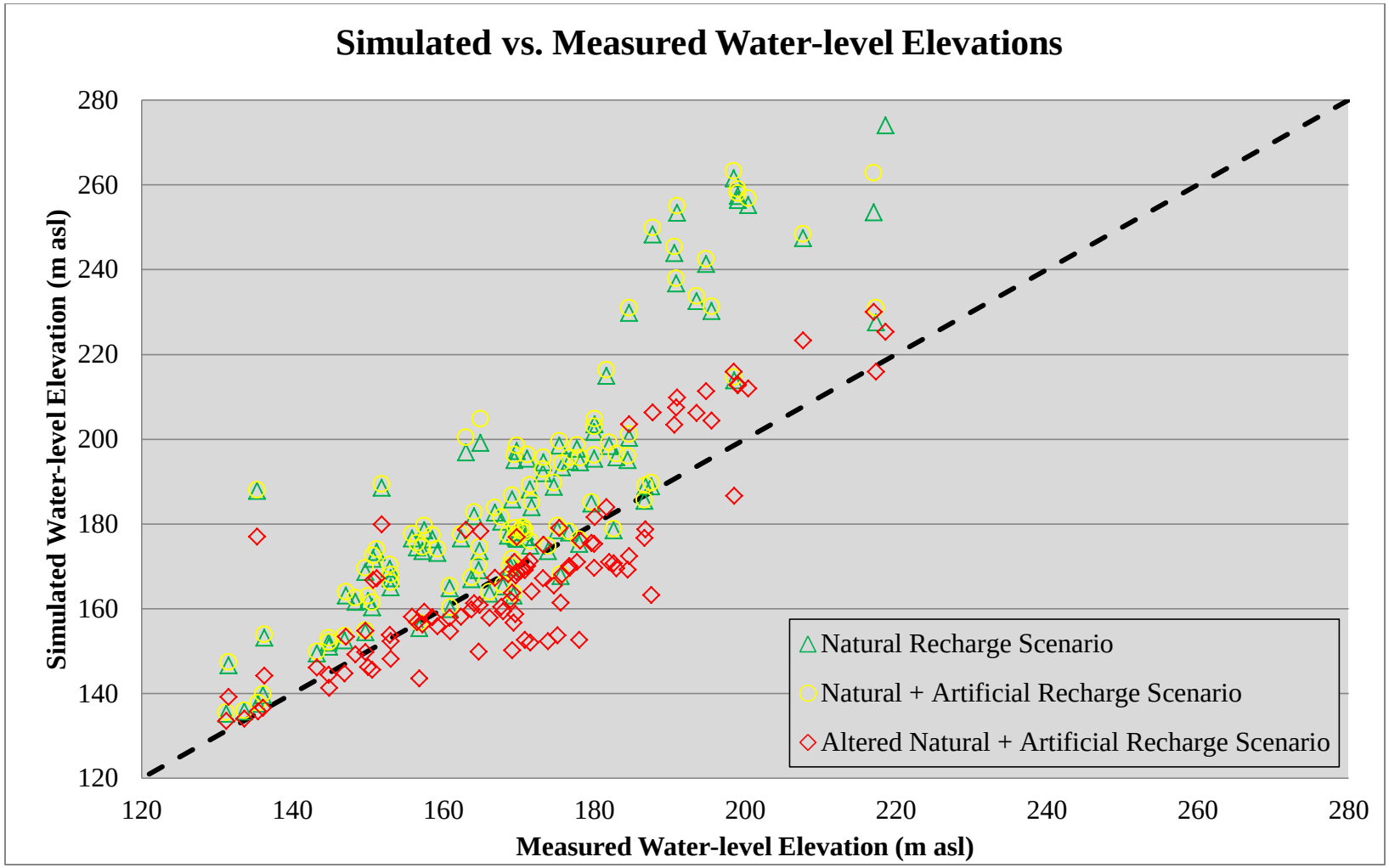

Figure 34: Plot of simulated versus measured water-level elevations.

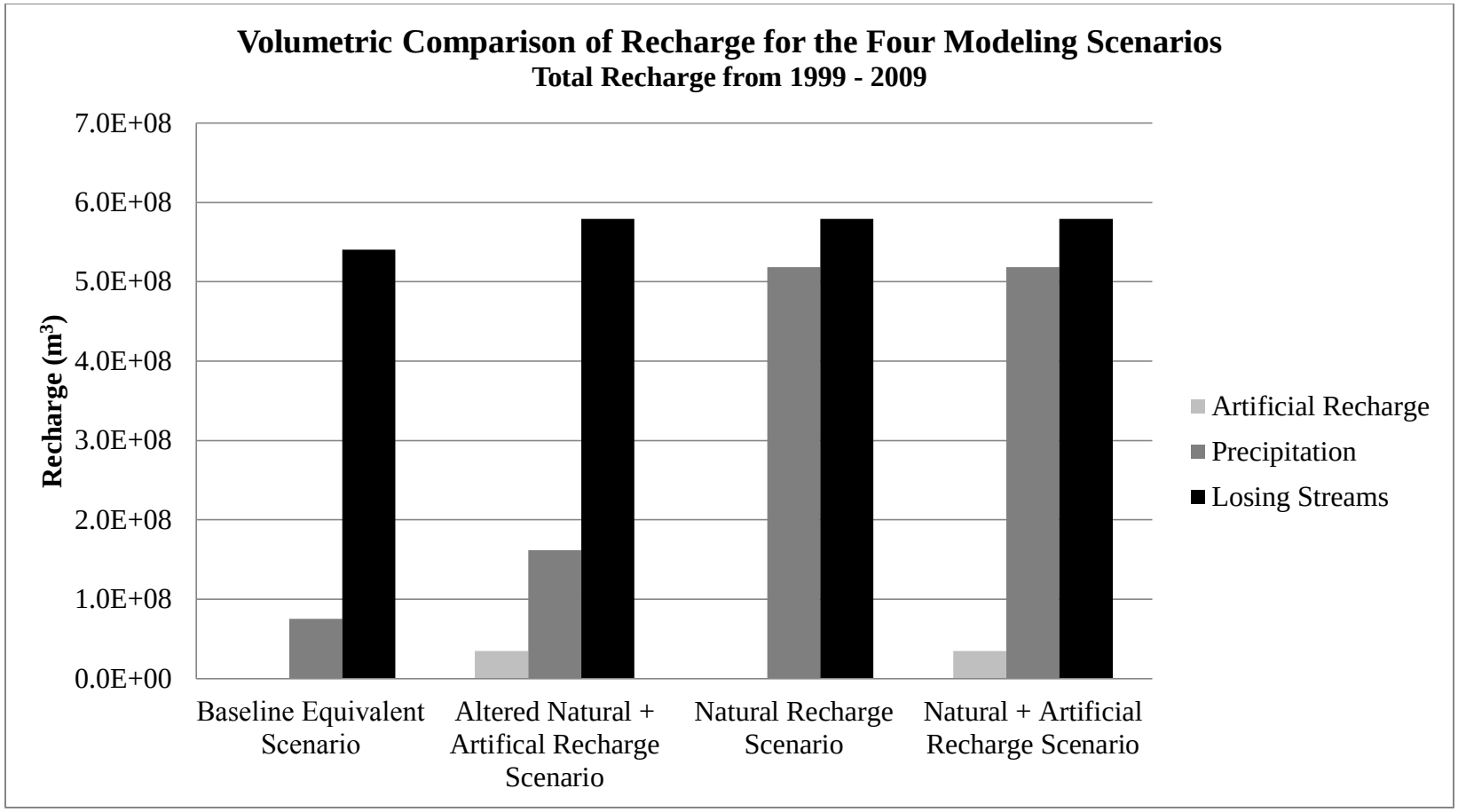

Figure 35: Comparison of total recharge inputs from natural and artificial sources for each modeling scenario (1999 - 2009).

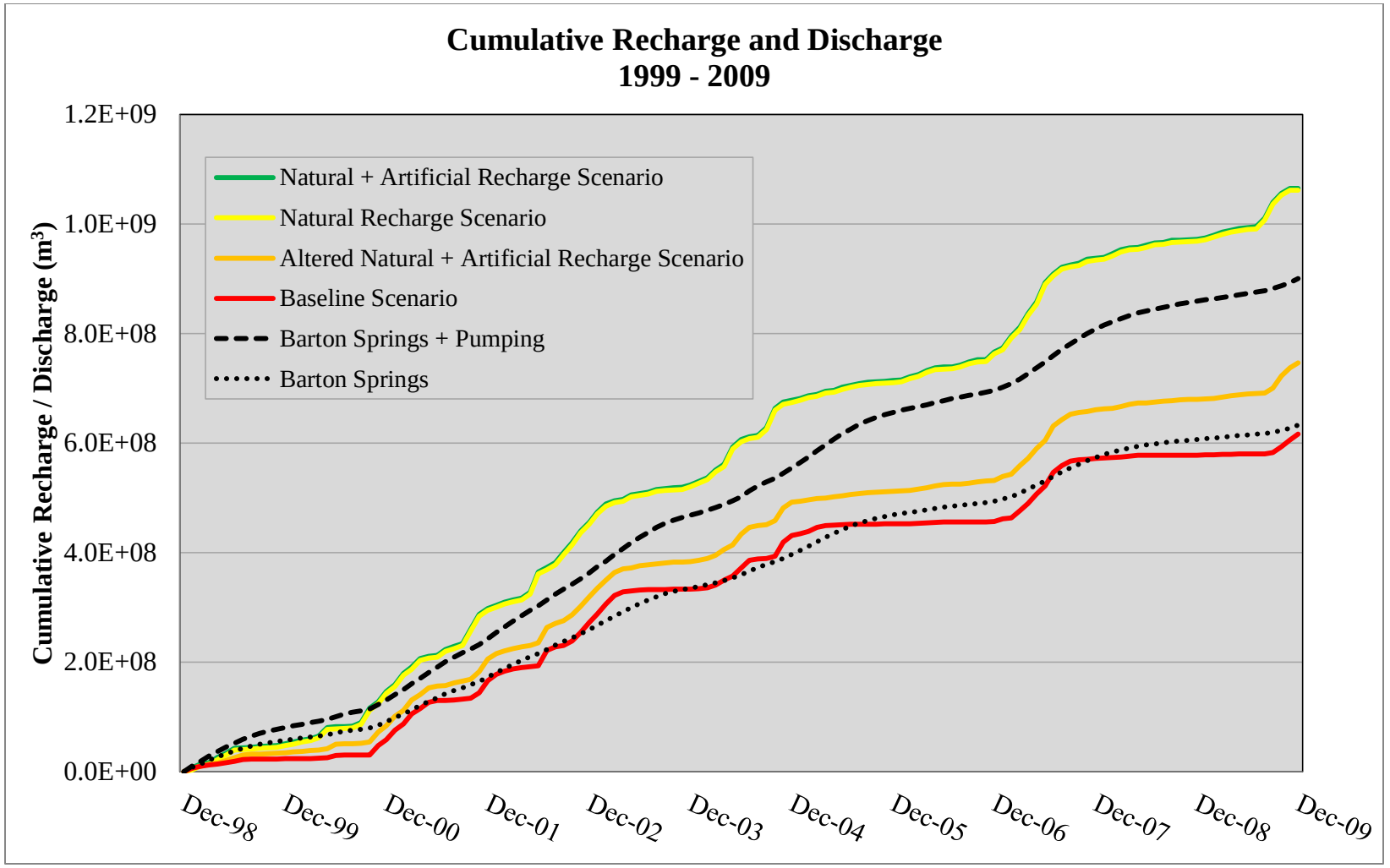

Figure 36: Cumulative Recharge and discharge for the four model scenarios.

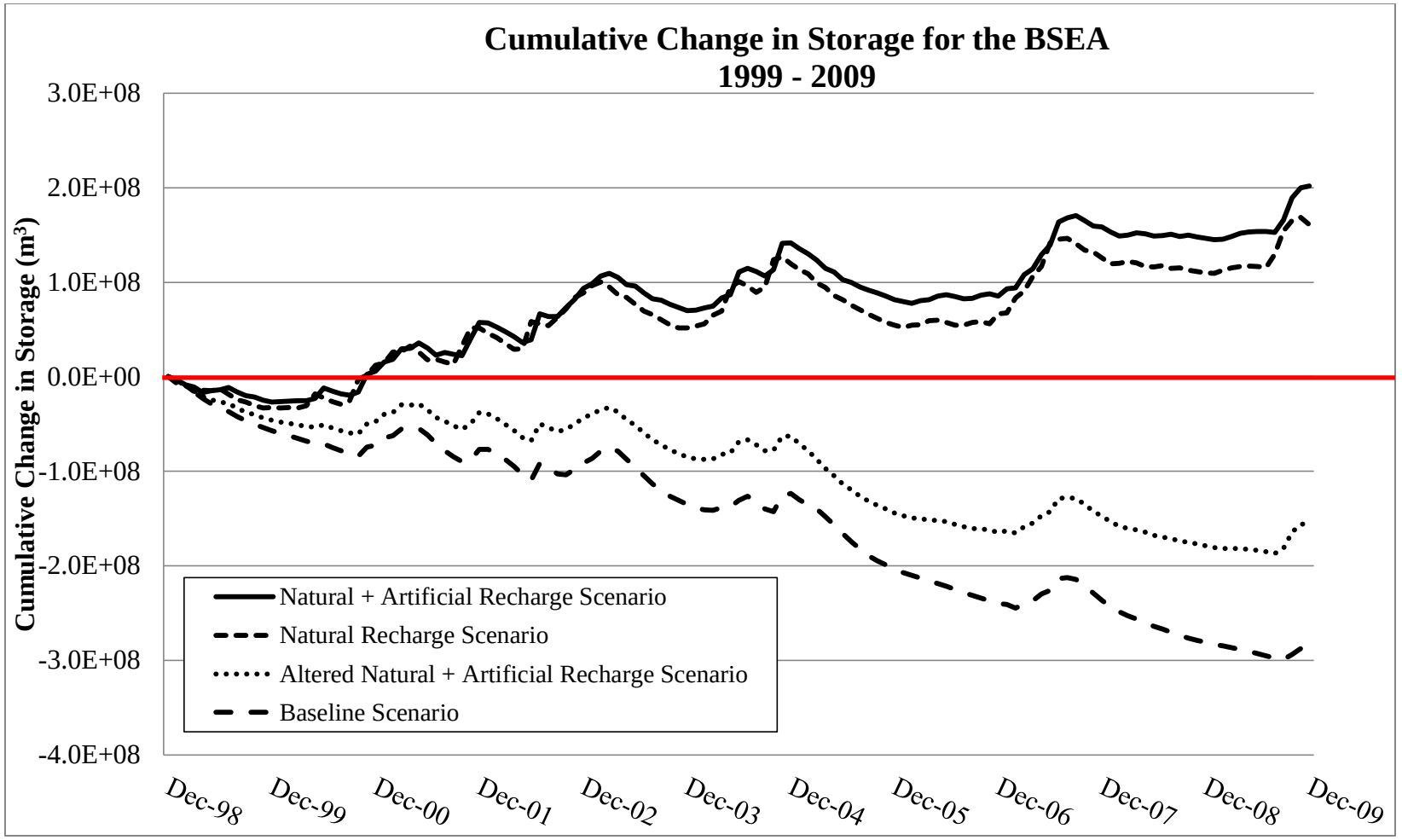

Figure 37: Cumulative change in storage for the four model scenarios (1999 - 2009).

Table 10: Residual statistics for simulated Barton Springs discharge (modified from Lindgren et al., 2009).

Type of simulation	Spring	Time Period	**Scanlon and others (2001)** RMSE (m^3/s)	**Smith and Hunt (2004)** RMSE (m^3/s)	**Winterle and others (2009)** RMSE (m^3/s)	**Baseline Scenario** RMSE (m^3/s)	**Natural Recharge Scenario** RMSE (m^3/s)	**Natural + Artificial Recharge Scenario** RMSE (m^3/s)	**Altered Natural + Artificial Recharge Scenario** RMSE (m^3/s)
Steady-state	Barton	Jul – Aug 1999	0	-	-	-	-	-	-
Transient	Barton	1989 – 98	0.34	-	-	-	-	-	-
Transient	Barton	1950 – 59	0.35	0.39	-	-	-	-	-
Transient	Barton	1950 – 59; flow less than 18 cfs	0.27	0.17	-	-	-	-	-
Transient	Barton	1999 - 2008	-	-	-	-	1.0	1.1	0.5

Table 11: Residual statistics for simulated water-level elevations for the BSEA (modified from Lindgren et al., 2009).

Type of simulation	Type of measurement	Time Period	Number of wells	**Scanlon and others (2001)** RMSE (m)	**Smith and Hunt (2004)** RMSE (m)	**Winterle and others (2009)** RMSE (m)	**Baseline Scenario** RMSE (m)	**Natural Recharge Scenario** RMSE (m)	**Natural + Artificial Recharge Scenario** RMSE (m)	**Altered Natural + Artificial Recharge Scenario** RMSE (m)
Steady-state	Synoptic	Jul – Aug 1999	99, 74	7	-	5.1	-	-	-	-
Transient	Synoptic	Mar – Apr 1994	27	9	-	-	-	-	-	-
Transient	Synoptic	Jul – Aug 1996	23	11	-	-	-	-	-	-
Transient	Synoptic	Jul – Aug 1998	35	20	-	-	-	-	-	-
Transient	Hydrographs	1989 – 98	8	1 – 26	-	-	-	-	-	-
Transient	Synoptic	1950 – 1959; lowest measured values	10	26	5.6	-	-	-	-	-
Transient	Synoptic	1999 – 2006; data from Hunt and Smith (2006)	104	-	-	-	-	22.6	24.0	10.5

Table 12: Change in storage for the four model scenarios (1999 - 2009).

Model Scenario	**Approximate Change in Storage (1999 -2009) (m^3)**
Baseline Scenario	-280,000,000
Natural Recharge Scenario	170,000,000
Natural + Artificial Recharge Scenario	200,000,000
Altered Natural + Artificial Recharge Scenario	-150,000,000

Water Budget Analyses

ARTIFICIAL RECHARGE SOURCES

Estimated artificial recharge from leaky water mains, leaky wastewater pipes, and irrigation return flow average 0.05, 0.022, and 0.022 $m^3 s^{-1}$ (1.9, 0.76, and 0.76 $ft^3 s^{-1}$), respectively (Figure 38, Table 13). Recharge from water mains and irrigation return flow oscillate between winter and summer months as water demands throughout the year peak during the summer. These peak recharge intervals coincide with months where lawn irrigation increases. Consequently, more water is transmitted through the water distribution network and is therefore available to leak or become irrigation return flow.

The range of recharge rates for each source varies. Wastewater leakage has the smallest estimated range of 0.017 - 0.032 $m^3 s^{-1}$ (0.59 – 1.12 $ft^3 s^{-1}$). Generally, water for irrigation is not transported to sewage treatment plants such that feedbacks to the treated volume of water are negligible. Therefore, there is not a concomitant increase in the volume of leakage from the wastewater network due to an increase in irrigation demands. Water main leakage rates range from 0.038 - 0.086 $m^3 s^{-1}$ (1.35 – 3.04 $ft^3 s^{-1}$) with peaks strongly correlating with summer months. Irrigation return flow has the greatest variance with a range of 0.000 - 0.171 $m^3 s^{-1}$ (0.00 – 6.05 $ft^3 s^{-1}$) and peaks during the summer months as well, although this can be altered by water rationing during droughts. The ranges of these two sources are best explained by the changes in irrigation demand throughout the year.

Leakage from water mains has a more constant rate of recharge since the majority of water distributed throughout the year is for municipal needs and is independent of the

seasons whereas irrigation return flow is clearly dependent upon the time of year since it affects PET and precipitation patterns. It is important to note that during time intervals where water demand for irrigation is high, recharge from irrigation return flow can be twice as large as recharge from both utility networks combined. However, for the majority of the year, recharge from leaky utility lines is greater than from irrigation return flow. The average total recharge from anthropogenic sources is 0.098 $m^3 s^{-1}$ (3.47 $ft^3 s^{-1}$) and ranges from 0.058 - 0.259 $m^3 s^{-1}$ (2.04 – 9.15 $ft^3 s^{-1}$).

The cumulative recharge from leaky water mains over the ten-year study period is approximately 1.8×10^7 m^3 (14,593 acre-feet) whereas the cumulative recharge for leaky wastewater pipes and irrigation return flow are approximately 7.3×10^6 m^3 and 8.2×10^6 m^3 (5,918 and 6,648 acre-feet), respectively (Figure 39, Table 13). Consequently, leakage from the water distribution network is the most significant source of artificial recharge in the study area. The cumulative recharge of each source increases approximately linearly. For irrigation return flow, cumulative recharge increases in a somewhat stair step pattern with sharp increases coinciding with summer months and increases in lawn irrigation.

When comparing the contribution of artificial recharge sources to the overall recharge of the study site and time period, artificial recharge constitutes approximately 4.34% of the total recharge to the BSEA from January, 1999, to December, 2009 (Figure 40, Table 13). In comparison to natural recharge sources, long-term artificial recharge is greater than Williamson (1.34%), Little Bear (3.26%), and Slaughter Creeks (4.33%). It is also comparable to Bear Creek which contributes approximately 5.60% of total recharge.

These contributions are ten-year averages and are highly variable on a month by month basis. In fact, the contribution to total monthly recharge from artificial recharge sources can range from <1 to 52%. This variance is not explained by significant fluctuations in artificial recharge, but rather changes in contributions from losing streams and precipitation. For months with little to no precipitation, recharge contributions from natural sources are comparable to artificial recharge sources. However, in wet months, artificial recharge is dwarfed by its natural counterparts. Three months representing minimal, maximum and mean recharge conditions are shown in Figures 41 and 42 to demonstrate how the relative contribution of artificial recharge can vary on a month by month basis.

It is important to note that limitations in the methods for calculating recharge from Little Bear Creek and precipitation artificially lower the relative contribution of artificial recharge sources for the minimal recharge condition (Figures 41 and 42). Because Little Bear Creek recharge is calculated as a percentage of Barton Springs discharge and Barton Springs never stopped flowing during the study period, there is always recharge taking place in this watershed. In reality, recharge for Little Bear Creek is similar to the other creeks in that for the majority of time it is dry and the watershed contributes only artificial recharge. These dry time intervals are offset by flashy storm events which result in flashy recharge events (see Figures 43 – 48). The same can be said for the diffuse recharge calculations.

Monthly NEXRAD precipitation data are interpolated from radar and rain gauges and do not have zero values. Consequently, for months where no rainfall takes place, there are values of precipitation within the NEXRAD data sets that are very small

(several decimal places) but not zero. This leads to overestimated diffuse recharge volumes for months where no actual precipitation takes place. Ultimately, the true relative contribution to total recharge from artificial sources for minimum recharge months is 100%.

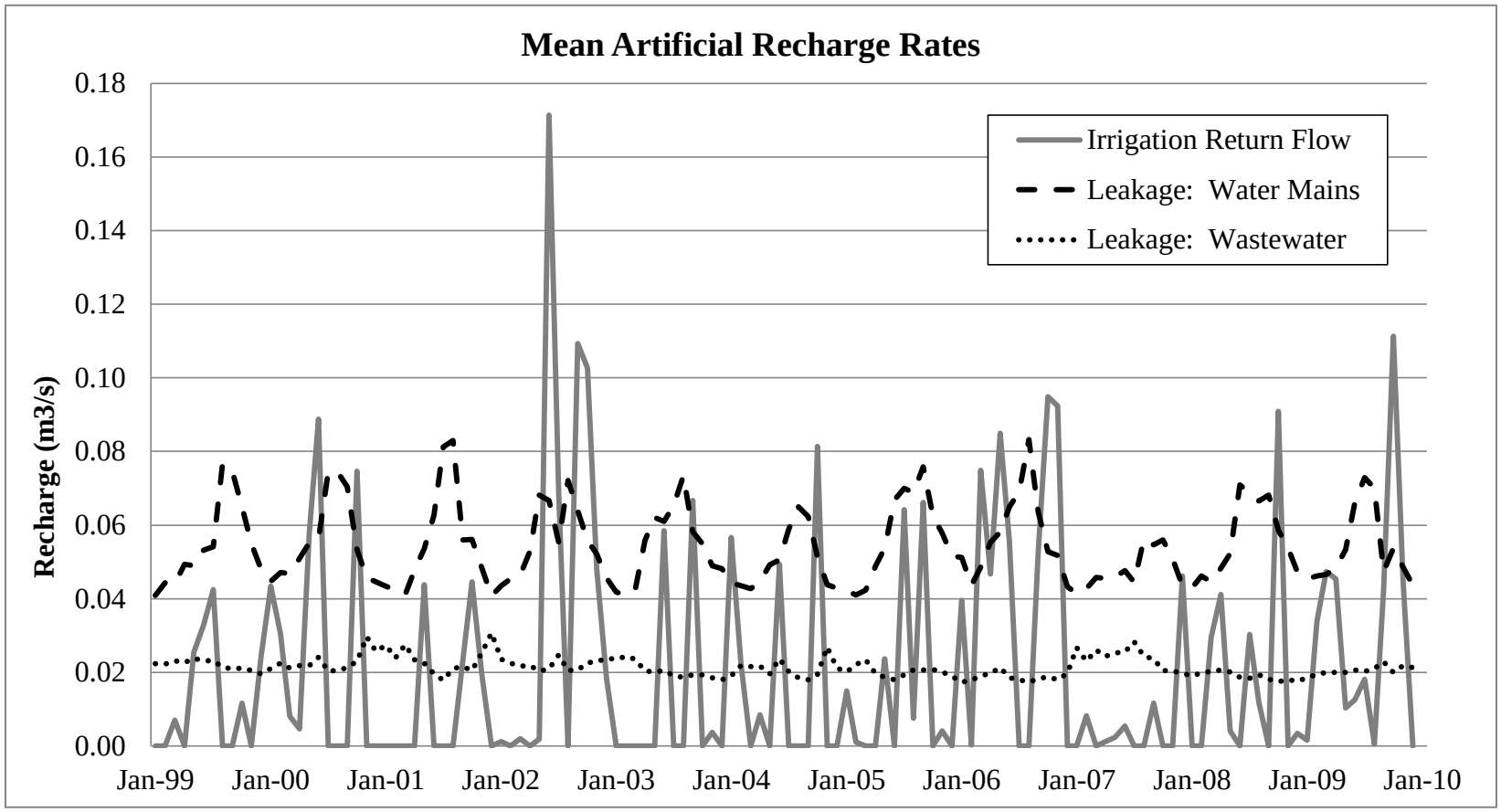

Figure 38: Graph of mean monthly recharge rates within the recharge zone of the BSEA from irrigation return flow, leaky water mains, and leaky wastewater pipes.

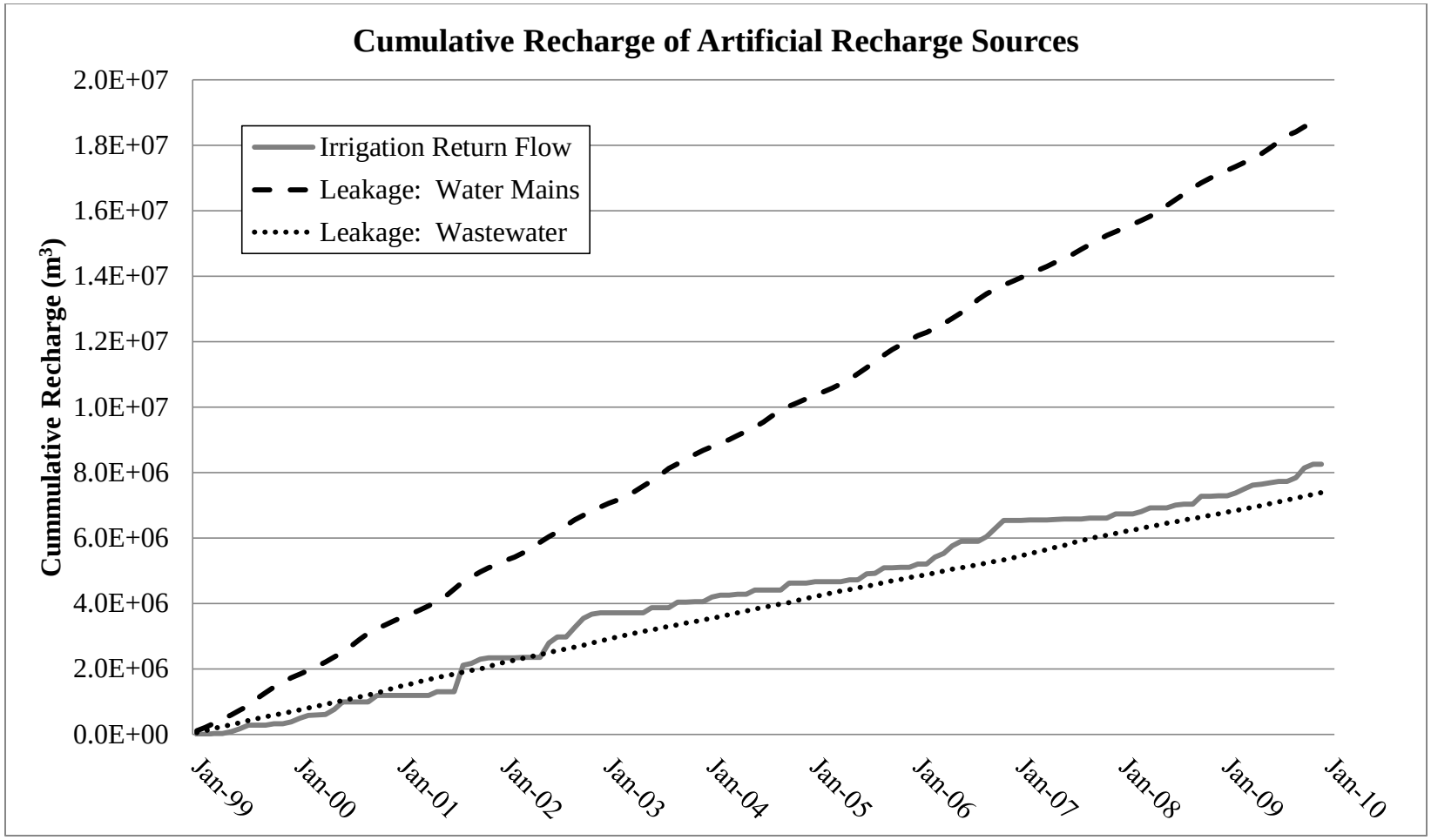

Figure 39: Graph of cumulative recharge volumes within the recharge zone of the BSEA from irrigation return flow, leaky water mains, and leaky wastewater pipes.

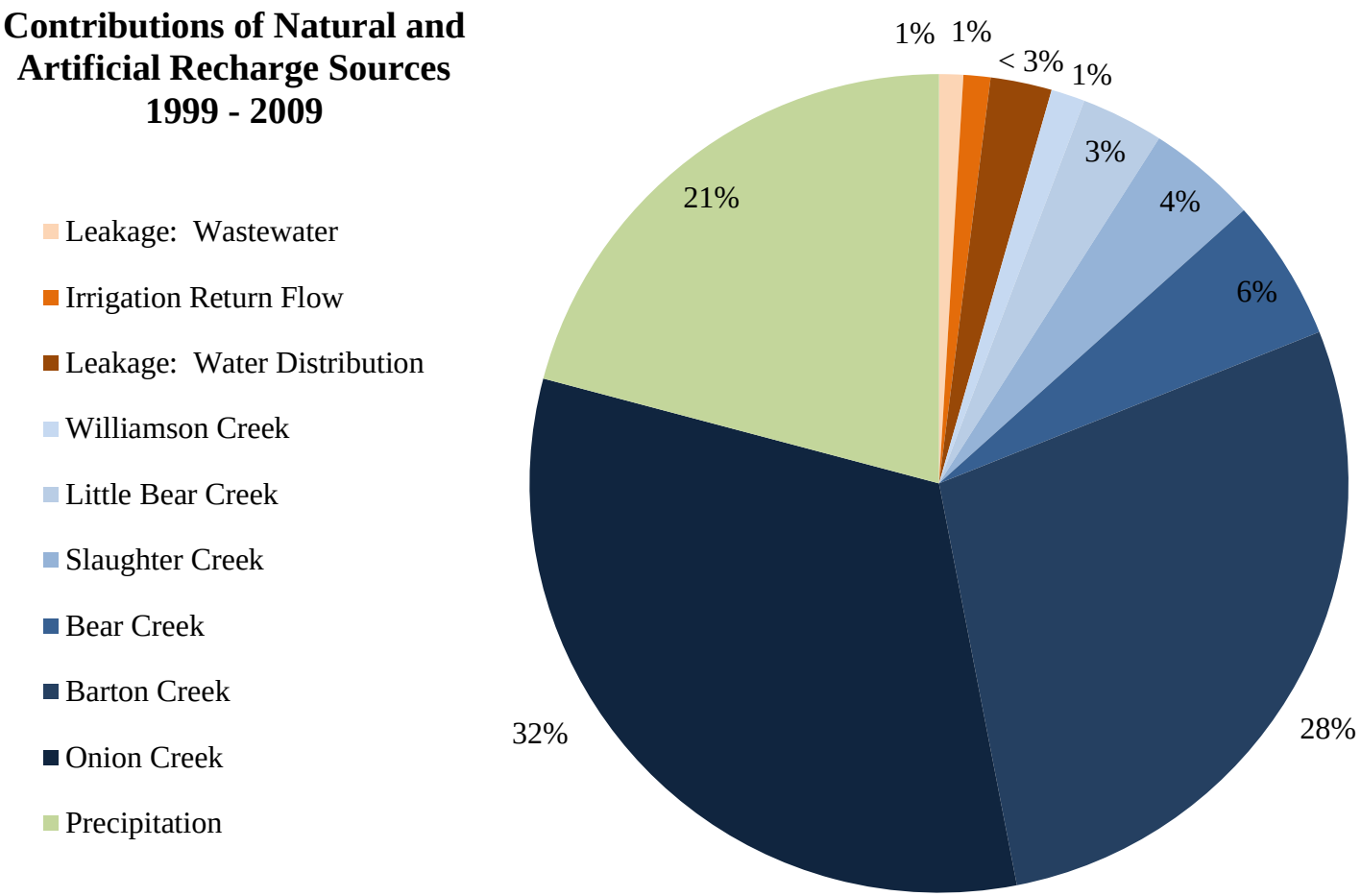

Figure 40: Comparison of artificial and natural recharge sources for the 10-year study period (January, 1999 - December, 2009). Artificial sources (orange) constitute approximately 5% of the total recharge.

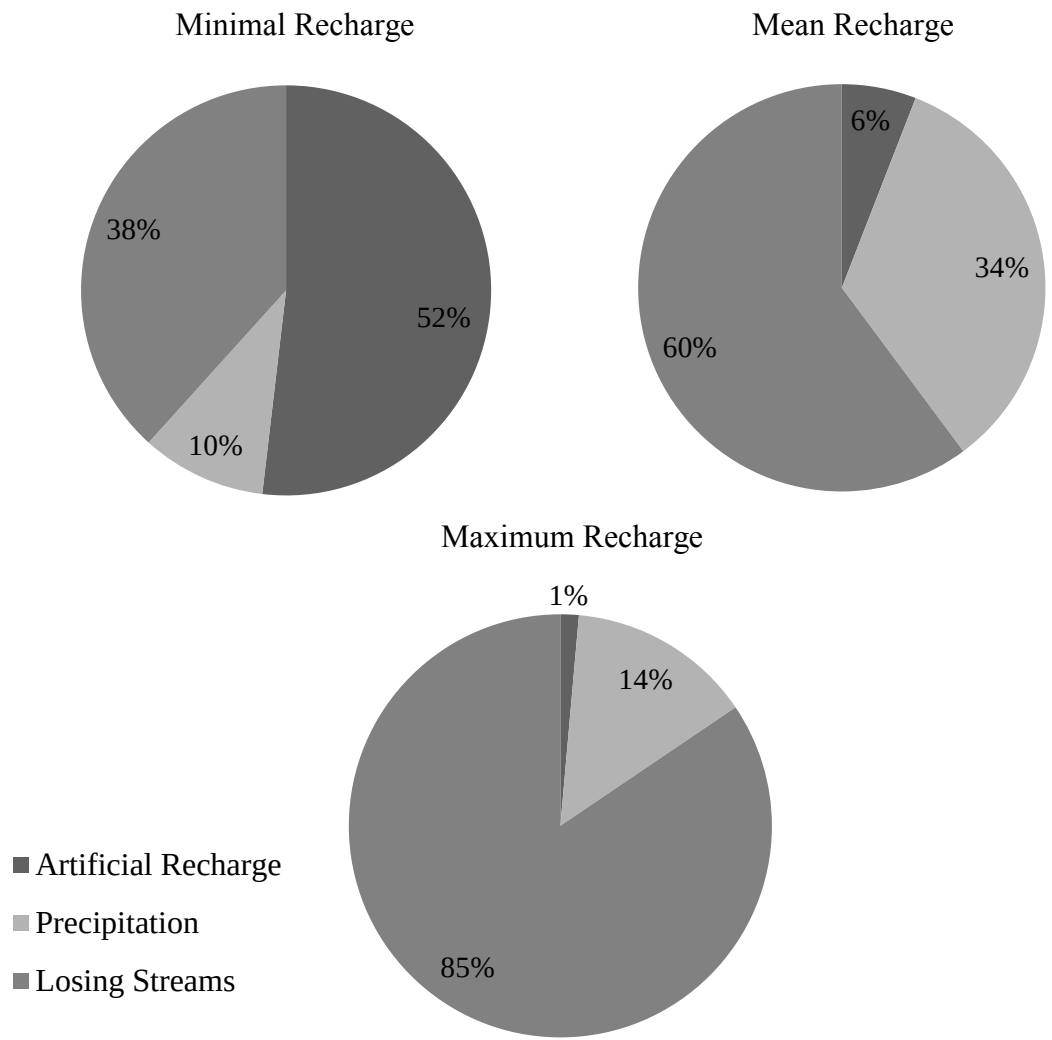

Figure 41: Comparison of recharge contributions from artificial and natural sources during varying recharge conditions.

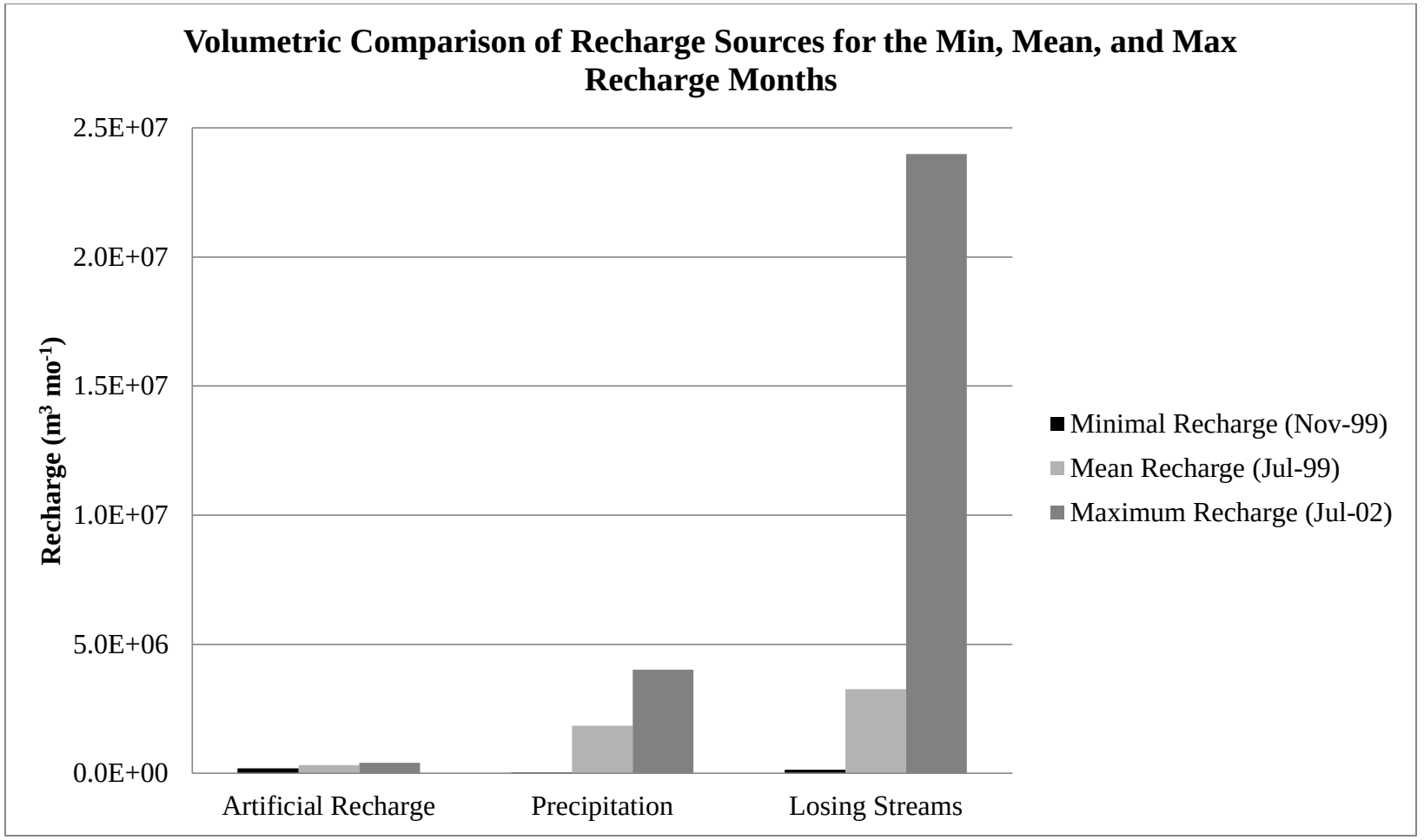

Figure 42: Volumetric comparison of artificial and natural recharge sources for the minimum, average, and maximum recharge months for the study period (January, 1999 – December, 1999).

Table 13: Minimum, maximum, and mean recharge rates for all recharge sources for the Altered Natural + Artificial Recharge scenario. *Minimum recharge rates for these recharge sources are 0.0 $m^3 s^{-1}$ in reality. Precipitation values are based upon interpolation techniques from NEXRAD gridded precipitation. The interpolation techniques do not allow for zero values, rather decimals that approach zero. Little Bear Creek's recharge was calculated as a percentage of Barton Springs discharge and therefore never reaches zero (see Methods, Figure 45).

Recharge Source	**Minimum ($m^3 s^{-1}$)**	**Maximum ($m^3 s^{-1}$)**	**Mean ($m^3 s^{-1}$)**	**Cumulative Recharge (m^3) 1999- 2009**	**Percentage of Total Recharge (%) 1999 - 2009**
Onion Creek	0.000	3.469	1.479	2.5×10^8	32.17
Barton Creek	0.000	6.128	1.315	2.1×10^8	27.98
Precipitation	0.014*	2.247	0.474	1.6×10^8	20.88
Bear Creek	0.000	0.781	0.260	4.3×10^7	5.60
Slaughter Creek	0.000	1.013	0.205	3.4×10^7	4.33
Little Bear Creek	0.017*	0.135	0.147	2.5×10^7	3.26
Total Artificial Recharge	0.058	0.259	0.098	3.4×10^7	4.34
Williamson Creek	0.000	0.271	0.063	1.0×10^7	1.34
Leakage: Water Distribution	0.038	0.086	0.055	1.8×10^7	2.42
Irrigation Return Flow	0.000	0.171	0.022	8.3×10^6	1.06
Leakage: Wastewater	0.017	0.032	0.022	7.4×10^6	0.95

Natural Recharge Sources

Natural recharge sources provide approximately 96% of long-term recharge for the BSEA (1999 – 2009) (Table 13). Losing streams contribute 75% of this total recharge while diffuse recharge is responsible for 21%. These values are consistent with previous studies but slightly differ in that the contribution to total recharge from losing streams is lowered and greater emphasis is placed upon diffuse recharge (Table 14). Recent studies have had similar findings and have also suggested that diffuse recharge contributes greater amounts than previously estimated (Hauwert, 2009; Hauwert et al., 2011 in press).

LOSING STREAMS

Recharge from losing streams is highly dependent upon precipitation events. All of the streams experience time intervals (1 – 6 months) of no stream flow due to insufficient precipitation. Therefore, there are time intervals of minimal recharge that coincide with these dry time periods (Figures 43 – 48). When precipitation events do take place in great enough magnitudes to generate stream flows, stream recharge increases dramatically resulting in flashy recharge events. This is evident not only by analyzing monthly recharge rates (Figures 43 – 48), but also apparent when plotting cumulative recharge volumes (Figure 49). All of the streams have a stair-step pattern for cumulative recharge explained by intervals of virtually no stream flow followed by sharp increases coinciding with precipitation events.

When comparing the streams to one another, Onion Creek is the largest contributor followed by Barton, Bear, Slaughter, Little Bear, and Williamson Creek

(Figures 50 and 51). Onion Creek contributes 42% of the total stream recharge for the study period which equates to approximately 2.5×10^8 m^3 (202, 678 acre-feet) or 32% of all recharge for the BSEA. Other individual stream contributions to total recharge for the BSEA are similar to values previously reported as well (Slade et al., 1986; Barrett and Charbeneau, 1996; Hauwert et al., 2011 in press) (Table 14).

PRECIPITATION

Values of diffuse recharge from this study and from previous work are by far the most questionable. They may be accurate but, in comparison to recharge estimates for other sources, they introduce the greatest amount of uncertainty. This is mainly due to the lack of data and the difficulty of taking direct measurements, land surface heterogeneity, and the general lack of understanding of how this recharge mechanism works. It is estimated from the Altered Natural + Artificial Recharge scenario that diffuse recharge constitutes approximately 21% of the total recharge to the BSEA (1999 – 2009) or 1.6×10^8 m^3 (129,714 acre-feet) (Figures 40; Table 13, 14). As discussed above in the Modeling Results section, this volume of recharge is insufficient to honor the assumption of no long-term change in aquifer storage. Therefore, there is a reduction of 1.56×10^8 m^3 (126,471 acre-feet) in storage over the ten-year study period (1999 – 2009). In order for there to be no change in storage, the precipitation infiltration percentage would have to be approximately 18.5%. This is within the range of previous studies (6 – 32%) (Hauwert, 2009; Wiles, 2007; Barrett and Charbeneau, 1996; Slade et al., 1985). However, utilizing this rate generates less agreement between simulated Barton Springs discharge and water-level elevations compared to the outputs from the Altered Natural + Artificial Recharge scenario (RMSE 0.58 vs. 0.50 m^3 s^{-1} and 14.3 vs.

10.5 m or 20.5 vs. 17.7 cfs and 46.9 vs. 34.5 feet) (Figures 53 - 55). These results indicate that simulated spring flows and water-level elevations are generally overestimated, suggesting that diffuse recharge is overestimated when using 18.5%. However, lowering the precipitation infiltration percentage induces deficits in aquifer storage according to the water budget analyses. Lack of agreement between the water budget analyses and the modeling analyses are most likely the result of the inherent limitation of the methods employed for determining diffuse recharge and the model framework. Additionally, the model probably inadequately represents true aquifer characteristics for hydraulic conductivity, transmissivity, specific yield, and storativity.

The method of employing precipitation infiltration percentages for calculating diffuse recharge is appropriate for long-term (yearly or greater) water budget analyses. However, the models analyzed in this study probably underestimates and/or overestimates recharge for short timescales (monthly or less). In reality, precipitation infiltration percentages may vary greatly from storm event to storm event and are a function of antecedent moisture conditions. This may explain why the model is unable to produce more accurate simulations of spring flows and water-level elevations as recharge inputs for the model are on monthly time steps, whereas the diffuse recharge quantification probably require sub-monthly if not sub-daily quantification. However, lack of agreement could also be explained by the inherent inaccuracy of the model and complexity of representing the karstic groundwater system as an equivalent porous media. Ultimately, the data from this study suggest that on average approximately 6 – 19% of annual precipitation recharge the aquifer for the BSEA.

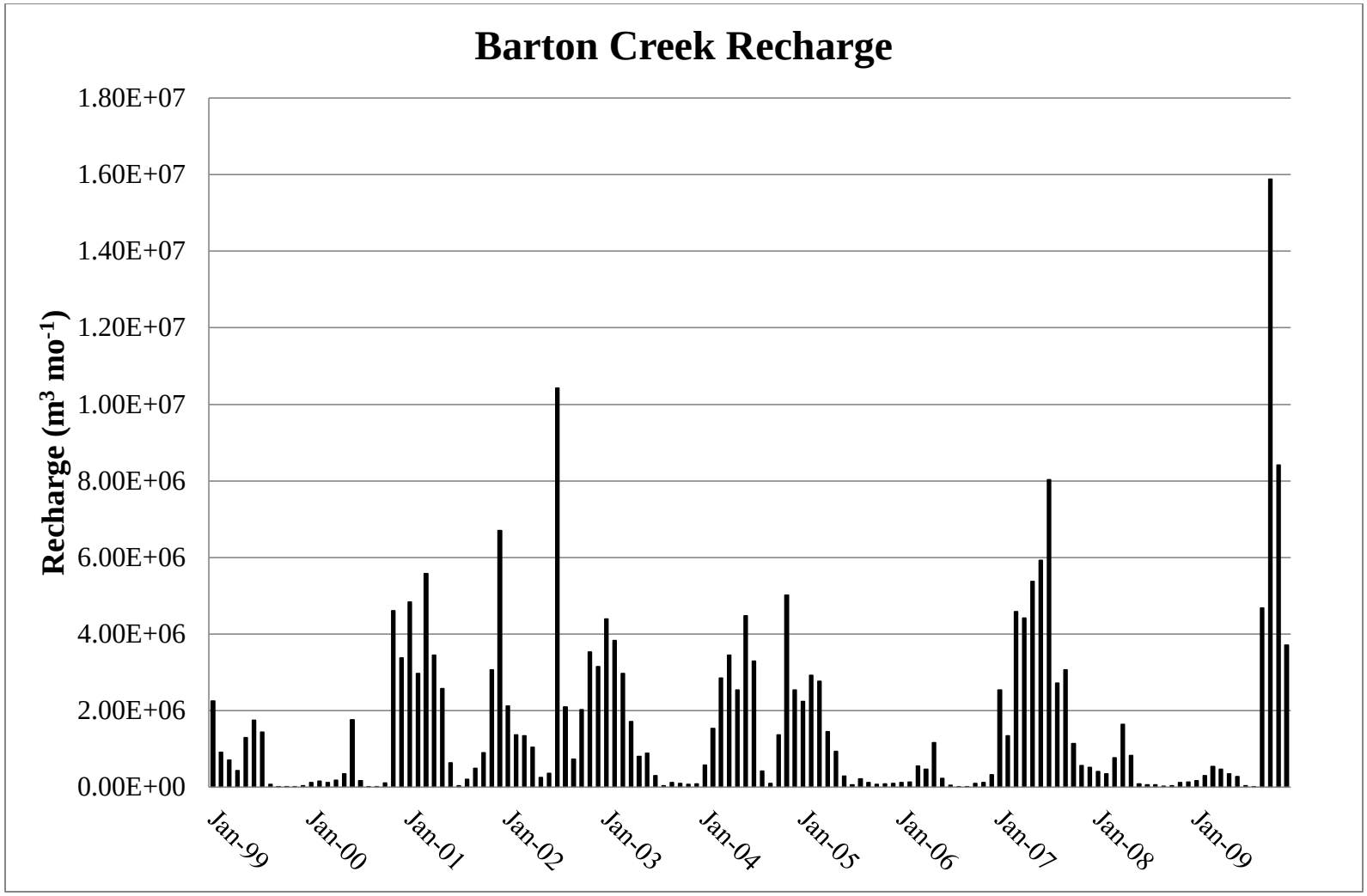

Figure 43: Monthly recharge for Barton Creek.

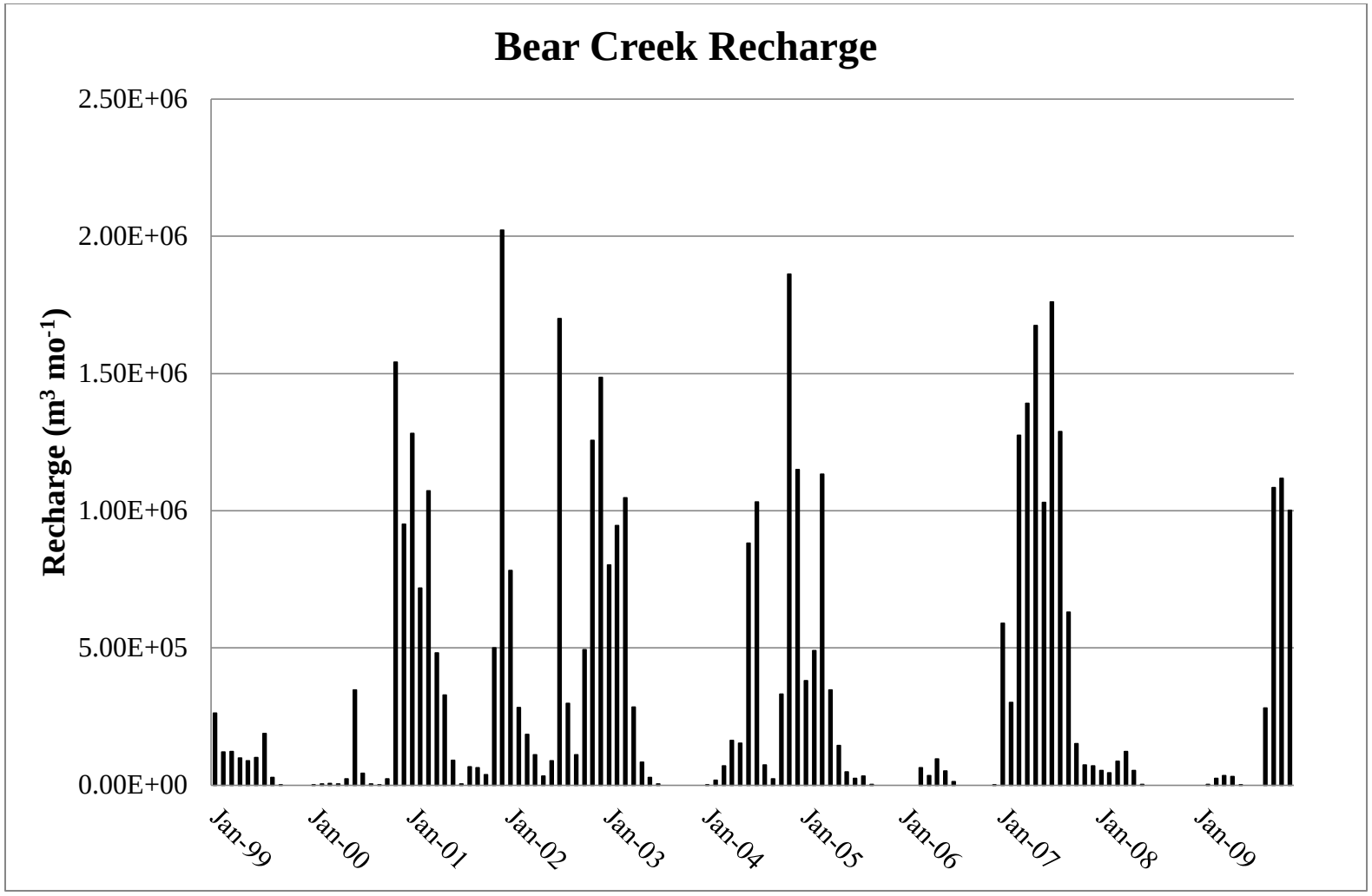

Figure 44: Monthly recharge for Bear Creek.

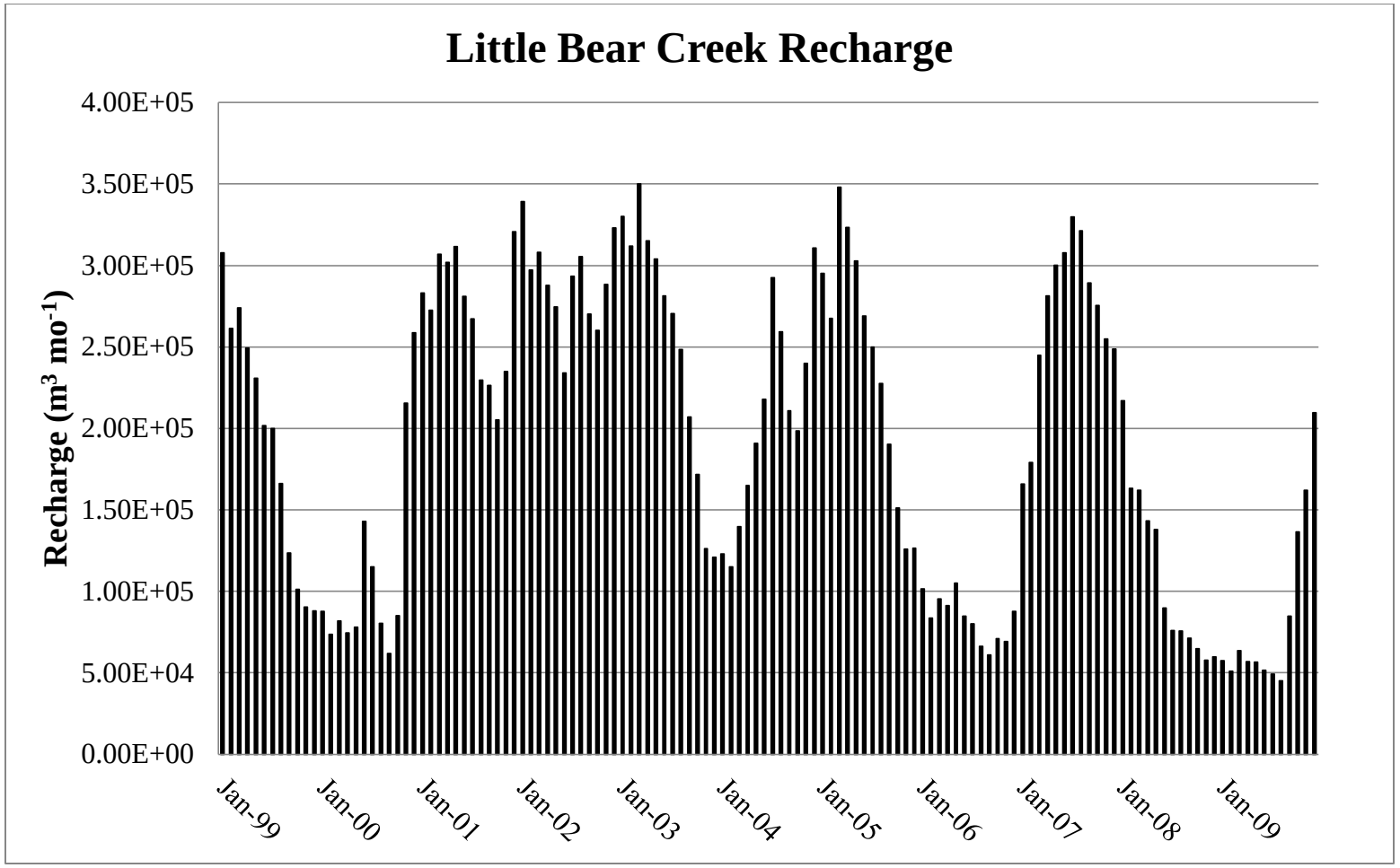

Figure 45: Monthly recharge for Little Bear Creek. These recharge volumes are calculated as a percentage of Barton Springs discharge (see Methods, Table 5) so no zero values exist. This is untrue for actual recharge but was determined this way since no stream gaging data existed.

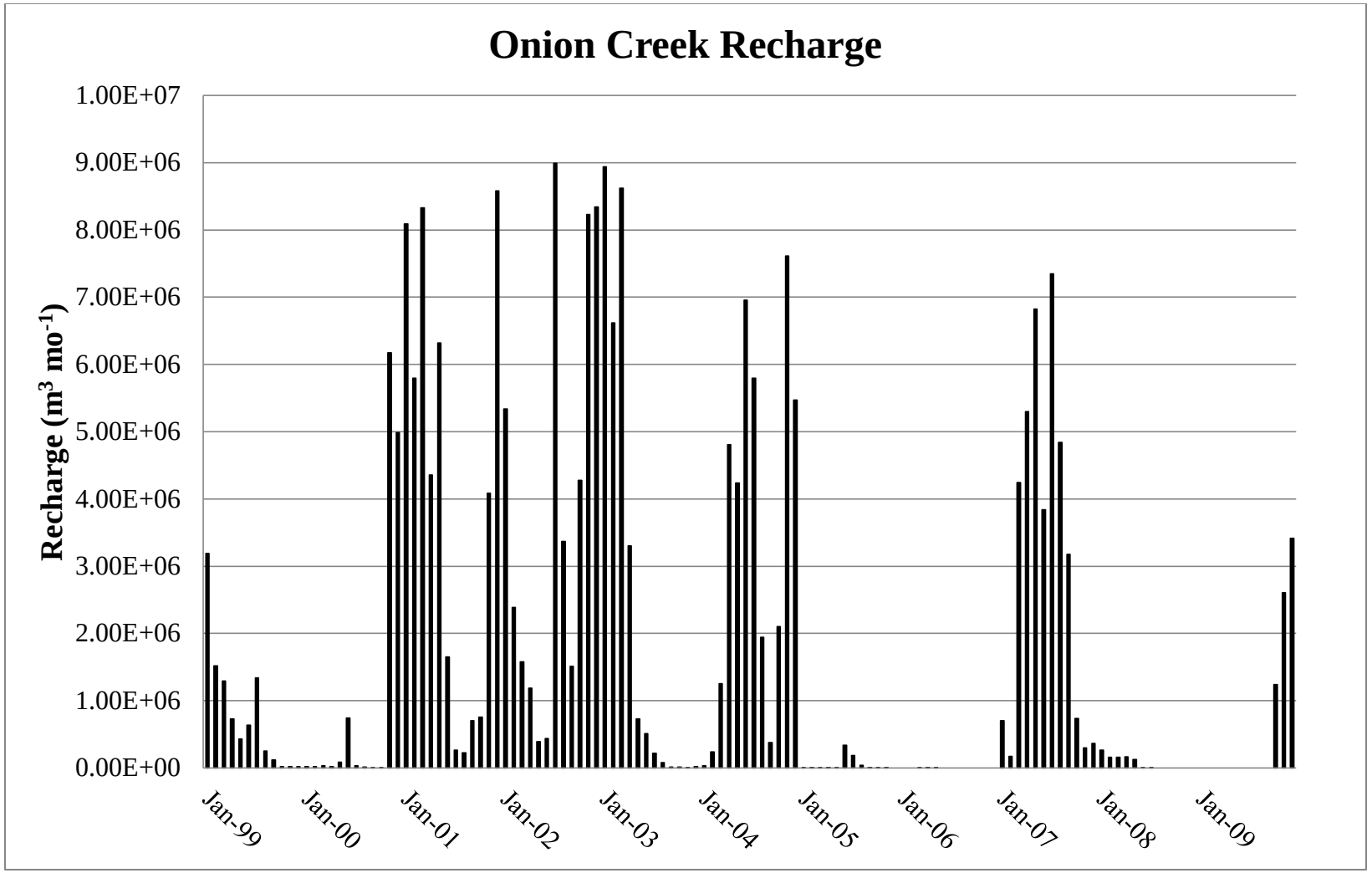

Figure 46: Monthly recharge for Onion Creek.

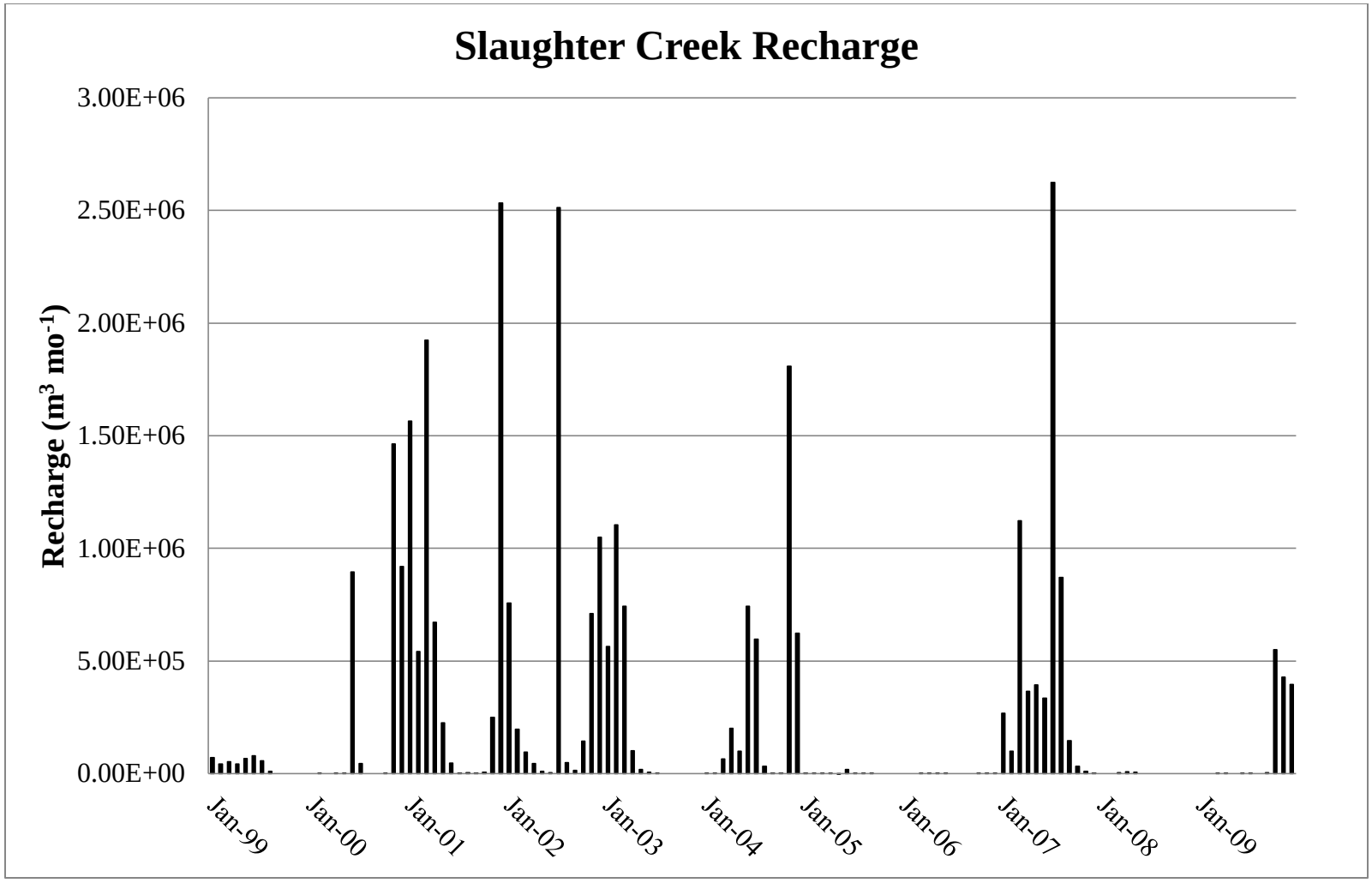

Figure 47: Monthly recharge for Slaughter Creek.

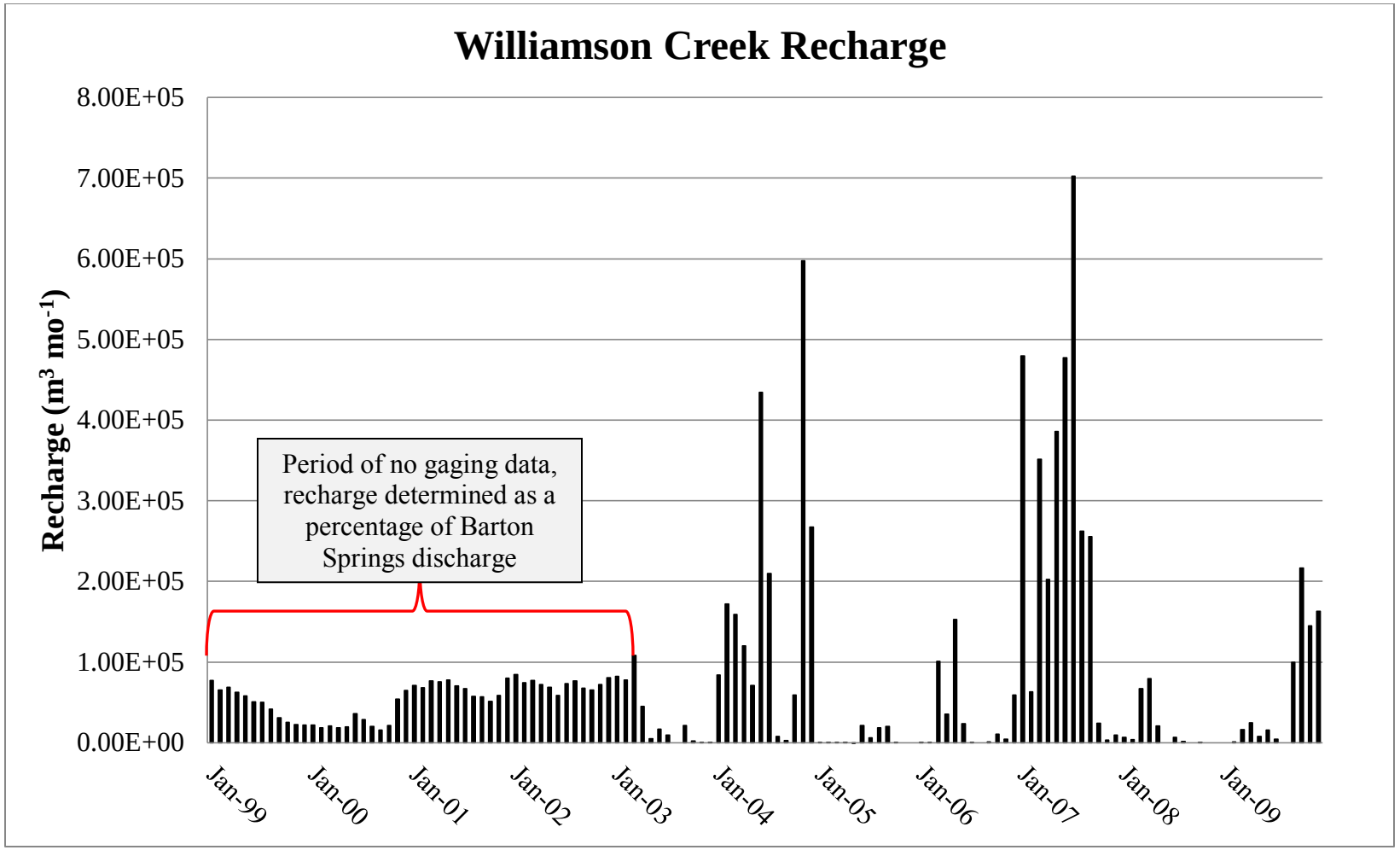

Figure 48: Monthly recharge for Williamson Creek. Periods when no gaging data existed were accounted for by calculating recharge as a percentage of Barton Springs discharge (see Methods).

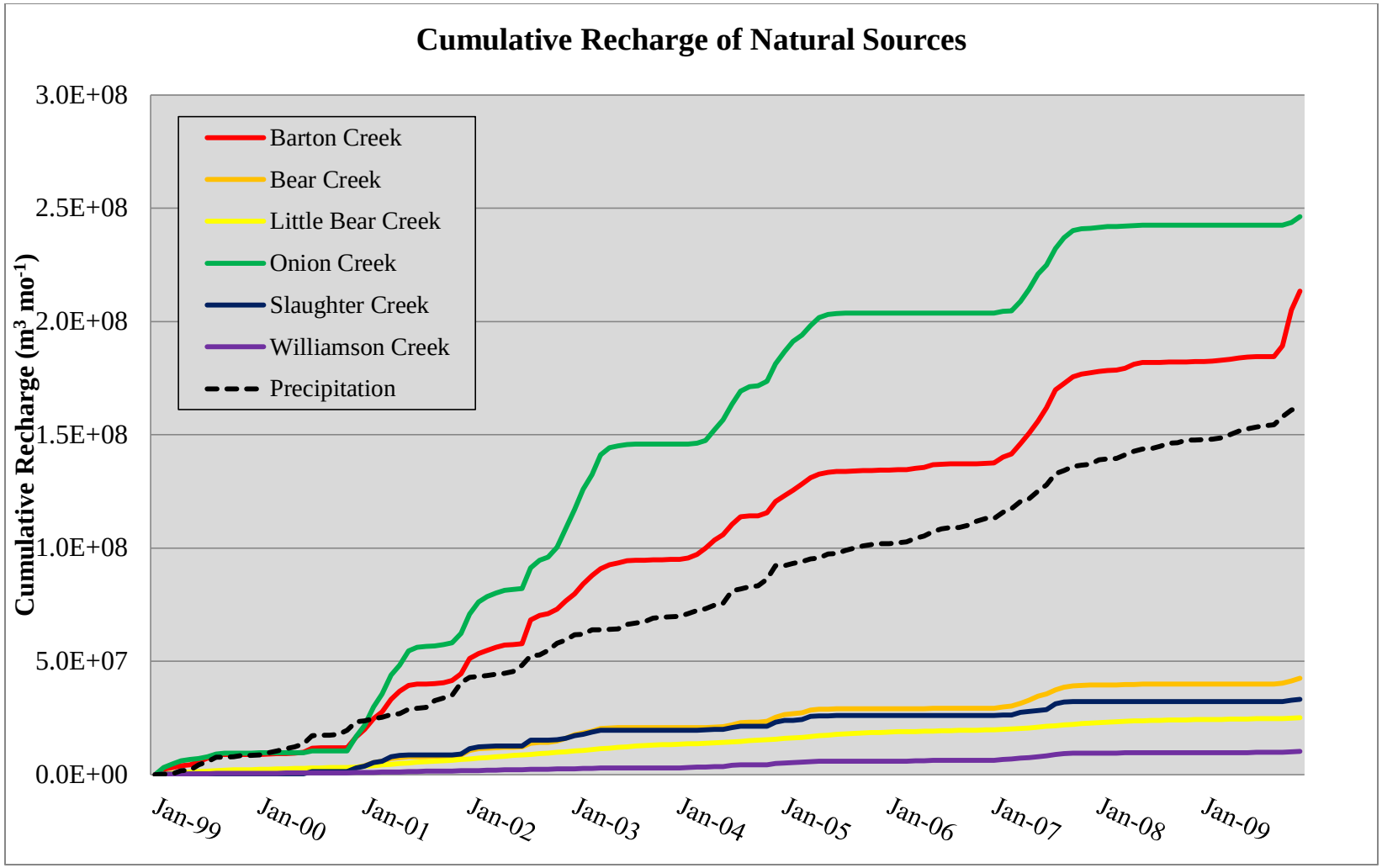

Figure 49: Cumulative recharge of natural sources within the BSEA (January, 1999 – December, 1999).

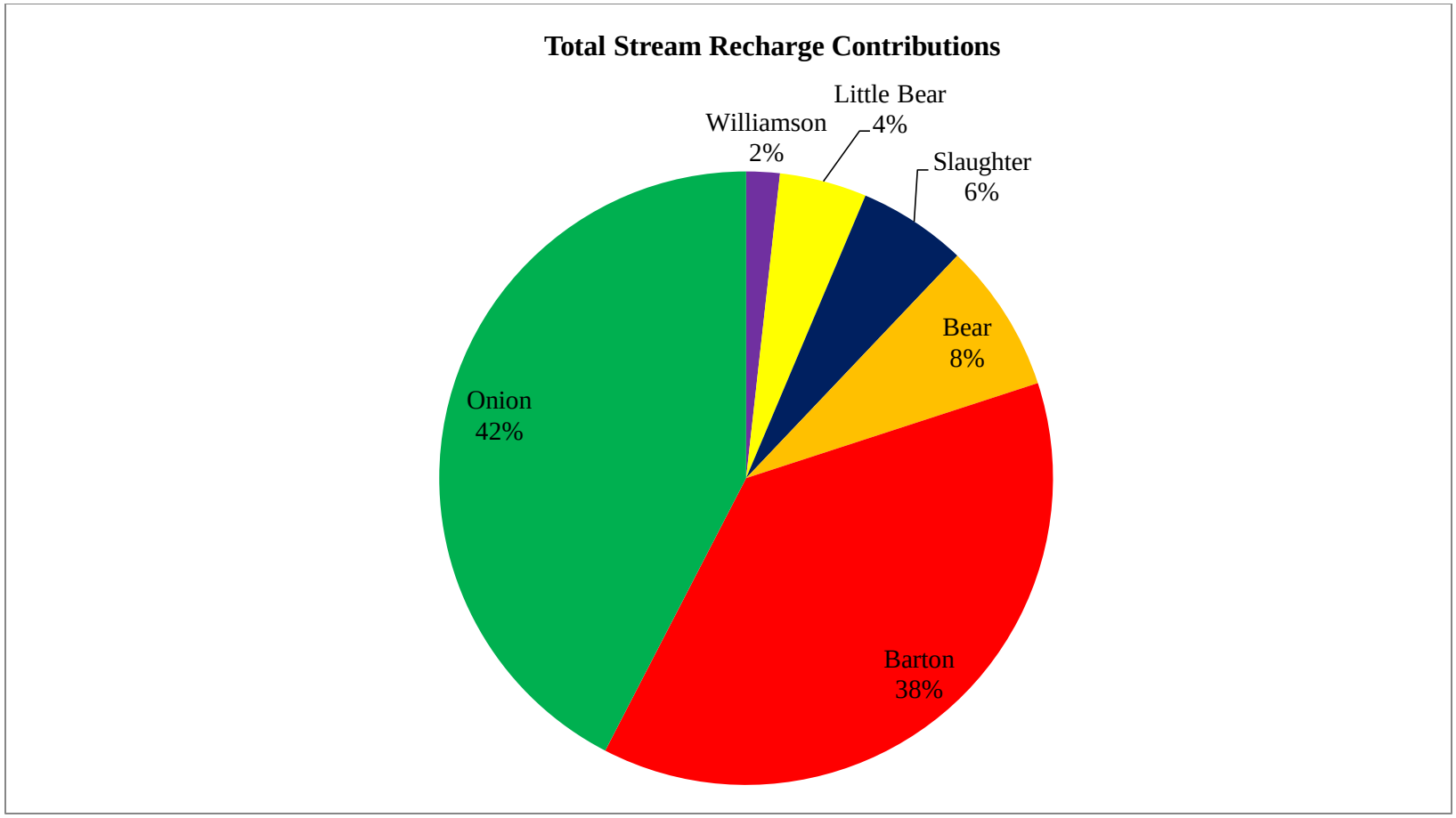

Figure 50: Recharge contributions of individual losing streams as a proportion of total stream recharge (January, 1999 – December, 1999).

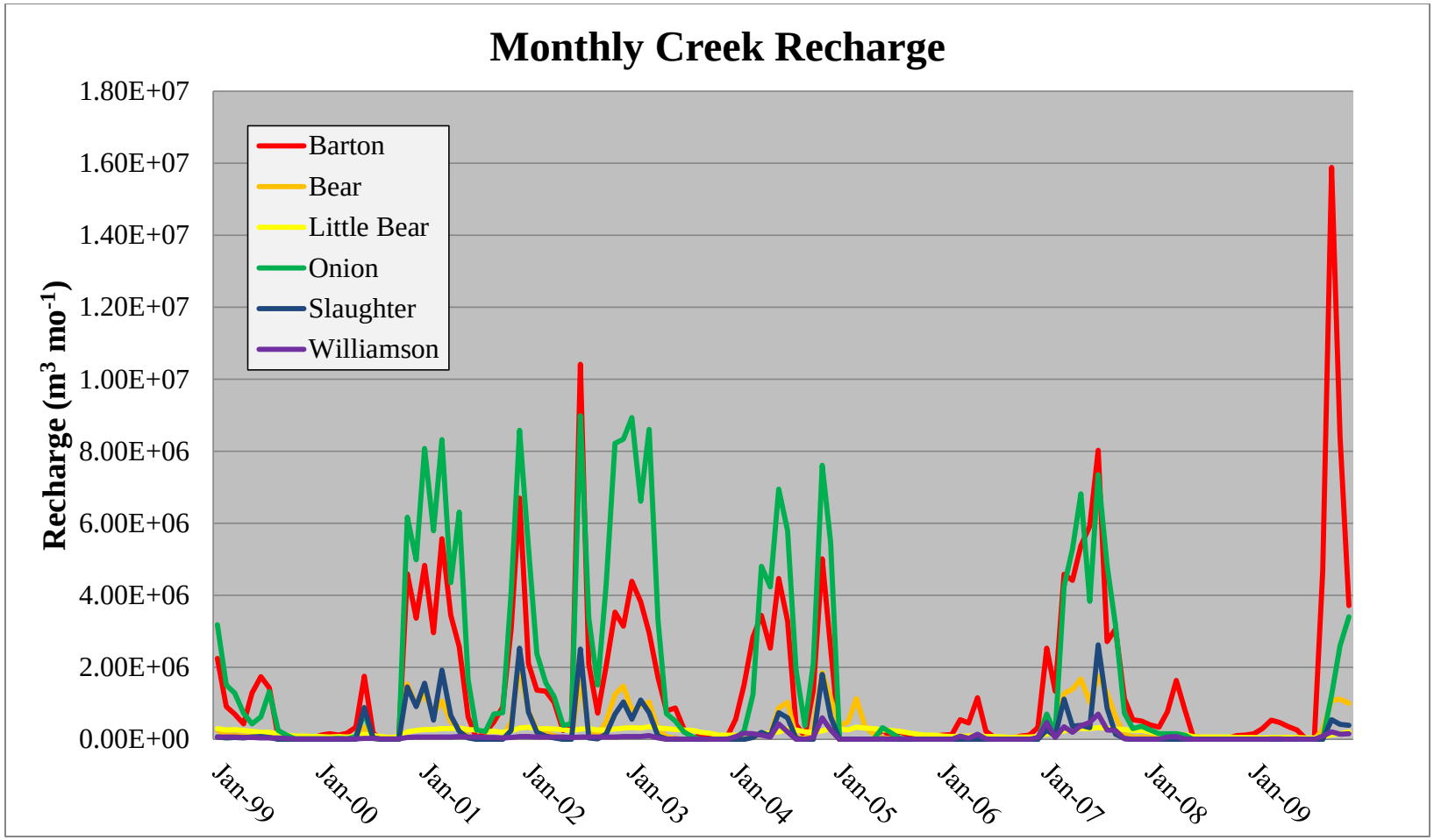

Figure 51: Monthly recharge volumes of individual losing streams within the BSEA (January, 1999 – December, 1999).

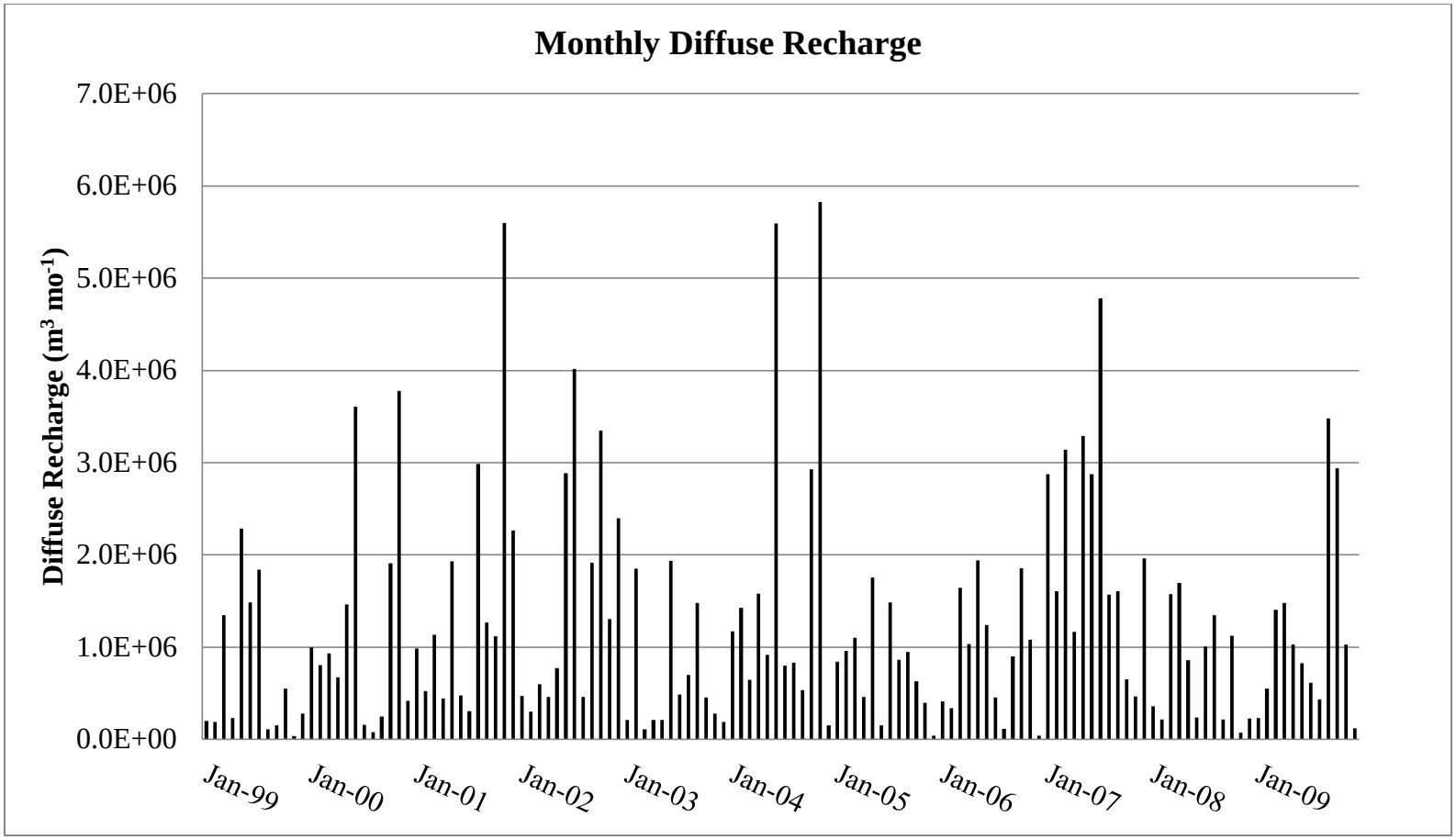

Figure 52: Plot of monthly diffuse recharge (1999 - 2009)

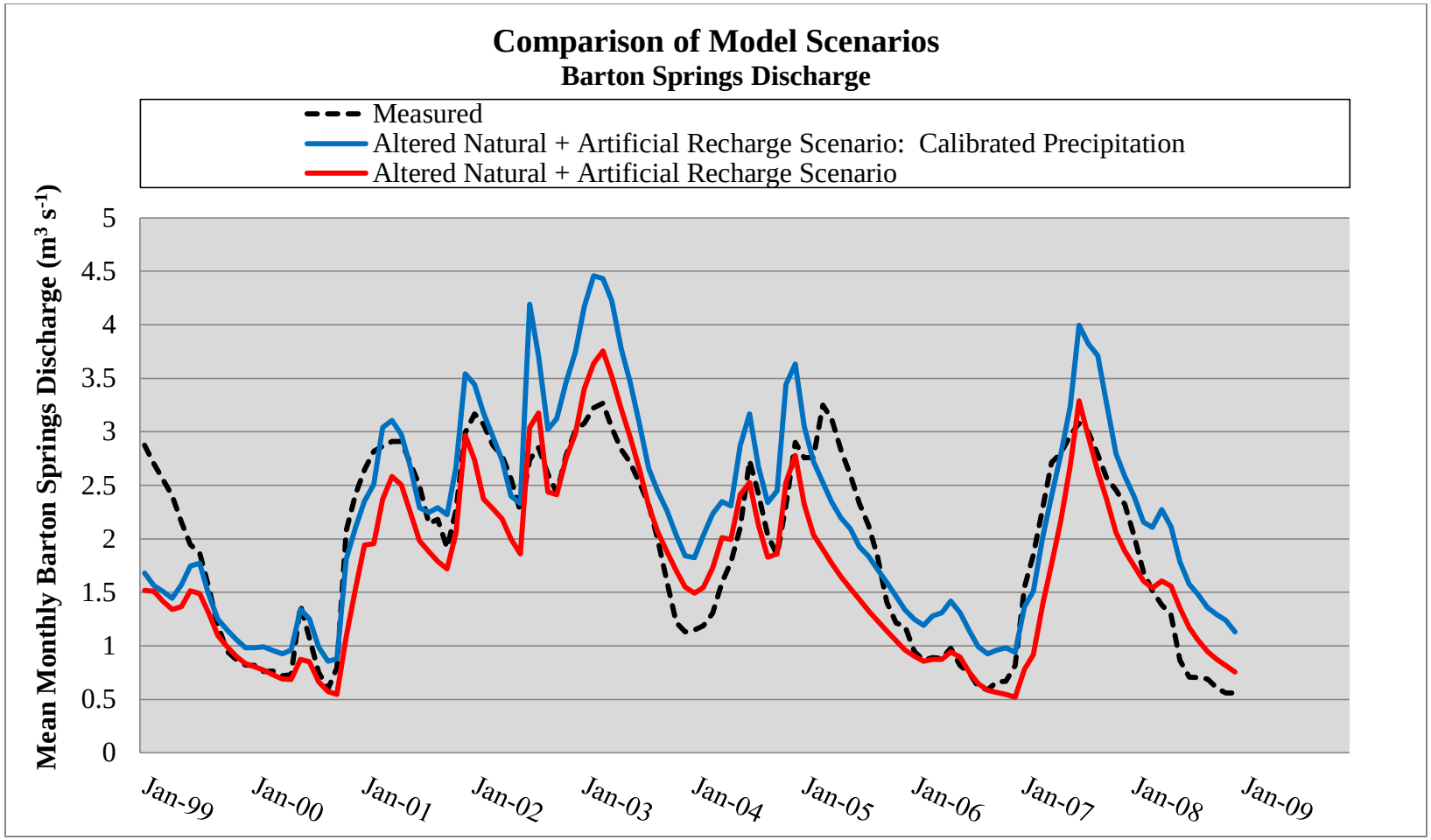

Figure 53: Graph of simulated and measured mean monthly Barton Springs discharge from January, 1999 – December, 2008 for the Altered Natural + Artificial Recharge scenario before (red) and after (blue) calibration. The calibrated version utilizes the precipitation infiltration percentage (18.5%) determined from the water budget analysis.

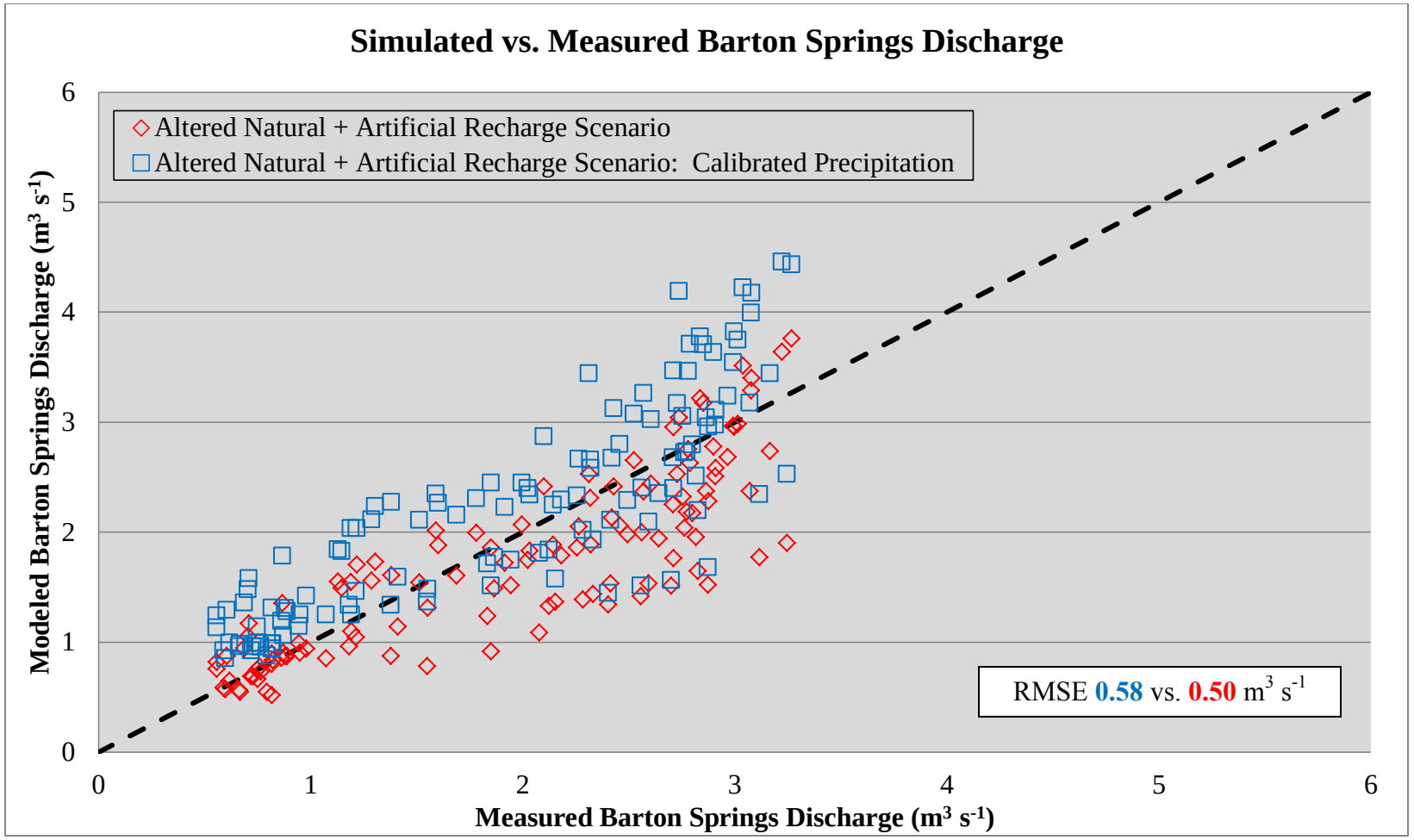

Figure 54: Scatter plot of simulated versus measured Barton Springs discharge from January, 1999 – December, 2008 for the Altered Natural + Artificial Recharge scenario before (red) and after (blue) calibration. The calibrated version utilizes the precipitation infiltration percentage (18.5%) determined from the water budget analysis.

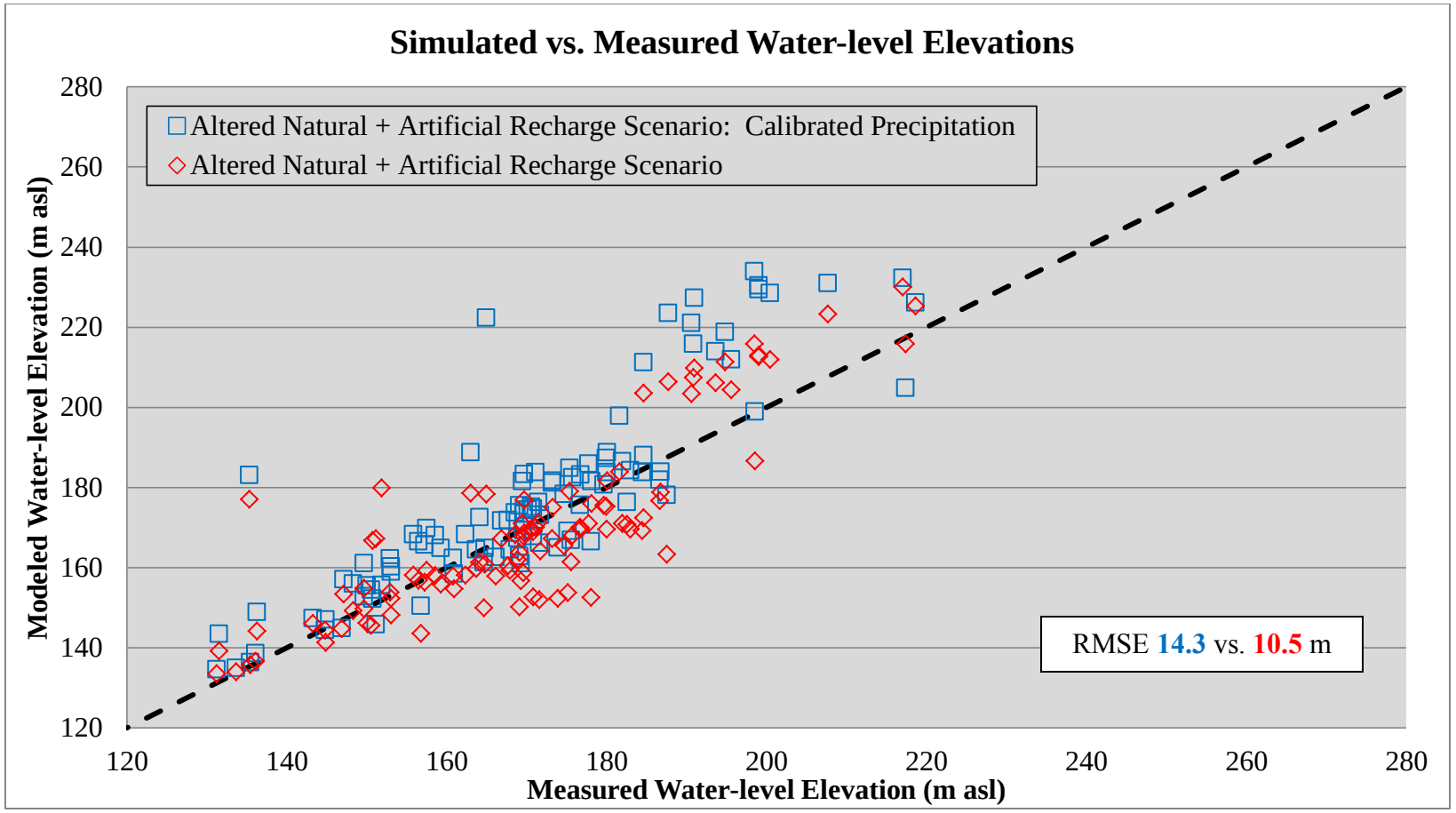

Figure 55: Scatter plot of simulated versus measured water-level elevations from January, 1999 – December, 2008 for the Altered Natural + Artificial Recharge scenario before (red) and after (blue) calibration. The calibrated version utilizes the precipitation infiltration percentage (18.5%) determined from the water budget analysis.

Table 14: Summary of total recharge percentages for the BSEA (modified from Hauwert et al., 2011 in press). Previous studies report values as creek channel sources to Barton Springs. This means they are assuming almost all recharge from these creeks discharge at Barton Springs so their calculations are coupled to Barton Springs discharge. This study reports values as total recharge percentages decoupled from Barton Springs discharge.

Stream	**Slade et al. (1986)**	**Barrett and Charbeneau (1996)**	**Hauwert et al. (2011, in press)**	**This Study**
Barton Creek Upstream of Highway 360	0.24	0.26	No Data	0.18
Barton Creek Downstream of Highway 360	No Data	No Data	< 0.12	0.10
Bear Creek	0.09	0.06	0.07	0.06
Little Bear Creek	0.09	0.06	0.04	0.03
Onion Creek	0.29	0.39	0.38	0.32
Slaughter Creek	0.10	0.05	0.08	0.04
Williamson Creek	0.05	0.03	0.01	0.01
Precipitation (diffuse recharge)	0.15	0.15	< 0.36	0.21

CHAPTER 7

CONCLUSIONS

New methods for quantifying and distributing recharge with greater spatial and temporal resolution for both artificial and natural sources have been developed for the BSEA. Artificial sources include leakage from water distribution and wastewater networks as well as irrigation return flows. Natural sources include stream loss from Barton, Bear, Little Bear, Onion, Slaughter, and Williamson Creek as well as diffuse recharge from precipitation. Recharge values calculated for these sources were quantified from newly available data sets (NEXRAD, City of Austin land use surveys, Austin Water Utility flow reports, USGS stream gauges) and were quantified from January, 1999 – December, 2009. These calculations have successfully decoupled recharge quantification from observed discharge, therefore reducing the uncertainty and circular reasoning inherent to the previously reported methods (Scanlon et al., 2001; Barrett and Charbeneau, 1996). Recharge values were spatially and temporally distributed within the BS GAM using new methods developed within this study. These methods are more representative of the actual system by accounting for karstic features, precipitation patterns, utility line locations, and impervious / pervious area locations. Water budget analyses from this study span a 10-year study period which is longer than those conducted by previous studies (Slade et al., 1985; Barrett and Charbeneau, 1996; Hauwert et al., 2011, in press). This longer study period coupled with the consideration of anthropogenic recharge sources provides the most accurate water budget analysis for the BSEA to date.

Modeling Conclusions

Four modeling scenarios were generated within this study to assess newly developed methods for quantifying and spatially distributing recharge values for the BS GAM. The recharge inputs calculated for the Altered Natural + Artificial Recharge scenario produced the most accurate results in terms of simulating Barton Springs discharge and water-level elevations from January, 1999 – December, 2009. This suggests that the water budget analyses for this scenario are also the most accurate as well as being substantiated by other recent studies.

It is important to note that there are discrepancies between the modeling and water budget analyses. In particular, there is a net deficit in aquifer storage for the ten-year study period for the Altered Natural + Artificial Recharge scenario according to water budget analyses. There is no long term loss in storage over the ten-year study period according to the BSEACD and suggested by stable long term water-level elevations. In order for there to be no change in storage, the precipitation infiltration percentage would need to be increased from 6 to 18.5% for the Altered Natural + Artificial Recharge scenario. However, the accuracy of the modeling results when using this new "calibrated" recharge input diminishes from the original input. This discrepancy is best explained by the inherent inaccuracies of representing a karst system as an equivalent porous media. Additionally, there may be other discharge features such as communication between the BSEA and the Colorado River via fissures and flow across "no flow boundaries" like the groundwater divide south of Onion Creek that are unaccounted for within the model.

Artificial Recharge Conclusions

Results indicate that recharge contributions from anthropogenic sources are significant to the overall water budget, especially during drought conditions. While the contribution of artificial recharge sources to the total aquifer recharge is approximately 4%, the relative contribution is highly variable and dependent upon seasonal conditions of both inputs and demand. The cumulative volume of recharge contributed by artificial recharge sources are of comparable magnitude with the six losing streams in the basin, and results indicate that artificial sources actually contribute more recharge than three of the streams.

With the introduction of new recharge sources from the urbanization of the Austin area, one would expect increases in springflow. Sharp and others (2009) document this observation at Barton Springs where cumulative discharge from Barton Springs has been increasing relative to precipitation since the 1960's. This deviation of discharge relative to precipitation was suggested to be from recharge from artificial sources with the onset of urbanization. However, results of this study demonstrate that cumulative recharge from artificial resources cannot account for the majority of the cumulative differences between Barton Springs discharge and precipitation estimated by Sharp and others (2009). If the recharge rates from artificial sources determined from this study were applied from 1960 to 2004, the cumulative recharge would be an order of magnitude short of the cumulative difference between discharge and precipitation reported by Sharp and others (2009). The most likely explanation for this discrepancy is that Sharp and others utilized a fitting constant from the first 5 years of the period of record that was an empirical function calculated from the time series that implicitly represented surface area,

slope, precipitation patterns, antecedent moisture conditions, and permeability to convert precipitation rates to recharge estimates. This fitting constant was assumed to remain constant through time. The results from this study imply that variability in the factor warrants refining to improve recharge estimates for the BSEA case study area. There also could be greater artificial recharge taking place than is presented in this study as our estimates are conservative, but it seems unlikely that this could account for the difference.

The City of Austin utilizes the Colorado River as its primary reservoir. Therefore, imported water is introduced into the BSEA via leaky utility lines, irrigation return flow, and other types of artificial recharge sources. This has essentially established a new baseflow for recharge to the aquifer as well as discharge from Barton and Cold Springs. This is important for managing water and environmental resources during drought intervals and, in particular, maintaining flow at Barton Springs, which hosts a federally-listed endangered species, the Barton Springs salamander (*Eurycea sosorum*). Managing the water resources of the BSEA, as with any urban aquifer system, requires knowledge about the complex components and feedbacks from shifting conditions and anthropogenic sources. The methods used in this study can be replicated in many urban areas to determine the relative importance of artificial recharge for specific systems. This research confirms that the common assumption of reduced recharge in urban settings does not hold and that artificial recharge can be an important source with buffering capacity against drought conditions and, where water quality is adequate, may actually serve to maintain flows for aquatic habitats.

Natural Recharge Conclusions

The results from the water budget analyses for the Altered Natural + Artificial Recharge scenario indicate that estimates of natural recharge derived from this study are comparable with previous studies (Slade et al., 1985; Barrett and Charbeneau, 1996; Hauwert et al., 2011, in press). The estimates presented within this study utilized the most current data (2010) that only recently have become available. Therefore, recharge from natural sources presented in this study is believed to be the most accurate estimate currently available. The majority of recharge is still attributed to losing streams (75%) with precipitation (21%) and artificial recharge (4%+) also being significant. As stated previously within the Modeling Conclusions section, these relative contributions are based on water budget analyses from the Altered Natural + Artificial Recharge scenario. This scenario yields and overall deficit in storage for the 10-year study period. If the precipitation infiltration percentage is increased from 6 to 18.5% in order to honor the observation of no change in storage, the relative contribution of these recharge sources are as follows: losing streams (62%), precipitation (35%), and artificial (3%). These values agree with the most recent values reported by Hauwert (2009) and Hauwert et al., (2011, in press).

Future Work

Further comparative modeling is needed with flow models that incorporate the recharge quantities and distributions developed in this study. A limitation of this study is the paucity of data. In order to enhance our estimates of recharge processes within the

BSEA, greater temporal and spatial resolution data sets are required for the following: Little Bear Creek stream gauge data, NEXRAD data, land-use, irrigation application, and utility line leaks. The greatest uncertainty in terms of recharge is from diffuse recharge. In order to estimate recharge from precipitation, new methods must be employed. Antecedent moisture conditions need to be considered as well as other parameters that control diffuse recharge (topography, land-use, soil and vegetation cover, etc). In addition, further geochemical work needs to be performed to verify the influence of artificial recharge presented within this study. Finally, improved scientific interpretation of recharge can be paired with numerical modeling for comparative analysis within a decision support context. Evaluation of the sensitivity of groundwater behavior across different scientific interpretations of input and modeled representations for the same aquifer pose an opportunity to evaluate the impact of uncertainty in groundwater science as it pertains to decision making for land use and groundwater management in the future.

APPENDIX A

Summary of *PP* values for wells reported within Hunt et al. (2006) for the year 2004.

	Proportion of Total Pumping (%)											
State Well Number	Jan	Feb	Mar	Apr	May	Jun	Jul	Aug	Sep	Oct	Nov	Dec
58-50-735	0.00	0.00	0.00	0.00	0.00	0.00	0.00	0.00	0.00	0.00	0.00	0.00
58-58-4LC	0.00	0.00	0.00	0.00	0.00	0.00	0.00	0.00	0.00	0.00	0.00	0.00
58-57-305	0.00	0.00	0.00	0.00	0.00	0.00	0.00	0.00	0.00	0.00	0.00	0.00
58-57-315	0.00	0.00	0.00	0.00	0.00	0.00	0.00	0.00	0.00	0.00	0.00	0.00
58-58-410	0.00	0.00	0.00	0.00	0.00	0.00	0.00	0.00	0.00	0.00	0.00	0.00
58-57-3H	0.00	0.00	0.00	0.00	0.00	0.00	0.00	0.00	0.00	0.00	0.00	0.00
58-58-126	0.00	0.00	0.00	0.00	0.00	0.00	0.00	0.00	0.00	0.00	0.00	0.00
58-58-1MT	0.00	0.00	0.00	0.00	0.00	0.00	0.00	0.00	0.00	0.00	0.00	0.00
58-58-122	0.00	0.00	0.00	0.00	0.00	0.00	0.00	0.00	0.00	0.00	0.00	0.00
58-50-738	0.00	0.00	0.00	0.00	0.00	0.00	0.00	0.00	0.00	0.00	0.00	0.00
58-50-7PC	0.00	0.00	0.00	0.00	0.00	0.00	0.00	0.00	0.00	0.00	0.00	0.00
58-50-729	0.00	0.00	0.00	0.00	0.00	0.00	0.00	0.00	0.00	0.00	0.00	0.00
58-50-8RRB	0.00	0.00	0.00	0.00	0.00	0.00	0.00	0.00	0.00	0.00	0.00	0.00
58-50-744	0.00	0.00	0.00	0.00	0.00	0.00	0.00	0.00	0.00	0.00	0.00	0.00
58-50-724	0.00	0.00	0.00	0.00	0.00	0.00	0.00	0.00	0.00	0.00	0.00	0.00
58-50-730	0.00	0.00	0.00	0.00	0.00	0.00	0.00	0.00	0.00	0.00	0.00	0.00
58-58-4MC	0.00	0.00	0.00	0.00	0.00	0.00	0.00	0.00	0.00	0.00	0.00	0.00
58-50-726	0.00	0.00	0.00	0.00	0.00	0.00	0.00	0.00	0.00	0.00	0.00	0.00
58-50-122	0.00	0.00	0.00	0.00	0.00	0.00	0.00	0.00	0.00	0.00	0.00	0.00
58-42-8VW	0.00	0.00	0.00	0.00	0.00	0.00	0.00	0.00	0.00	0.00	0.00	0.00
58-42-825	0.00	0.00	0.00	0.00	0.00	0.00	0.00	0.00	0.00	0.00	0.00	0.00
58-42-821	0.00	0.00	0.00	0.00	0.00	0.00	0.00	0.00	0.00	0.00	0.00	0.00
58-42-913	0.00	0.00	0.00	0.00	0.00	0.00	0.00	0.00	0.00	0.00	0.00	0.00
58-58-1JS	0.00	0.00	0.00	0.00	0.00	0.00	0.00	0.00	0.00	0.00	0.00	0.00
58-50-8LB	0.00	0.00	0.00	0.00	0.00	0.00	0.00	0.00	0.00	0.00	0.00	0.00
58-50-8KL	0.00	0.00	0.00	0.00	0.00	0.00	0.00	0.00	0.00	0.00	0.00	0.00
58-58-407	0.02	0.02	0.02	0.02	0.01	0.02	0.02	0.01	0.02	0.02	0.02	0.02
58-58-415	0.01	0.01	0.01	0.01	0.01	0.01	0.01	0.01	0.01	0.01	0.01	0.01
58-58-414	0.08	0.06	0.07	0.07	0.06	0.05	0.06	0.06	0.06	0.06	0.07	0.09
58-58-406	0.00	0.00	0.00	0.00	0.00	0.00	0.00	0.00	0.00	0.00	0.00	0.00
58-58-423	0.00	0.00	0.00	0.00	0.00	0.00	0.00	0.00	0.00	0.00	0.00	0.00
58-58-418	0.00	0.00	0.00	0.00	0.00	0.00	0.00	0.00	0.00	0.00	0.00	0.00

58-58-509	0.00	0.00	0.00	0.00	0.00	0.00	0.00	0.00	0.00	0.00	0.00	0.00
58-50-7MO	0.00	0.00	0.00	0.00	0.00	0.00	0.00	0.00	0.00	0.00	0.00	0.00
58-50-861	0.00	0.00	0.00	0.00	0.00	0.00	0.00	0.00	0.00	0.00	0.00	0.00
58-50-862	0.00	0.00	0.00	0.00	0.00	0.00	0.00	0.00	0.00	0.00	0.00	0.00
58-50-859	0.00	0.00	0.00	0.00	0.00	0.00	0.00	0.00	0.00	0.00	0.00	0.00
58-50-860	0.00	0.00	0.00	0.00	0.00	0.00	0.00	0.00	0.00	0.00	0.00	0.00
58-50-835	0.00	0.01	0.03	0.06	0.07	0.09	0.08	0.07	0.05	0.06	0.03	0.01
58-50-414	0.00	0.00	0.00	0.00	0.00	0.00	0.00	0.00	0.00	0.00	0.00	0.00
58-50-123	0.00	0.00	0.00	0.00	0.00	0.00	0.00	0.00	0.00	0.00	0.00	0.00
58-50-1NF	0.00	0.00	0.00	0.00	0.00	0.00	0.00	0.00	0.00	0.00	0.00	0.00
58-50-5A	0.00	0.00	0.00	0.00	0.00	0.00	0.00	0.00	0.00	0.00	0.00	0.00
58-50-231	0.00	0.00	0.00	0.00	0.00	0.00	0.00	0.01	0.01	0.00	0.00	0.00
58-42-9NC	0.01	0.01	0.01	0.01	0.01	0.01	0.01	0.01	0.01	0.01	0.02	0.03
58-58-4GF	0.08	0.06	0.07	0.07	0.07	0.07	0.06	0.06	0.06	0.06	0.06	0.06
58-50-731	0.02	0.02	0.03	0.03	0.05	0.03	0.04	0.04	0.04	0.03	0.03	0.02
58-57-9N1	0.10	0.15	0.11	0.13	0.11	0.10	0.06	0.08	0.09	0.12	0.10	0.11
58-57-6M3	0.00	0.00	0.00	0.00	0.00	0.00	0.01	0.00	0.01	0.00	0.00	0.00
58-57-607	0.00	0.00	0.00	0.00	0.00	0.00	0.00	0.00	0.00	0.00	0.00	0.00
58-57-606	0.00	0.00	0.00	0.00	0.00	0.00	0.00	0.00	0.00	0.00	0.00	0.00
58-57-608	0.00	0.00	0.00	0.00	0.00	0.00	0.01	0.00	0.01	0.00	0.00	0.00
58-58-417	0.00	0.00	0.00	0.00	0.00	0.00	0.00	0.00	0.00	0.00	0.00	0.01
58-58-708	0.09	0.09	0.08	0.08	0.08	0.10	0.09	0.08	0.08	0.09	0.10	0.11
58-57-312	0.00	0.00	0.00	0.00	0.00	0.00	0.00	0.00	0.00	0.00	0.00	0.00
58-58-125	0.00	0.00	0.00	0.00	0.00	0.00	0.00	0.00	0.00	0.00	0.00	0.00
58-58-426	0.00	0.00	0.00	0.00	0.00	0.00	0.00	0.00	0.00	0.00	0.00	0.00
58-57-307	0.01	0.00	0.00	0.00	0.00	0.00	0.00	0.00	0.00	0.00	0.00	0.00
58-57-314	0.01	0.01	0.01	0.01	0.01	0.01	0.01	0.01	0.01	0.01	0.01	0.01
58-57-3Z4	0.01	0.01	0.01	0.01	0.01	0.01	0.01	0.01	0.01	0.01	0.01	0.01
58-57-308	0.01	0.01	0.01	0.01	0.01	0.01	0.01	0.01	0.01	0.01	0.01	0.01
58-58-413	0.03	0.03	0.03	0.03	0.03	0.03	0.03	0.03	0.03	0.03	0.03	0.03
58-58-403	0.03	0.03	0.03	0.03	0.03	0.03	0.03	0.03	0.03	0.03	0.03	0.03
58-58-119	0.01	0.01	0.01	0.01	0.01	0.01	0.01	0.01	0.01	0.01	0.00	0.01
58-58-106	0.03	0.03	0.03	0.03	0.03	0.03	0.03	0.03	0.03	0.03	0.03	0.03
58-58-409	0.01	0.01	0.01	0.01	0.01	0.01	0.01	0.01	0.01	0.01	0.01	0.01
58-49-911	0.00	0.00	0.00	0.00	0.00	0.00	0.00	0.00	0.00	0.00	0.00	0.00
58-58-127	0.00	0.00	0.00	0.00	0.00	0.00	0.00	0.00	0.00	0.00	0.00	0.00
58-58-107	0.01	0.01	0.01	0.01	0.01	0.01	0.01	0.01	0.01	0.01	0.00	0.01
58-58-121	0.02	0.02	0.01	0.01	0.01	0.01	0.02	0.02	0.02	0.01	0.01	0.01
58-58-501	0.08	0.06	0.07	0.07	0.07	0.07	0.06	0.06	0.06	0.06	0.06	0.06
58-58-118	0.01	0.01	0.01	0.01	0.01	0.01	0.01	0.01	0.01	0.01	0.00	0.01

58-58-120	0.01	0.01	0.01	0.01	0.01	0.01	0.01	0.01	0.01	0.01	0.00	0.01
58-58-102	0.01	0.01	0.01	0.01	0.01	0.01	0.02	0.02	0.02	0.01	0.01	0.01
58-58-117	0.00	0.00	0.00	0.00	0.00	0.00	0.00	0.00	0.00	0.00	0.00	0.00
58-58-115	0.00	0.00	0.00	0.00	0.00	0.00	0.00	0.00	0.00	0.00	0.00	0.00
58-58-111	0.00	0.00	0.00	0.00	0.00	0.00	0.00	0.00	0.00	0.00	0.00	0.00
58-58-114	0.04	0.04	0.04	0.04	0.04	0.04	0.05	0.05	0.05	0.04	0.04	0.03
58-49-915	0.00	0.00	0.00	0.00	0.00	0.00	0.00	0.00	0.00	0.00	0.00	0.00
58-49-927	0.01	0.01	0.01	0.01	0.01	0.01	0.01	0.01	0.01	0.00	0.00	0.01
58-50-727	0.00	0.00	0.00	0.00	0.00	0.00	0.00	0.00	0.00	0.00	0.00	0.00
58-50-704	0.01	0.01	0.01	0.01	0.01	0.01	0.01	0.01	0.01	0.01	0.01	0.01
58-50-728	0.00	0.00	0.00	0.00	0.00	0.00	0.00	0.00	0.00	0.00	0.00	0.00
58-50-718	0.01	0.01	0.00	0.00	0.00	0.00	0.01	0.00	0.01	0.00	0.00	0.00
58-50-732	0.00	0.00	0.00	0.00	0.00	0.00	0.00	0.00	0.00	0.00	0.00	0.00
58-50-7AD	0.00	0.00	0.00	0.00	0.00	0.00	0.00	0.00	0.00	0.00	0.00	0.00
58-58-215	0.01	0.01	0.01	0.01	0.01	0.01	0.01	0.01	0.01	0.01	0.01	0.01
58-50-8AS	0.00	0.00	0.00	0.00	0.00	0.00	0.00	0.00	0.00	0.00	0.00	0.00
58-58-202	0.00	0.00	0.00	0.00	0.00	0.00	0.00	0.00	0.00	0.00	0.00	0.00
58-50-845	0.01	0.01	0.01	0.01	0.01	0.01	0.01	0.01	0.01	0.01	0.01	0.01
58-58-207	0.00	0.00	0.00	0.00	0.00	0.00	0.00	0.00	0.00	0.00	0.00	0.00
58-50-737	0.00	0.00	0.00	0.00	0.00	0.00	0.00	0.00	0.00	0.00	0.00	0.00
58-58-209	0.01	0.01	0.02	0.02	0.01	0.01	0.01	0.01	0.02	0.01	0.02	0.01
58-50-858	0.01	0.01	0.00	0.01	0.00	0.00	0.00	0.00	0.00	0.01	0.00	0.00
58-50-846	0.07	0.07	0.06	0.06	0.05	0.06	0.05	0.04	0.05	0.05	0.07	0.06
58-50-849	0.07	0.07	0.06	0.06	0.05	0.06	0.05	0.04	0.05	0.05	0.07	0.06
58-50-723	0.00	0.00	0.00	0.00	0.00	0.00	0.00	0.00	0.00	0.00	0.00	0.00
58-50-842	0.00	0.00	0.00	0.00	0.00	0.00	0.00	0.00	0.00	0.00	0.00	0.00
58-50-843	0.00	0.00	0.00	0.00	0.00	0.00	0.00	0.00	0.00	0.00	0.00	0.00
58-50-838	0.01	0.00	0.00	0.01	0.01	0.01	0.01	0.01	0.01	0.01	0.00	0.00
58-50-855	0.01	0.01	0.01	0.01	0.01	0.01	0.01	0.01	0.01	0.01	0.01	0.01
58-50-852	0.00	0.00	0.00	0.00	0.00	0.00	0.00	0.00	0.00	0.01	0.00	0.00
58-50-830	0.01	0.00	0.01	0.00	0.01	0.01	0.01	0.01	0.01	0.00	0.01	0.01
58-50-215	0.01	0.01	0.01	0.01	0.01	0.00	0.01	0.01	0.01	0.01	0.01	0.01
58-42-816	0.01	0.00	0.01	0.01	0.01	0.01	0.01	0.01	0.01	0.01	0.00	0.01

APPENDIX B

Summary of monthly recharge inputs for this study (m^3)

Precip A: diffuse recharge input for the Natural and Natural + Artificial Recharge scenarios
Precip B: diffuse recharge input for the Altered Natural + Artificial Recharge scenario
WL: leakage from water distribution system
WW: leakage from waste water network
IRF: irrigation return flow

Date	Precip A	Precip B	WL	WW	IRF	Barton	Bear	L. Bear	Onion	Slaughter	Williamson
Jan-99	656,079	199,883	109,673	59,875	0	2,255,743	262,273	307,926	3,187,888	71,464	76,981
Feb-99	595,657	190,617	107,262	53,656	0	909,881	121,350	261,412	1,516,877	41,934	65,353
Mar-99	4,326,179	1,346,979	118,023	62,098	18,719	706,082	122,329	273,948	1,289,345	51,916	68,487
Apr-99	735,057	233,644	128,066	58,782	0	428,640	99,013	249,257	727,612	41,372	62,314
May-99	7,560,291	2,284,605	131,261	63,651	67,942	1,290,079	88,297	230,869	432,555	66,351	57,717
Jun-99	4,758,487	1,484,925	138,055	60,020	85,214	1,748,568	100,603	201,696	635,376	78,217	50,424
Jul-99	5,921,941	1,841,989	144,986	62,205	113,906	1,438,342	188,876	199,924	1,336,320	55,635	49,981
Aug-99	340,738	109,101	205,314	57,497	0	66,547	27,402	166,250	251,997	9,052	41,562
Sep-99	484,383	154,563	193,470	54,203	0	3,768	1,566	123,601	121,008	0	30,900
Oct-99	1,800,225	548,202	174,046	56,817	31,294	1,908	0	101,327	15,976	0	25,332
Nov-99	121,157	37,164	142,732	53,201	0	16,637	0	90,425	15,071	0	22,606
Dec-99	908,291	281,526	128,624	52,574	64,835	36,160	0	87,979	15,707	0	21,995
Jan-00	3,151,278	996,177	119,962	56,380	116,400	117,754	587	87,675	18,667	0	21,919
Feb-00	2,637,721	807,975	114,099	54,461	73,595	158,538	3,915	73,710	18,374	367	18,428
Mar-00	3,195,691	934,323	125,512	56,569	21,690	121,839	6,410	81,911	30,313	0	20,478
Apr-00	2,188,887	670,708	132,150	56,704	11,927	175,419	4,869	74,572	18,374	220	18,643

May-00	4,781,797	1,465,392	147,648	58,652	155,078	347,658	22,900	77,967	84,138	685	19,492
Jun-00	11,787,237	3,608,111	145,853	62,417	230,010	1,757,791	347,487	142,978	738,034	894,003	35,744
Jul-00	469,705	158,571	199,484	54,766	0	168,814	43,745	114,979	30,851	44,699	28,745
Aug-00	256,751	79,646	198,708	54,848	0	4,502	5,015	80,394	9,493	0	20,099
Sep-00	792,636	245,989	182,344	55,150	0	49	73	61,947	465	0	15,487
Oct-00	6,239,630	1,908,805	142,909	61,650	199,859	102,805	23,071	84,945	1,492	98	21,236
Nov-00	12,027,020	3,776,017	118,409	76,859	0	4,607,146	1,542,297	215,494	6,172,979	1,463,786	53,874
Dec-00	1,301,519	419,580	119,501	68,918	0	3,375,540	951,718	258,779	4,988,568	919,423	64,695
Jan-01	3,140,355	986,622	116,177	73,273	0	4,836,880	1,282,006	283,049	8,088,379	1,565,074	70,762
Feb-01	1,665,343	525,399	102,457	57,960	0	2,967,696	717,825	272,646	5,795,937	541,672	68,162
Mar-01	3,581,237	1,134,588	110,275	73,785	0	5,578,192	1,073,313	307,016	8,333,036	1,924,232	76,754
Apr-01	1,452,433	442,175	123,922	60,683	0	3,447,225	481,975	301,810	4,357,351	670,851	75,452
May-01	6,290,480	1,929,054	143,665	60,381	117,434	2,573,797	328,575	311,567	6,319,505	225,330	77,892
Jun-01	1,544,814	474,393	162,663	50,826	0	635,376	90,939	280,965	1,650,949	46,950	70,241
Jul-01	991,057	308,071	217,632	48,023	0	37,555	4,184	267,274	266,921	2,398	66,818
Aug-01	9,443,869	2,984,647	222,165	56,307	0	201,794	66,987	229,655	224,253	3,939	57,414
Sep-01	4,025,023	1,268,946	145,022	55,853	59,833	491,272	63,171	226,357	701,923	1,346	56,589
Oct-01	3,513,971	1,121,133	150,214	55,113	119,417	902,542	37,873	205,385	752,322	4,600	51,346
Nov-01	17,870,950	5,598,780	125,497	65,670	50,878	3,064,581	499,615	234,871	4,083,579	248,327	58,718
Dec-01	7,287,935	2,263,403	109,173	82,154	0	6,706,064	2,023,073	320,668	8,585,034	2,532,695	80,167
Jan-02	1,480,358	471,940	116,731	63,166	3,282	2,113,841	782,170	339,174	5,335,981	757,704	84,793
Feb-02	922,334	298,762	109,952	54,577	0	1,367,146	282,335	297,308	2,387,858	195,481	74,327
Mar-02	1,963,364	597,287	124,262	58,116	5,324	1,344,149	184,227	308,229	1,578,041	95,612	77,057
Apr-02	1,496,517	460,466	137,273	56,492	0	1,038,082	109,802	287,717	1,189,036	44,699	71,929
May-02	2,514,717	771,905	182,553	54,574	4,823	257,429	33,273	274,555	392,920	10,618	68,639
Jun-02	9,315,537	2,888,004	172,768	54,377	444,251	361,946	88,811	233,990	434,756	3,596	58,498
Jul-02	13,267,663	4,014,794	148,239	66,204	183,319	10,422,412	1,700,859	293,364	8,991,165	2,513,856	73,341

Aug-02	1,407,979	458,092	193,287	54,860	0	2,100,140	297,504	305,499	3,368,935	48,736	76,375
Sep-02	6,321,821	1,915,037	165,599	53,548	283,501	729,324	110,708	270,102	1,511,984	14,117	67,525
Oct-02	10,774,615	3,346,412	149,601	60,450	275,221	2,028,456	493,009	260,296	4,277,103	143,492	65,074
Nov-02	4,115,351	1,303,818	135,026	59,238	124,662	3,532,855	1,256,561	288,304	8,230,280	710,241	72,076
Dec-02	7,533,590	2,399,206	122,407	63,858	49,150	3,143,850	1,486,784	323,095	8,342,823	1,048,602	80,774
Jan-03	621,224	208,634	112,154	62,984	0	4,391,603	802,966	330,072	8,937,340	563,691	82,518
Feb-03	5,917,271	1,852,431	98,786	58,987	0	3,826,444	946,091	311,831	6,620,433	1,103,161	77,958
Mar-03	350,972	112,631	113,663	63,189	0	2,970,143	1,047,379	350,095	8,619,286	743,270	107,992
Apr-03	621,224	208,634	144,929	52,693	0	1,713,826	284,047	315,021	3,299,207	101,141	45,164
May-03	621,224	208,634	166,095	53,877	0	799,541	83,184	303,982	725,777	18,349	4,942
Jun-03	6,196,426	1,935,079	158,202	53,104	151,483	881,501	27,548	281,258	507,249	5,921	17,053
Jul-03	1,562,204	484,712	175,155	51,185	0	303,302	3,645	270,611	214,149	563	9,640
Aug-03	2,249,671	700,768	196,876	50,113	28	33,273	0	248,464	76,186	0	0
Sep-03	4,683,247	1,477,040	151,090	50,193	172,895	117,362	0	206,980	9,297	0	21,089
Oct-03	1,464,553	452,649	147,219	51,903	0	92,872	0	171,710	10,227	0	1,884
Nov-03	860,531	278,576	126,808	48,000	9,667	69,532	0	126,243	7,193	0	196
Dec-03	589,914	191,497	129,147	48,102	0	80,052	0	121,047	17,982	0	147
Jan-04	3,738,086	1,169,279	118,858	51,195	151,729	568,951	1,003	122,867	31,169	489	84,064
Feb-04	4,455,619	1,425,145	105,366	52,823	54,256	1,529,550	17,982	115,087	238,688	489	171,945
Mar-04	2,145,470	646,019	114,477	57,894	41	2,850,603	69,948	139,856	1,250,200	64,027	159,027
Apr-04	5,163,179	1,581,026	115,567	56,202	22,090	3,447,225	162,208	164,997	4,805,074	199,763	120,225
May-04	2,974,765	915,064	131,691	52,492	0	2,541,992	152,666	190,823	4,237,469	98,891	71,171
Jun-04	17,776,178	5,593,126	131,115	61,388	127,810	4,476,989	881,110	217,843	6,958,550	741,704	434,487
Jul-04	2,568,120	800,444	157,812	54,145	0	3,292,112	1,032,210	292,454	5,796,182	597,209	210,014
Aug-04	2,799,105	833,337	173,918	49,535	178	414,450	74,131	259,386	1,939,131	31,047	7,854
Sep-04	1,735,952	535,368	161,608	46,634	0	99,551	22,729	210,797	377,384	171	2,691
Oct-04	9,458,188	2,929,135	137,535	52,262	217,826	1,365,630	331,095	198,407	2,103,150	514	59,158

Nov-04	18,726,542	5,823,400	113,646	69,484	0	5,016,458	1,862,578	239,862	7,615,456	1,808,802	597,331
Dec-04	477,321	150,671	114,766	56,690	0	2,539,545	1,150,135	310,656	5,472,500	622,898	267,460
Jan-05	2,696,712	844,844	113,009	53,793	40,223	2,232,745	381,176	295,184	4,546,471	118,463	118,219
Feb-05	3,086,311	958,821	99,122	53,524	2,621	2,921,211	490,294	267,440	2,796,436	274,922	145,767
Mar-05	3,571,456	1,102,026	113,581	62,925	0	2,769,524	1,132,520	347,972	4,071,102	1,554,946	321,260
Apr-05	1,466,057	460,444	126,509	51,114	0	1,448,862	347,169	323,242	3,554,385	171,016	58,008
May-05	5,671,110	1,756,939	143,847	50,098	63,365	931,901	144,544	302,769	1,454,563	46,827	27,475
Jun-05	448,324	151,781	173,075	46,716	0	284,977	48,418	268,928	335,254	18,374	21,285
Jul-05	4,821,881	1,483,908	187,611	51,626	171,818	63,758	24,294	249,981	182,099	245	5,994
Aug-05	2,862,512	863,849	184,406	55,271	20,258	214,271	33,714	227,532	36,821	440	18,325
Sep-05	2,929,169	950,949	196,492	53,400	171,586	121,032	3,034	190,246	7,584	318	20,356
Oct-05	2,031,845	630,785	167,272	55,523	0	72,981	0	151,081	4,184	0	465
Nov-05	1,257,491	397,383	149,894	52,272	10,615	82,939	0	125,950	73	0	0
Dec-05	148,953	43,822	138,392	50,767	0	97,129	0	126,508	0	0	0
Jan-06	1,303,952	411,865	137,090	46,550	105,923	117,191	0	101,631	0	0	73
Feb-06	1,061,702	336,969	105,541	43,203	725	132,604	0	83,575	0	0	661
Mar-06	5,102,072	1,646,313	130,051	51,176	200,471	549,501	64,002	95,260	1,492	758	101,044
Apr-06	3,296,056	1,032,991	143,426	51,094	121,198	461,326	35,280	91,306	3,963	269	35,402
May-06	6,106,524	1,939,088	155,753	57,175	227,562	1,155,224	95,661	104,968	196	1,615	152,715
Jun-06	4,057,519	1,240,516	168,327	48,182	143,850	222,002	50,693	84,847	0	294	23,781
Jul-06	1,441,558	453,076	184,980	48,047	0	52,870	13,163	80,091	0	0	24
Aug-06	350,131	113,632	222,888	46,583	0	6,068	0	66,136	0	0	0
Sep-06	2,859,332	902,969	164,934	47,471	136,267	16,050	0	61,067	0	0	856
Oct-06	5,851,985	1,854,660	141,478	50,473	253,976	93,263	0	70,990	0	73	10,716
Nov-06	3,612,903	1,082,828	134,118	46,621	239,277	118,170	0	69,287	0	147	4,159
Dec-06	149,754	43,921	115,760	52,965	0	327,107	1,395	87,675	0	612	59,232
Jan-07	8,884,096	2,873,932	110,797	71,528	0	2,538,077	589,527	165,946	702,412	267,949	479,798

Feb-07	5,096,186	1,605,684	103,505	55,787	19,970	1,340,234	300,684	179,207	169,303	99,820	63,195
Mar-07	10,106,470	3,138,397	122,479	69,781	0	4,587,329	1,274,421	244,824	4,246,521	1,122,146	351,548
Apr-07	3,743,224	1,166,065	117,997	63,248	2,981	4,420,962	1,392,101	281,258	5,297,325	363,977	202,650
May-07	10,357,253	3,286,783	122,843	67,708	6,487	5,377,573	1,675,904	300,038	6,822,863	393,923	386,143
Jun-07	8,884,096	2,873,932	123,334	66,235	14,197	5,928,053	1,030,498	307,681	3,836,230	334,985	477,156
Jul-07	15,120,460	4,781,920	119,172	75,702	0	8,027,214	1,761,534	329,769	7,349,513	2,624,686	702,754
Aug-07	4,984,412	1,567,165	150,523	65,082	0	2,715,699	1,288,856	321,275	4,838,592	869,929	262,126
Sep-07	5,096,186	1,605,684	141,833	61,435	30,066	3,065,559	630,238	289,185	3,172,964	145,791	255,251
Oct-07	2,010,950	653,992	149,884	55,116	0	1,134,477	151,443	275,465	731,771	31,365	24,294
Nov-07	1,456,274	463,478	131,788	52,758	0	557,330	74,180	254,835	298,972	9,444	3,205
Dec-07	6,174,734	1,960,067	116,686	52,789	123,611	517,940	69,972	248,768	366,252	1,223	9,493
Jan-08	1,155,467	357,089	115,296	51,024	0	412,248	52,846	216,913	263,741	0	6,704
Feb-08	676,873	214,300	111,597	47,898	0	345,212	44,405	163,314	157,755	0	3,572
Mar-08	5,059,144	1,573,559	119,354	54,200	79,233	770,916	87,269	162,002	158,416	2,911	67,012
Apr-08	5,335,880	1,699,117	125,088	53,567	106,641	1,635,780	121,595	143,271	165,144	7,829	79,294
May-08	2,713,193	859,379	139,903	54,056	10,900	830,612	52,357	138,036	123,919	6,092	20,894
Jun-08	726,432	236,394	183,981	48,348	0	87,734	3,034	89,838	465	0	0
Jul-08	3,245,303	1,007,976	183,625	49,302	81,199	62,143	0	75,844	196	0	6,410
Aug-08	4,611,486	1,345,026	178,135	51,709	31,519	59,329	0	75,540	0	0	1,810
Sep-08	697,351	218,471	176,748	46,940	0	23,047	0	71,342	0	0	0
Oct-08	3,457,916	1,125,139	157,061	46,709	243,538	33,078	0	64,922	0	0	73
Nov-08	204,193	70,765	139,163	46,582	0	116,090	0	57,837	0	0	0
Dec-08	704,646	228,147	126,474	46,983	9,328	126,733	0	59,765	0	0	0
Jan-09	729,382	232,248	121,644	49,655	4,323	162,208	0	57,338	0	0	0
Feb-09	1,753,486	550,382	111,743	46,976	81,764	303,375	3,058	50,967	0	0	1,150
Mar-09	4,497,777	1,405,594	124,798	53,522	126,728	535,800	24,074	63,709	0	24	16,172
Apr-09	4,756,135	1,478,452	125,409	51,695	117,523	469,009	34,301	56,956	0	24	24,906

May-09	3,323,113	1,026,593	142,698	53,692	27,663	352,062	30,998	56,428	0	0	7,487
Jun-09	2,505,829	825,836	171,375	53,587	32,629	271,448	245	51,672	0	73	15,438
Jul-09	1,840,752	616,900	195,291	54,311	48,661	35,818	0	49,147	0	49	4,477
Aug-09	1,389,052	433,008	187,532	56,412	1,594	4,379	0	45,203	0	0	0
Sep-09	11,134,783	3,480,687	122,961	59,292	110,286	4,680,152	281,063	84,847	0	3,401	99,918
Oct-09	9,465,925	2,936,458	143,867	53,606	298,199	15,883,609	1,083,833	136,519	1,238,897	549,990	216,473
Nov-09	3,293,657	1,028,666	125,840	56,631	115,622	8,416,220	1,118,574	162,061	2,608,294	427,025	145,033
Dec-09	390,095	121,243	117,004	57,247	0	3,713,902	1,000,894	209,623	3,413,218	394,461	162,795

REFERENCES

Asquith, W.H., and Roussel, M.C., 2007, An initial-abstraction constant-loss model for unit hydrograph modeling for applicable watersheds in Texas: U.S. Geological Survey Scientific Investigations Report 2007-5243, p. 82

Barton Springs / Edwards Aquifer Conservation District (BSEACD), 2003, Summary of Groundwater Dye Tracing Studies (1996 – 2002), Barton Springs Segment of the Edwards Aquifer, Electronic document, accessible at: http://www.bseacd.org/uploads/AquiferScience/Dye_BSEACD_report_2002.pdf

Barrett, M.E. and Charbeneau, R.J., 1997, A Parsimonious Model for Simulation of Flow and Transport in a Karst Aquifer, *Journal of Hydrology*, **196**, 47–65.

Barrett, M.E. and Charbeneau, R.J., 1996, A Parsimonious Model for Simulation of Flow and Transport in a Karst Aquifer: Technical Report Center for Research in Water Resources, Report No. 269

Berg, A., Byrne, J., and Rogerson, R., 1996, An urban water balance study, Lethbridge Alberta: Estimation of urban lawn overwatering and potential effects on local water tables: Canadian Water Resources Journal, v. 21, no. 4, p. 17 -27.

Brassington, F.C. and Rushton, K.R., 1987, Rising water table in central Liverpool, Q J Eng Geol 20:151-158.

Cain, W.O., Pierce, S.A., Barnes, J.W., Ciarleglio, M., Lowry, T.S., Sharp, J.M., Jr., and Tidwell, V.C., 2008, CADRE: A negotiation support system for sustainable water management: Water Down Under 2008, p. 2106-2117.

Capital Area Council of Governments, accessed, March, 2011, Geospatial Data, Electronic document available at http://www.capcog.org/information-clearinghouse/geospatial-data

Caran, S.C., Woodruff, C.M., Jr., and Thompson, E.J., 1981, Lineament analysis and inference of geologic structure – examples of the Balcones-Ouachita trend of Texas, Trans., Gulf Coast Assoc. Geol. Societies, v. 31, p. 59 - 69

City of Austin, accessed August, 2010, City of Austin GIS Data Sets, Electronic document, available at ftp://ftp.ci.austin.tx.us/GIS-Data/Regional/coa_gis.html

Christian, L.N., Banner, J.L., and Mack, L.E., 2011, Sr isotopes as tracers of anthropogenic influences on stream water in the Austin, Texas, area, Chemical Geology, Vol. 282, p. 84 - 97

Coldewey, W.G., and Meβer, J., 1997, The effects of urbanization on groundwater recharge in the Ruhr region of Germany, in Chilton, J., ed., Groundwater in the urban environment: Problems, processes and management: Rotterdam, Netherlands, Balkema, p. 115 – 119

Danielson, R.E., Hart, W.E., Feldhake, C.M., and Haw, P.M., 1980, Water requirements for urban lawns in Colorado, CWRRI Report No. 97, Colorado State University, Fort Collins, Colorado.

Drouin-Brisebois, I.A., 2002, Predicting local and regional effects of urbanisation on the subsurface water balance of North Pickering Agricultural Lands: unpublished M.S. thesis, Univ Toronto, Toronto, Ontario, Canada, p. 90

Fieseler, R., 1998, Implementation of Best Management Practices to Reduce Nonpoint Source Loadings to Onion Creek Recharge Features, report to the Barton Springs Aquifer Conservation District, Austin, Texas

Flores, R., 1990, Test Well Drilling Investigation to Delineate the Downdip Limits of Usable-Quality Groundwater in the Edwards Aquifer in the Austin Region, Texas. Texas Water Development Board Report 325, p. 70

Foster, S.S.D., Morris, B.L., and Lawrence, A.R., 1994, Effects of urbanization on groundwater recharge, in Wilkinson, W.B., ed., Groundwater problems in urban areas: London, Thomas Telford, p. 43 – 63.

Foster, S.S.D., 1990, Impacts of urbanization on groundwater, in Massing, H., et al., eds., Hydrological processes and water management in urban areas: Wallingford, UK, International Association of Hydrological Sciences Publication 198, p. 362

Garcia-Fresca B. and Sharp J.M., 2005, Hydrogeologic considerations of urban development – Urban-induced recharge. In: *Humans as Geologic Agents*, Ehlen J., Haneberg W. and Larson R. (eds.), Geol. Soc. America, Reviews in Engineering Geology, vol 16, pp. 123-136.

Garcia-Fresca, B., 2004, Urban Effects on Groundwater Recharge in Austin, Texas: unpublished M.S. thesis, University of Texas, Austin, TX, p. 74 – 80.

Garza, S., 1962, Recharge, discharge, and changes in ground-water storage in the Edwards and associated limestones, San Antonio area, Texas, a progress report on studies, 1955-59: Texas Board of Water Engineers Bulletin 6201, p. 51

Grischeck, T., Nestler, W., Piechniczek, K., and Fischer, T., 1996, Urban groundwater in Dresden, Germany, Hydrogeology Journal, v. 4, p. 48 – 63.

Harbaugh, A.W. and McDonald, M.G., 1996, User's documentation for MODFLOW-96, an update to the U.S. Geological Survey modular finite-difference ground-water flow model: U.S. Geological Survey Open-File Report 96-485

Halihan, T., Sharp, J.M., Jr., and Mace, R., 1999, Interpreting flow using permeability at multiple scales. Karst modeling: proceedings of the symposium held February 24 through 27, 1999, Charlottesville, Virginia / edited by Arthur N. Palmer, Margaret V. Palmer, and Ira D. Sasowsky

Hauwert, N.M., 2011, personal communication, City of Austin, Watershed Protection Department, P.O. Box 1088, Austin, TX, 78767, Nico.Hauwert@ci.austin.tx.us

Hauwert, N., Beery, J., and Slade, R., 2011 in press, Recharge to the Barton Springs Segment of the Edwards Aquifer from Major Creek and River Channel Contributions: City of Austin Short Report, Austin, TX.

Hauwert, N., 2009, Groundwater Flow and Recharge within the Barton Springs Segment of the Edwards Aquifer, Southern Travis and Northern Hays Counties, Texas. PhD thesis, Jackson School of Geosciences, Department of Geology, The University of Texas at Austin

Hauwert, N.M., Johns, D.A., Sansom, J.W., Aley, T.J., 2004, Groundwater Tracing of the Barton Springs Edwards Aquifer, southern Travis and northern Hays Counties, Texas: Report by the Barton Springs/Edwards Aquifer Conservation District and the City of Austin Watershed Protection and Development Review Department, p. 100

Hauwert, N.M., Johns, D.A., Sansom, J.W., and Aley, T.J., 2002, Groundwater Tracing of the Barton Springs Edwards Aquifer, Travis and Hays Counties, Texas: Gulf Coast Associations of Geological Societies Transactions, v. 52, p. 377 - 384

Hovorka, S., Mace, R., and Collins, E., 1998, Permeability Structure of the Edwards Aquifer, South Texas – Implications for Aquifer Management: The University of Texas at Austin, Bureau of Economic Geology, Report of Investigations No. 250, p. 55

Hovorka, S., Dutton, A., Ruppel, S., and Yeh, J., 1996, Edwards Aquifer Ground-Water Resources: Geologic Controls on Porosity Development in Platform Carbonates, Sourth Texas: The University of Texas at Austin, Bureau of Economic Geology, Report of Investigations N. 238, p. 75

Howell, T.A., Schnieder, A.D., and Jensen, M.E., 1991, History of lysimeter design and use for evapotranspiration measurements, Proceedings International Symposium on Lysimetry, ASCE, New York, N.Y., p. 1 – 9.

Hunt, B.B., Smith, B.A., and Beery, J., 2007, Potentiometric Maps for Low to High Flow Conditions, Barton Springs Segment of the Edwards Aquifer, Central Texas, Barton Springs / Edwards Aquifer Conservation District (BSEACD), Report of Investigations 2007-1201, Electronic document, accessible at http://www.bseacd.org/uploads/AquiferScience/HR_PotMap_BSEACD_2007.pdf

Hunt, B.B. and Smith, B.A., 2006, Groundwater Levels in the Balcones Fault Zone, Hays and Travis Counties, Texas, 1937 – 2005, Barton Springs/Edwards Aquifer Conservation District (BSEACD), Report of Investigations 2006-1025, Electronic

document, accessible at http://www.bseacd.org/uploads/AquiferScience/HR_WaterLevels_BSEACD_DataSeries_2006.pdf

Hunt, B.B., Smith, B.A., Beery, J., Johns, D., and Hauwert, N., 2006, Summary of 2005 Groundwater Dye Tracing, Barton Springs Segment of the Edwards Aquifer, Hays and Travis Counties, Central Texas, Barton Springs / Edwards Aquifer Conservation District Report of Investigations 2006-0530, Electronic document, accessible at: http://www.bseacd.org/uploads/AquiferScience/HR_Dye_BSEACD_report_2006.pdf

Hutchinson, A.S., and Woodside, G.D., 2002, The Santa Ana River: The challenge of maximizing the use of an urban river, in Dillon, P.J., ed., Management of aquifer recharge for sustainability: Proceedings 4th International Symposium on Artificial Recharge of Groundwater, Adelaide, Australia, Lisse, Netherlands, Swets and Zeitlinger, p. 509 – 514

Klemt, W.B.; Knowles, T.R.; Edler, G.R.; and Sieh, T.W., 1979, Groundwater resources and model applications for the Edwards (Balcones fault zone) aquifer in the San Antonio region: Texas Water Development Board Report 239

Klenzendorf, J.B., Eck, B.J., Charbeneau, R.J., and Barrett, M.E., 2011 in press, Quantifying the behavior of porous asphalt overlays with respect to drainage hydraulics and runoff water quality, Environmental and Engineering Geoscience

Knisel, W.G., 1993, GLEAMS: Groundwater Loading Effects of Agricultural Management Systems. University of Georgia, Coastal Plain Experiment Station, Biological and Agricultural Engineering Department, Publication No. 5, p. 260

Konikow, L.F., 1986, Predictive Accuracy of a Ground-Water Model – Lessons from a Postaudit, Ground Water, vol. 24, no. 2, p. 173 – 184.

Larkin, T.J., and Bomar, G.W., 1983, Climatic atlas of Texas: Austin, Teas, Department of Water Resources, p. 151

LGB-Guyton Associates, 1994, Edwards Aquifer Ground-Water Divides Assessment San Antonio Region, Texas: Report 95-01 Prepared for the Edwards Underground Water District, p. 35

Legget, R.F., 1969, Man as a geological agent: National Research Council of Canada, Division of Building Research Technical Paper 304, p. 8

Leopold, L.B., 1968, Hydrogeology for Urban Planning – A Guidebook on the Hydrologic Effects of Urban Land Use: U.S. Geological Survey Circular 554, p. 18.

Lerner, D.N., 2002, Identifying and quantifying urban recharge: A review: Hydrogeology Journal, v. 10, p. 143 – 152, doi: 10.1007/s10040-001-0177-1.

Lerner, D.N., 1997, Too much or too little: Recharge in urban areas, in Chilton, J. (ed.), Groundwater in the Urban Environment: Problems, Processes and Management: International Association of Hydrogeologists, Balkema, Rotterdam, p. 41 – 47.

Lerner, D.N., 1990, Groundwater recharge in urban areas: Atmospheric Environment, v. 24B, p. 29 – 33

Lerner, D.N., 1986, Leaking pipes recharge ground water: Groundwater, v. 24, p. 654 – 662.

Lindgren, R.J.; Taylor, C.J. and Houston, N.A., 2009, Description and evaluation of numerical groundwater flow models for the Edwards aquifer, south-central Texas: U.S. Geological Survey Scientific Investigations Report 2009-5183, p. 25

Lindgren, R.J., 2006, Diffuse-flow conceptualization and simulation of the Edwards aquifer, San Antonio region, Texas: U.S. Geological Survey Scientific Investigations Report 2006 – 5319

Lindgren, R.J.; Dutton, A.R.; Hovorka, S.D.; Worthington, S.R.H. and Painter, Scott, 2004, Conceptualization and simulation of the Edwards aquifer, San Antonio regions Texas: U.S. Geological Survey Scientific Investigations Report 2006 – 5277

Lowe, M.D., 1992, Shaping Cities, in State of the World 1992. New York: W.W. Norton

Maclay, R.W., and Small, T.A., 1986, Carbonate Geology and Hydrogeology of the Edwards Aquifer in the San Antonio Area, Texas: Texas Water Development Board, Report 296, p. 90

Massei, N., Mahler, B.J., Bakalowicz, M., Fournier, M., and Dupont, J.P., 2007, Quantitative Interpretation of Specific Conductance Frequency Distribution in Karst, in Groundwater, May-June 2007, Vol. 45, No.3, p. 288 – 293

McDonald, M.G., and Harbaugh, A.W., 1988, A modular three-dimensional finite-difference ground-water flow model: Techniques of Water-Resources Investigations of the United States Geological Survey, Book 6, Chapter A1, 586 p.

Moore, C.H., 1996, Anatomy of a sequence boundary – Lower Cretaceous Glen Rose/Fredericksburg, Central Texas Platform: Gulf Coast Association of Geological Societies Transactions, v. 46, p. 313 – 320

National Oceanographic and Atmospheric Administration (NOAA) (a), accessed November, 2010, Past Palmer Drought Severity Index Maps by Week for 1998 – current, Electronic document, available at: http://www.cpc.ncep.noaa.gov/products/monitoring_and_data/drought.shtml/

National Oceanographic and Atmospheric Administration (NOAA) (b), accessed October, 2010, Gridded Rainfall Data, Electronic document, accessible at: http://water.weather.gov/precip/download.php

Oad, R., and DiSpigno, M., 1997, Water rights to return flow from urban landscape irrigation, Journal of Irrigation and Drainage Engineering, 123(4), p. 293 – 299.

Oad, R., Lusk, K., and Podmor, T., 1997, Consumptive use and return flows in urban lawn water use, Journal of Irrigation and Drainage Engineering, 123(1), p. 62 – 69.

Painter, S.L., Sun, A., and Green, R.T., 2007, Enhanced characterization and representation of flow through karst aquifers – Phase II, Revision 1: San Antonio, Southwest Research Institute, final technical report prepared for Southwest Florida Water Management District, Brooksville Fla., and Edwards Aquifer Authority under SwRI Project 20-11674

Pierce, S.A., Dulay, M.M., Sharp, J.M., Lowry, T.S., Tidwell, V.C., 2006, Defining tenable groundwater management: Integrating stakeholder preferences, distributed parameter models, and systems dynamics to aid groundwater resource allocation. MODFLOW and More. International Groundwater Modeling Center, Golden, Colorado.

Pierce, S.A., Ciarleglio, M., Dulay, M., Lowry, T.S., Sharp, J.M., Jr., Barnes, J.W., Eaton, D.J., and Tidwell, V.C., 2006, Solving for efficiency or decision criteria: When the non-unique nature of solutions becomes a benefit: EOS, American Geophysical Union.

Pierce, S.A., Sharp, J.M., Jr., Lowry, T.S., and Tidwell, V.C., 2006, Interactive management models to guide groundwater allocation policy [abs.]: The Abstract Book of the 2006 Ground Water Summit Program, National Ground Water Association, Westerville, OH, p. 167.

Pierce, S.A., 2006, Groundwater Decision Support: An integrated assessment linking causal narratives, numerical models, and combinatorial search techniques to determine available yield for an aquifer system, PhD thesis, Jackson School of Geosciences, Department of Geology, The University of Texas at Austin

Price, M., Reed, D.W., 1989, The influence of mains leakage and urban drainage on groundwater levels beneath conurbations in the UK. Proc Inst Civil Eng (Design and Construction) 86 (part 1): 31-39

Ramsey, M.S., 2003, Mapping the city landscape from space: The Advanced Spaceborne Thermal Emission and Reflectance Radiometer (ASTER) urban environmental monitoring program: in Earth Sciences in the City (Heiken, G., Fakundiny, R., and Sutter, J., eds.), Am. Geophysical Union, Washington, DC, Ch. 9, p. 337 – 376.

Rushton, K.R., Alothman, A.A.R., 1994, Control of rising groundwater levels in Riyadh, Saudi Arabia, in Wilkinson, W.B., (ed) Groundwater problems in urban areas, Thomas Telford, London, p. 299 – 309.

Rushton, K.R., Kawecki, M.W., and Brassington, F.C., 1988, Groundwater model of conditions in Liverpool sandstone aquifer, J Inst Water Environ Manage 2(1): 67 – 84.

Rushton, K.R., and Redshaw, S.C., 1979, Seepage and groundwater flow-numerical analysis by analog and digital methods; New York, John Wiley and Sons

Scanlon, B.R., Mace, R.E., Barrett, M.E., Smith, B., 2003, Can we simulate regional groundwater flow in a karst system using equivalent porous media models? Case Study, Barton Springs Edwards aquifer, USA, Journal of Hydrology, v. 276, p. 137 – 158.

Scanlon, B.R.; Mace, R.E.; Smith, B.A.; Hovorka, S.D.; Dutton, A.R. and Reedy, R.C., 2001, Groundwater Availability of the Barton Springs Segment of the Edwards Aquifer, Texas – Numerical Simulations through 2050: The University of Texas at Austin, Bureau of Economic Geology, final report prepared for the Lower Colorado River Authority, under contract no. UTA99-0

Schueler, T.J., 1994, Importance of imperviousness: Watershed protection techniques, v.1, p. 100 – 111

Senger, R.K. and Kreithler, C.W., 1984, Hydrogeology of the Edwards aquifer, Austin, area, Central Texas: The University of Texas at Austin, Bureau of Economic Geology Report of Investigations No. 141, p. 35

Sharp, J.M., Jr., 2010, The impacts of urbanization on groundwater systems and recharge: Aqua Mundi, v.1., p.51-56 . DOI 10.44409/Am-004-10-0008.

Sharp, J.M., Llado, L.E., and Budge, T.J., 2009, Urbanization-induced trends in spring discharge from a karstic aquifer – Barton Springs, Austin, Texas, USA: in Proceedings, 15th International Congres of Speleology (White, W.B., ed.), Kerrville, TX, v. 2, p. 1211 – 1216.

Sharp, J.M., Jr., Pierce, S.A. Smith, B.A., Dulay, M.P., and Eaton, D.J., 2008, Conflict resolution and integration of science in groundwater policy development: Water Down Under 2008, p. 2453-2462.

Sharp, J.M., Hansen, J.M., and Krothe, J.N., 2001, Effects of urbanization on hydrogeological systems: The physical effects of utility trenches, in Seiler, K.P. and Wohnlich, S. (eds.) New Approaches Characterizing Groundwater Flow: XXXI Congress, supplement volume, International Association of Hydrogeologists, Munich, p. 4

Sharp, J.M., 1997, Ground-water supply issues in urban and urbanizing areas, in Chilton, J., et al., eds., Groundwater in the urban environment: Problems, processes and management: Rotterdam, Netherlands, Balkema, p. 67 – 74

Sharp, J.M., Jr., 1990, Stratigraphic, Geomorphic and Structural Controls of the Edwards Aquifer, Texas, U.S.A., in Selected Papers on Hydrogeology (eds., E.S. Simpon and J.M. Sharp, Jr.), 1, 67_82, International Association of Hydrogeologists, Heise, Hannover, 1990.

Shelton, G.P., 2010, personal communication, National Oceanographic and Atmospheric Administration, National Weather Service River Forecast Center, West Gulf River Forecast Center, Fort Worth, TX, 817-831-3289 x323

Sherlock, R.L., 1922, Man as a Geological Agent: H.F. & G. Witherby, London, p. 372

Slade, R.M., Jr.; Dorsey, M.E. and Stewart S.L., 1986, Hydrology and water quality of the Edwards Aquifer associated with Barton Springs in the Austin area, Texas. US Geological Survey, Water Resource Investigation Report, 86-4036

Slade, R.M., Jr.; Linda, R. and Slagle, D., 1985, Simulation of the Flow System of Barton Springs and Associated Edwards Aquifer in the Austin Area, Texas: U.S. Geological Survey, Water-Resources Investigations Report 85-4299

Small, T.A., Hanson, J.A., and Hauwert, N.M., 1996, Geologic framework and hydrogeologic characteristics of the Edwards aquifer outcrop (Barton Springs segment), northeastern Hays and southwestern Travis Counties, Texas: U.S. Geological Survey, Water-Resources Investigations WRI 96-4306, p. 15

Smith, B.A., 2011, personal communication, Barton Springs Edwards Aquifer / Conservation District, 1124 Regal Row, Austin, TX 78748, brians@bseacd.org

Smith, B.A., Hunt, B.B., and Schindel, G.M., 2005, Groundwater Flow in the Edwards Aquifer: Comparison of Groundwater Modeling and Dye Trace Results, Barton Springs/Edwards Aquifer Conservation District, Electronic document, accessible at http://www.bseacd.org/uploads/AquiferScience/HR_DyeModeling_ASCE_SinkholeConf_paper_2005.pdf

Smith, B.A. and Hunt, B.B., 2004, Evaluation of the sustainable yield of the Barton Springs segment of the Edwards aquifer, Hays and Travis Counties, central Texas: Austin, Barton Springs/Edwards Aquifer Conservation District

Smith, B.A., Hunt, B.B., Helmcamp, S., Johns, D., Hauwert, N., 2001, Water Quality and Flow Loss Study of the Barton Springs Segment of the Edwards Aquifer: EPA – funded 319h grant report by the Barton Springs/Edwards Aquifer Conservation District and City of Austin, submitted to the Texas Commission on Environmental Quality (formerly TNRCC), August 2001, p. 85

Stein, W.G., 1995, Edwards aquifer ground-water divides assessment, San Antonio region, Texas: Edwards Underground Water District Report 95-01 prepared by LBG-Guyton Associates

Stewart, M. and Langevin, C., 1999, Post Audit of a Numerical Prediction of Wellfield Drawdown in a Semiconfined Aquifer System, Ground Water, vol. 37, no. 2, p. 245 - 252

Texas Water Development Board, accessed March, 2011, Ground Water Availability Modeling, accessible at http://www.twdb.state.tx.us/gam/

Texas Water Development Board, accessed March, 2011, GIS Data, Electronic document, available at http://www.twdb.state.tx.us/mapping/gisdata.asp

TexasET, accessed November, 2010, Crop coefficients, Turf coefficients, Texas Average ET_0, Electronic document, available at http://texaset.tamu.edu/etinfo

Thorkildsen, D.F. and McElhaney, P.D., 1992, Model refinement and applications for the Edwards (Balcones fault zone) aquifer in the San Antonio region, Texas: Texas Water Development Board Report 340

Trescott, P.C.; Pinder, G.F. and Larson, S.P., 1976, Finite-difference model for aquifer simulation in two dimensions with results of numerical experiments: U.S. Geological Survey Techniques of Water-Resources Investigations, Book 7, Chapter C1, p. 116

Trow, S and Farley, M, 2004, Developing a strategy for leakage management in water distribution systems, Water Science and Technology: Water Supply, vol. 4, no. 3, p. 149 - 168

Underwood, J.R., Jr., 2001, Anthropic rocks as a fourth basic class: Environmental and Engineering Geoscience, v. 7, p. 104-110

United Nations, 1991, World urbanization prospects 1990: New York, United Nations Population Division, Department of Economic and Social Affairs, p. 100

United States Environmental Protection Agency, accessed March 23, 2011, Heat Island Effect – Basic Information, Electronic document, accessible at http://www.epa.gov/heatisld/about/index.htm

Wiles, T.J., and Sharp, J.M., Jr., 2008, The secondary permeability of impervious cover: Environmental and Engineering Geoscience, v. 14(4), p. 251 – 265.

Winterle, J.R., Painter, S.L., and Green, R.T., 2009, Update of Groundwater Availability Model for Barton Springs Segment of the Edwards Aquifer Utilizing the MODFLOW-DCM code, Southwest Research Institute, final technical report prepared for Barton Springs Edwards Aquifer Conservation District and Texas Water Development Board, SwRI Project 20-12074, Electronic document, accessible at http://www.bseacd.org/uploads/AquiferScience/HR_DCM_SWRI_Report_2009.pdf

Yang, Y., Lerner, D.N., Barrett, M.H., and Tellam, J.H., 1999, Quantification of groundwater recharge in the city of Nottingham, UK: Environmental Geology, v. 38, p. 183 – 198, doi: 10.1007/s002540050414

Zahm, C., 1998, Regional Groundwater Flow Measurements, Barton Springs Segment, Edwards Aquifer, M.S. Thesis, Department of Geology, The Jackson School of Geoscience, The University of Texas at Austin

VITA

Michael Charles Passarello was born in Charleston, South Carolina on May 19th, 1987. He is the eldest son of Mike and Ruth Passarello and brother to Drew. He attended Pinewood Preparatory School where he graduated in 2005. After high school, he attended the College of Charleston where he obtained his B.S. in Geology and Environmental Geosciences. While at the College of Charleston, he participated in undergraduate research with his advisor and friend Dr. Timothy J. Callahan. He also received the Outstanding Student and Departmental Honors awards from the Geology Department and was President of the Geological Society at the College of Charleston.

After graduating from the College of Charleston, he substituted at his high school during the spring semester of 2009. Soon after, he was accepted to the Jackson School of Geoscience at the University of Texas at Austin where he pursued his Masters of Science in Geology. As a graduate student, he was co-supervised by Jack Sharp and Suzanne Pierce and was a teaching assistant for Introduction to Geology, Sedimentary Rocks, and Applied Hydrogeology. He was Secretary and Member at Large for the Graduate Student Executive Council for the Jackson School of Geoscience and mentored one undergraduate honors thesis project and one independent study research project. He is a member of the Association of Environmental and Engineering Geologists, American Association of Petroleum Geologists, and the Geological Society of America. Upon graduation he will be moving to Houston, Texas to begin his career as a geologist with ExxonMobil.

Permanent Contact: mcpassarello@gmail.com

This thesis was typed by the author